Search for new physics in the 2011 opposite sign dilepton sample

D. Barge, C. Campagnari, P. Kalavase, D. Kovalskyi, V. Krutelyov, J. Ribnik

University of California, Santa Barbara

W. Andrews, G. Cerati, D. Evans, F. Golf, I. Macneill, S. Padhi, Y. Tu, F. Würthwein, A. Yagil, J. Yoo

University of California, San Diego

L. Bauerdick, I. Bloch, K. Burkett, I. Fisk, Y. Gao, O. Gutsche, B. Hooberman, S. Jindariani, J. Linacre

Fermi National Accelerator Laboratory, Batavia, Illinois

Version v2

Abstract

We present the results of a search for new physics in the opposite-sign leptons + jets + missing energy final state based on 204 pb^{-1} of 2011 CMS data.

Contents

1 Introduction **2**

2 Datasets, Triggers, Luminosity **2**

3 Event Preselection **3**

3.1 Event Cleanup . . . 3

3.2 Muon Selection . . . 3

3.3 Electron Selection . . . 4

3.4 Invariant mass requirement . . . 4

3.5 Trigger Selection . . . 4

4 Trigger efficiency **5**

5 Dilepton Yields **6**

6 Preselection yields: Data/MC Comparison **6**

7 Properties of data passing the preselection **7**

8 Definition of the signal region **7**

9 Data Driven Background Estimation Methods **11**

9.1 ABCD method . . . 12

9.2 Dilepton p_T method . . . 14

9.3 Opposite-Flavor Subtraction . . . 15

9.3.1 OF subtraction: Application to high p_T lepton sample . . . 15

9.3.2 OF subtraction: Application to low p_T lepton sample . . . 15

10 Results **17**

10.1 Background estimate from the ABCD method . . . 17

10.2 Background estimate from the $P_T(\ell\ell)$ method . . . 21

10.3 Background estimate from OF subtraction . . . 21

10.4 Summary of results . . . 22

Appendix A Fakeable Object Definitions **25**

Appendix B The ABCD' Technique **26**

Appendix C Data/MC Comparison: Preselection Region **29**

Appendix D Data/MC Comparison: 2010 Signal Region **50**

1 Introduction

In this note we describe a search for new physics in the opposite sign isolated dilepton sample (ee, $e\mu$, and $\mu\mu$) based on 204 pb^{-1} of 2011 data. The main source of isolated dileptons at CMS is Drell Yan and $t\bar{t}$. Here we concentrate on dileptons with invariant mass inconsistent with $Z \to ee$ and $Z \to \mu\mu$, thus $t\bar{t}$ is the most important background. A separate search for new physics in the Z sample is described in a separate note [1]. This is an update of a (soon to be) published analysis performed on 2010 data [2, 3].

The search strategy is the following

- We start out with a pre-selection which is as close as possible to the published $t\bar{t}$ dilepton analysis [4] (same lepton ID, same jet definitions, etc.). We do make a couple of substantive modifications:

  1. The top analysis requires two leptons of $P_T > 20$ GeV. In this analysis we search for new physics in 2 data samples. The first data sample is collected with high p_T dilepton triggers; for this sample we require leptons with $p_T >$ (20,10) GeV (leading lepton $p_T > 20$ GeV, trailing lepton $p_T > 10$ GeV. The second data sample is collected with dilepton-H_T cross triggers; for this sample we require leptons with $p_T >$ (10,5) GeV. This is motivated by our desire to maintain sensitivity to possible SUSY signals with relatively low p_T leptons generated in the cascade decays of heavy objects.
  2. The top analysis requires at least two jets of $p_T > 30$ GeV with $\mathrm{E_T^{miss}} > 30$ GeV (ee and $e\mu$) or $\mathrm{E_T^{miss}} > 20$ GeV ($e\mu$). We tighten the $\mathrm{E_T^{miss}}$ cut to 50 GeV and we also require that the scalar sum of the p_T of all jets with $p_T > 30$ GeV be > 100 GeV. These requirements considerably reduce backgrounds to the $t\bar{t}$ sample, *e.g.*, backgrounds from Drell Yan and W+jets.

- The pre-selection consists mostly of $t\bar{t}$ events. We perform data $-$ Monte Carlo comparisons of kinematical distributions. Assuming reasonable agreeement for the bulk of $t\bar{t}$ we move on to a search for new physics in the tails of the $t\bar{t}$ $\mathrm{E_T^{miss}}$ and H_T distributions.

- Our prejudice is that new physics would manifest itself in an excess of events with high $\mathrm{E_T^{miss}}$ and significant hadronic activity. We define a a-priori search regions by tightening the $\mathrm{E_T^{miss}}$ and hadronic activity requirements.

- We perform a counting experiment in the signal regions. We compare observed yields with expectations from Monte Carlo and with three independent data driven techniques (see Sections 9.1, 9.2 and 9.3).

2 Datasets, Triggers, Luminosity

We combine the official May10ReReco and June 3rd prompt reco json files, yielding a luminosity of 204 pb^{-1}.

We use two data samples, one collected with high p_T dilepton triggers and the other with dilepton-H_T cross triggers. These samples are complementary, since the dilepton-H_T trigger sample extends to lower lepton p_T, while the high p_T dilepton trigger sample does not include requirements on the hadronic activity in the event.

Currently we use data reconstructed in CMSSW 4_2_X and Spring11 MC reconstructed in CMSSW 3_11_X. We will update the MC when the Summer11 madgraph MC samples become available.

- Datasets
  - High p_T dilepton trigger sample
    * `DoubleElectron_Run2011A-May10ReReco-v1_AOD`
    * `DoubleMu_Run2011A-May10ReReco-v1_AOD`
    * `MuEG_Run2011A-May10ReReco-v1_AOD`
    * `DoubleElectron_Run2011A-PromptReco-v4_AOD`
    * `DoubleMu_Run2011A-PromptReco-v4_AOD`
    * `MuEG_Run2011A-PromptReco-v4_AOD`
  - Dilepton-H_T cross trigger sample
    * `ElectronHad_Run2011A-May10ReReco-v1_AOD`
    * `MuHad_Run2011A-May10ReReco-v1_AOD`

    * ElectronHad_Run2011A-PromptReco-v4_AOD
    * MuHad_Run2011A-PromptReco-v4_AOD

- Monte Carlo samples
  - TTJets_TuneZ2_7TeV-madgraph-tauola_Spring11-PU_S1_START311_V1G1-v1
  - DYToEE_M-10To20_TuneZ2_7TeV-pythia6_Spring11-PU_S1_START311_V1G1-v1
  - DYToMuMu_M-10To20_TuneZ2_7TeV-pythia6_Spring11-PU_S1_START311_V1G1-v1
  - DYToTauTau_M-10To20_CT10_TuneZ2_7TeV-powheg-pythia-tauola_Spring11-PU_S1_START311_V1G1-v2
  - DYToEE_M-20_CT10_TuneZ2_7TeV-powheg-pythia_Spring11-PU_S1_START311_V1G1-v1
  - DYToMuMu_M-20_CT10_TuneZ2_7TeV-powheg-pythia_Spring11-PU_S1_START311_V1G1-v1
  - DYToTauTau_M-20_CT10_TuneZ2_7TeV-powheg-pythia-tauola_Spring11-PU_S1_START311_V1G1-v1
  - DYJetsToLL_TuneD6T_M-50_7TeV-madgraph-tauola_Spring11-PU_S1_START311_V1G1-v1
  - WWTo2L2Nu_TuneZ2_7TeV-pythia6_Spring11-PU_S1_START311_V1G1-v1
  - WZtoAnything_TuneZ2_7TeV-pythia6-tauola_Spring11-PU_S1_START311_V1G1-v1
  - ZZtoAnything_TuneZ2_7TeV-pythia6-tauola_Spring11-PU_S1_START311_V1G1-v1
  - WJetsToLNu_TuneZ2_7TeV-madgraph-tauola_Spring11-PU_S1_START311_V1G1-v1
  - TToBLNu_TuneZ2_s-channel_7TeV-madgraph_Spring11-PU_S1_START311_V1G1-v1
  - TToBLNu_TuneZ2_t-channel_7TeV-madgraph_Spring11-PU_S1_START311_V1G1-v1
  - TToBLNu_TuneZ2_tW-channel_7TeV-madgraph_Spring11-PU_S1_START311_V1G1-v1

3 Event Preselection

The purpose of the preselection is to reject backgrounds other than $t\bar{t} \rightarrow$ dileptons. We compare the kinematical properties of this sample with expectations from $t\bar{t}$ Monte Carlo.

The preselection is based on the $t\bar{t}$ analysis [4]. We select events with two opposite sign, well-identified and isolated leptons (ee, $e\mu$, or $\mu\mu$); one of the leptons must have $p_T > 20$ GeV, the other one must have $p_T > 10$ GeV. Events with dilepton mass consistent with $Z \rightarrow ee/\mu\mu$ are rejected. In case of events with more than two such leptons, we select the pair that maximizes the scalar sum of lepton p_T's. There must be at least two pfjets of $p_T > 30$ GeV and $|\eta| < 3.0$; jets must pass loose `pfJetId` and be separated by $\Delta R > 0.4$ from any lepton with $p_T > 10$ GeV passing the selection. The scalar sum H_T of the p_T of all such jets must exceed 100 GeV, for the dilepton-H_T sample this requirement is increased to 200 GeV since these triggers have large inefficiency below this threshold. Finally $\mathrm{E_T^{miss}} > 50$ GeV (we use pfmet). More details are given in the subsections below.

3.1 Event Cleanup

- Require at least one good deterministic annealing (DA) vertex
  - not fake
  - ndof > 4
  - $|\rho| < 2$ cm
  - $|z| < 24$ cm.

3.2 Muon Selection

Muon candidates are RECO muon objects passing the following requirements:

- $p_T > 5$ GeV and $|\eta| < 2.4$
- Global Muon and Tracker Muon
- χ^2/ndof of global fit < 10
- At least 11 hits in the tracker fit
- Impact parameter with respect to the first DA vertex $d_0 < 200$ μm and $d_z < 1$ cm

- $Iso \equiv E_T^{\rm iso}/p_T < 0.15$, $E_T^{\rm iso}$ is defined as the sum of transverse energy/momentum deposits in ecal, hcal, and tracker, in a cone of 0.3
- At least one of the hits from the standalone muon must be used in the global fit
- Require tracker $\Delta p_T/p_T < 0.1$. This cut was not in the original top analysis. It is motivated by the observation of poorly measured muons in data with large relative p_T uncertainty, giving significant contributions to the $\rm E_T^{miss}$

3.3 Electron Selection

Electron candidates are RECO GSF electrons passing the following requirements:

- $p_T > 10$ GeV and $|\eta| < 2.5$.
- Veto electrons with a supercluster in the transition region $1.4442 < |\eta| < 1.556$.
- VBTF90 identification[5] with requirements tightened to match the CaloIdT and TrkIdVL HLT requirements:
  - $\sigma_{i\eta i\eta} < 0.01$ (EB), 0.03 (EE)
  - $\Delta\phi < 0.15$ (EB), 0.10 (EE)
  - $\Delta\eta < 0.007$ (EB), 0.009 (EE)
  - $H/E < 0.1$ (EB), 0.075 (EE)
- Impact parameter with respect to the first DA vertex $d_0 < 400$ μm and $d_z < 1$ cm.
- $Iso \equiv E_T^{\rm iso}/p_T < 0.15$. $E_T^{\rm iso}$ is defined as the sum of transverse energy/momentum deposits in ecal, hcal, and tracker, in a cone of 0.3. A 1 GeV pedestal is subtracted from the ecal energy deposition in the EB, however the ecal energy is never allowed to go negative.
- Electrons with a tracker or global muon within ΔR of 0.1 are vetoed.
- The number of missing expected inner hits must be less than two [6].
- Conversion removal via partner track finding: any electron where an additional GeneralTrack is found with dist < 0.02 cm and $\Delta \cot\theta < 0.02$ is vetoed [6].

We estimate the contributions from fake leptons using the data-driven fake rate (FR) method. The requirements defining the fakeable objects are listed in App. A.

3.4 Invariant mass requirement

We remove e^+e^- and $\mu^+\mu^-$ events with invariant mass between 76 and 106 GeV. We also remove events with invariant mass < 12 GeV, since this kinematical region is not well reproduced in CMS Monte Carlo and to remove events with Upsilons.

In addition, we remove $Z \to \mu\mu\gamma$ candidates with the γ collinear with one of the muons. This is done as follows: if the ecal energy associated with one of the muons is greater than 6 GeV, we add this energy to the momentum of the initial muon, and we recompute the $\mu\mu$ mass. If this mass is between 76 and 106 GeV, the event is rejected.

3.5 Trigger Selection

We do not make any requirements on HLT bits in the Monte Carlo. Instead, as discussed in Section 4, a trigger efficiency weight is applied to each event, based on the trigger efficiencies measured on data (see Sec. 4).

We select data events using the following triggers. An event in the ee channel is required to pass a DoubleElectron trigger, an event in the $\mu\mu$ channel is required to pass a DoubleMu trigger, and an event in the $e\mu$ channel is required to pass a Ele-Mu trigger.

- High p_T dilepton trigger sample
  - `HLT_Ele17_CaloIdL_CaloIsoVL_Ele8_CaloIdL_CaloIsoVL`
  - `HLT_DoubleMu7`
  - `HLT_Mu13_Mu7`
  - `HLT_Mu17_Ele8_CaloIdL`
  - `HLT_Mu8_Ele17_CaloIdL`
- Lepton H_T cross trigger sample
  - `HLT_DoubleMu3_HT150`
  - `HLT_DoubleMu3_HT160`
  - `HLT_Mu3_Ele8_CaloIdL_TrkIdVL_HT150`
  - `HLT_Mu3_Ele8_CaloIdT_TrkIdVL_HT150`
  - `HLT_Mu3_Ele8_CaloIdL_TrkIdVL_HT160`
  - `HLT_Mu3_Ele8_CaloIdT_TrkIdVL_HT160`
  - `HLT_DoubleEle8_CaloIdL_TrkIdVL_HT150`
  - `HLT_DoubleEle8_CaloIdT_TrkIdVL_HT150`
  - `HLT_DoubleEle8_CaloIdL_TrkIdVL_HT160`
  - `HLT_DoubleEle8_CaloIdT_TrkIdVL_HT160`

4 Trigger efficiency

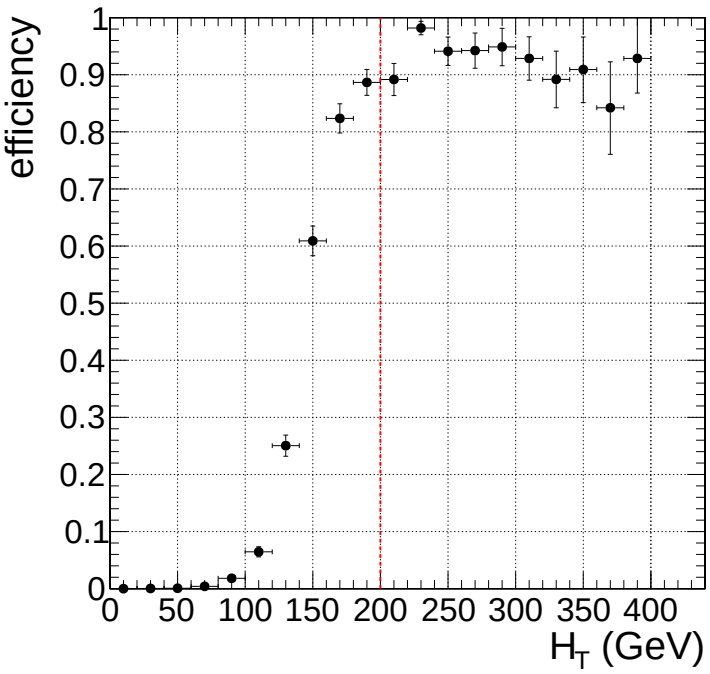

Figure 1: Efficiency for the dimuon-H_T trigger HLT_DoubleMu3_HT150 as a function of the offline H_T. Events are selected with the high p_T dilepton trigger HLT_DoubleMu7 and required to have 2 muons passing analysis selection. The vertical dashed line indicates the requirement $H_T > 200$ GeV, which is used in the preselection for the dilepton-H_T trigger sample.

For the high p_T dilepton triggers, the efficiencies have been measured to be approximately 100% (DoubleEle), 90% (DoubleMu), and 95% (Mu-Ele) [7]. In the following, unless otherwise specified we weight the ee, $\mu\mu$ and $e\mu$ MC events by these efficiencies. We do not apply any efficiency correction for the hadronic part of the dilepton-H_T triggers. We have verified that the efficiencies for these triggers with respect to an offline selection of $H_T >$ 200 GeV is high ($\sim$90–95%), as shown in Fig. 1.

5 Dilepton Yields

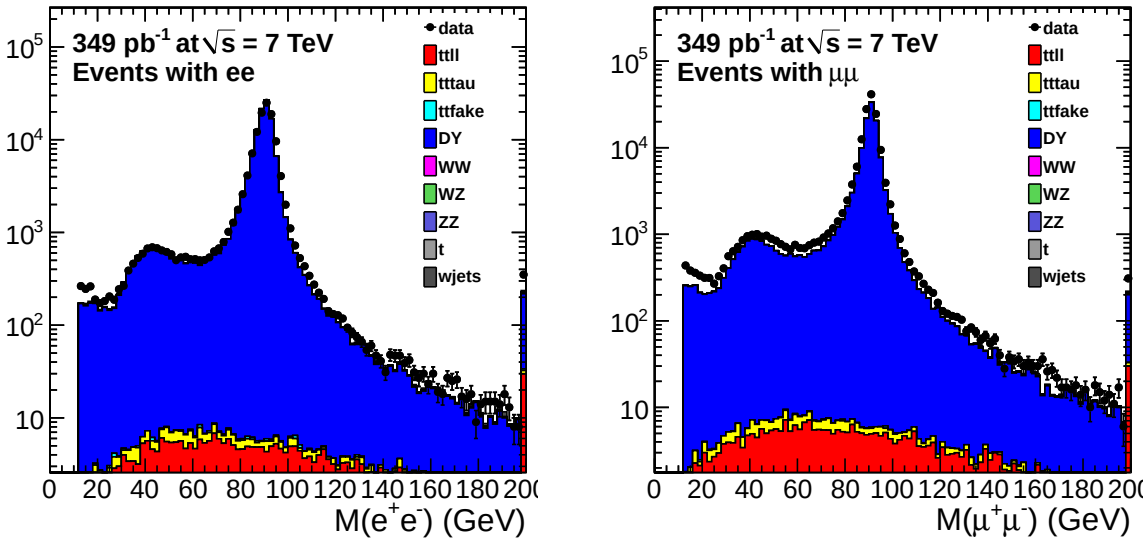

Figure 2: Distributions of dilepton mass in data and MC, in the ee channel (left) and $\mu\mu$ channel (right).

Table 1: The data and MC yields in the ee and $\mu\mu$ final states for events with 2 selected leptons with invariant mass 76–106 GeV.

Sample	ee	$\mu\mu$
data	110402	140191
MC	107089	125998
data/MC	1.03	1.11

The data and MC dilepton mass distributions for events with 2 selected leptons are displayed in Fig. 2. The yields of Z events in the mass range 76–106 GeV are indicated in Table 1. In data we observe a slight excess with respect to MC expectations, of 3% (11%) in the ee ($\mu\mu$) channel, which we attribute to uncertainties in trigger efficiency, lepton selection efficiency, and integrated luminosity. We use the ratio of $Z \to \mu^+\mu^-$ to $Z \to e^+e^-$ yields in data to estimate the ratio of muon to electron selection efficiencies, and find $R_{\mu e} = \mathrm{eff}(\mu)/\mathrm{eff}(\mathrm{e}) = 1.13$.

6 Preselection yields: Data/MC Comparison

The data yields and the MC predictions for the dilepton trigger sample are given in Table 2. As anticipated, the MC predicts that the preselection is dominated by $t\bar{t}$. We observe a slight excess in data with respect to MC expectations. We also look for an excess of low lepton p_T events using the dilepton-H_T trigger sample, and requiring the leptons to pass lepton $p_T >$ (10,5) GeV but not pass lepton $p_T >$ (20,10) GeV (to remove overlap with the dilepton trigger sample), as summarized in Table 3. We observe reasonable agreement between the data and MC yields in this region. Finally, we compare in Table 4 the data samples collected with high p_T dilepton triggers and lepton-H_T cross triggers, including the requirements $H_T > 200$ GeV and lepton $p_T >$ (20,10) GeV. We find slightly fewer events in the dilepton-H_T trigger sample, consistent with the small inefficiency of the hadronic part of the trigger for an offline selection of $H_T > 200$ GeV.

The MC yields are normalized to 204 pb^{-1} using the cross-sections from Reference [8]. The MC is scaled by the approximate trigger efficiency (100% for ee, 95% for $\mu\mu$, and 95% for $e\mu$) and has been reweighted such that the distribution of reconstructed DA vertices matches that in data. The DY contribution is dominated by DY$\to \tau^+\tau^-$, and we have verified with the data-driven $R_{out/in}$ method [4] that the contributions from DY$\to e^+e^-$ and DY$\to \mu^+\mu^-$ are negligible. Also shown are the yields for LM1 and LM3, two of the LM points which are benchmarks for SUSY analyses at CMS. The LM yields are calculated at NLO using process-dependent k-factors computed from Prospino.

Table 2: High p_T dilepton trigger data and Monte Carlo yields for the preselection (njets ≥ 2, H_T>100 GeV, $\mathrm{E_T^{miss}}$ > 50 GeV, lepton p_T > (20,10) GeV).

Sample	ee	$\mu\mu$	$e\mu$	tot
$t\bar{t} \to \ell^+\ell^-$	120.1 ± 2.9	133.1 ± 2.9	320.3 ± 4.6	573.5 ± 6.1
$t\bar{t} \to \ell^\pm\tau^\mp/\tau^+\tau^-$	27.5 ± 1.4	33.3 ± 1.4	71.5 ± 2.2	132.3 ± 3.0
$t\bar{t} \to$ fake	4.5 ± 0.6	1.3 ± 0.3	8.1 ± 0.7	13.9 ± 1.0
DY	6.6 ± 1.8	9.5 ± 2.1	13.4 ± 2.6	29.6 ± 3.8
W^+W^-	1.4 ± 0.2	1.5 ± 0.2	3.4 ± 0.2	6.3 ± 0.3
$W^\pm Z^0$	0.3 ± 0.0	0.4 ± 0.0	0.7 ± 0.1	1.3 ± 0.1
Z^0Z^0	0.1 ± 0.0	0.1 ± 0.0	0.2 ± 0.0	0.4 ± 0.0
single top	4.5 ± 0.2	5.0 ± 0.2	11.9 ± 0.3	21.4 ± 0.5
W + jets	4.5 ± 1.9	0.0 ± 0.0	2.8 ± 1.7	7.3 ± 2.6
tot SM MC	169.7 ± 4.2	184.3 ± 3.9	432.2 ± 6.0	786.1 ± 8.3
data	193	201	485	879

Table 3: Dilepton-H_T trigger data and Monte Carlo yields for the preselection (njets ≥ 2, $H_T > 200$ GeV, $\mathrm{E_T^{miss}}$ > 50 GeV, lepton p_T > (10,5) GeV and not lepton p_T > (20,10) GeV).

ttll	0.6 ± 0.2	3.7 ± 0.5	4.1 ± 0.5	8.4 ± 0.7
tttau	0.6 ± 0.2	3.9 ± 0.5	3.5 ± 0.5	8.0 ± 0.7
ttfake	0.1 ± 0.1	1.3 ± 0.3	1.5 ± 0.3	2.9 ± 0.4
DY	0.0 ± 0.0	3.7 ± 1.4	0.6 ± 0.6	4.3 ± 1.5
WW	0.0 ± 0.0	0.0 ± 0.0	0.0 ± 0.0	0.0 ± 0.0
WZ	0.0 ± 0.0	0.0 ± 0.0	0.0 ± 0.0	0.0 ± 0.0
ZZ	0.0 ± 0.0	0.0 ± 0.0	0.0 ± 0.0	0.0 ± 0.0
t	0.0 ± 0.0	0.3 ± 0.1	0.3 ± 0.1	0.6 ± 0.1
wjets	0.0 ± 0.0	0.0 ± 0.0	0.0 ± 0.0	0.0 ± 0.0
tot SM MC	1.3 ± 0.3	12.9 ± 1.6	10.1 ± 1.0	24.3 ± 1.9
data	1	9	8	18

7 Properties of data passing the preselection

A number of kinematical distributions for events passing the preselection in data are compared with MC in Appendix C. Although we observe a slight overall excess of data, in general we find that the MC does a good job of reproducing the shapes of the kinematical distributions. Therefore we turn our attention to the tails of the $t\bar{t}$ events.

8 Definition of the signal region

We define signal regions to look for possible new physics contributions in the opposite sign isolated dilepton sample. The choice of signal region is driven by three observations:

1. astrophysical evidence for dark matter suggests that we concentrate on the region of high $\mathrm{E_T^{miss}}$;
2. new physics signals should have high $\sqrt{\hat{s}}$;
3. observable high cross section new physics signals are likely to be produced strongly; thus, we expect significant hadronic activity in conjunction with the two leptons.

Table 4: Comparison of data yields in the high-p_T dilepton and dilepton-H_T trigger samples, passing the selection njets ≥ 2, $\mathrm{E_T^{miss}} > 50$ GeV, H_T>200 GeV, lepton p_T> (20,10) GeV.

Sample	ee	$\mu\mu$	$e\mu$	tot
high-p_T dilepton trigger	88	75	190	353
dilepton-H_T trigger	85	74	185	344

Following these observations, we define the following 3 signal regions by adding requirements of large hadronic activity and missing transverse energy to the preselection of Section 3.

- 2010 signal region: $H_T > 300$ GeV and $y > 8.5$ GeV$^{1/2}$.
- high y signal region: $H_T > 300$ GeV and $y > 13$ GeV$^{1/2}$.
- high H_T signal region: $H_T > 600$ GeV and $y > 8.5$ GeV$^{1/2}$.

We cut on the quantity $y \equiv \mathrm{E_T^{miss}}/\sqrt{\mathrm{H_T}}$ rather than $\mathrm{E_T^{miss}}$ because the variables H_T and y are largely uncorrelated for the dominant $t\bar{t}$ background. This allows us to use a data-driven ABCD method to estimate the background (see Section 9.1). In the future, we plan to cut instead on $\mathrm{E_T^{miss}}$ and H_T, since we observe that $\mathrm{E_T^{miss}}$ is a better discriminant between $t\bar{t}$ vs. SUSY. We have developed a novel technique, which is a variation of the ABCD method, to estimate the background in a signal region defined by $\mathrm{E_T^{miss}}$ and H_T requirements (see App. B).

The 2010 signal region is the same as the one used in the 2010 analysis, and was chosen to preserve about 1% of the $t\bar{t}$ sample. The additional signal regions (high y and high H_T) have tightened requirements on y and H_T, respectively, which reduce the expected background by roughly an order of magnitude.

For each signal region, we search in the high p_T dilepton trigger sample requiring lepton $p_T >$ (20,10) GeV, and separately in the dilepton-H_T trigger sample requiring lepton $p_T >$ (10,5) GeV and not passing lepton $p_T >$ (20,10) GeV, to remove overlap with the high p_T dilepton trigger sample. For the high p_T dilepton sample, for which we have prior experience with the 2010 analysis, we apply the ABCD, $p_T(\ell\ell)$, and OF subtraction background estimates. For the dilepton-H_T sample we currently apply only the OF subtraction background estimate.

We present the data and MC expected yields in the 3 signal regions in Tables 5-7 for the high p_T dilepton trigger sample and in Tables 8-10.

Table 5: High p_T dilepton trigger data and MC yields in the 2010 signal region. MC errors are statistical only.

Sample	ee	$\mu\mu$	$e\mu$	tot
$t\bar{t} \to \ell^+\ell^-$	0.9 ± 0.2	1.4 ± 0.2	2.6 ± 0.3	5.0 ± 0.4
$t\bar{t} \to \ell^\pm\tau^\mp/\tau^+\tau^-$	0.4 ± 0.1	0.4 ± 0.1	1.2 ± 0.2	2.0 ± 0.3
$t\bar{t} \to$ fake	0.1 ± 0.1	0.0 ± 0.0	0.2 ± 0.1	0.3 ± 0.1
DY	0.2 ± 0.2	0.4 ± 0.4	0.4 ± 0.4	1.0 ± 0.6
W^+W^-	0.0 ± 0.0	0.0 ± 0.0	0.1 ± 0.0	0.2 ± 0.0
$W^\pm Z^0$	0.0 ± 0.0	0.0 ± 0.0	0.0 ± 0.0	0.0 ± 0.0
Z^0Z^0	0.0 ± 0.0	0.0 ± 0.0	0.0 ± 0.0	0.0 ± 0.0
single top	0.0 ± 0.0	0.0 ± 0.0	0.0 ± 0.0	0.1 ± 0.0
$W +$ jets	0.0 ± 0.0	0.0 ± 0.0	0.0 ± 0.0	0.0 ± 0.0
tot SM MC	1.8 ± 0.3	2.3 ± 0.5	4.5 ± 0.6	8.6 ± 0.8
data	4	3	7	14
LM1	6.4 ± 0.2	7.6 ± 0.2	3.9 ± 0.2	18.0 ± 0.4
LM3	1.3 ± 0.1	1.5 ± 0.1	2.0 ± 0.1	4.8 ± 0.1

Table 6: High p_T dilepton trigger data and MC yields in the high y signal region. MC errors are statistical only.

Sample	ee	$\mu\mu$	$e\mu$	tot
$t\bar{t} \to \ell^+\ell^-$	0.2 ± 0.1	0.3 ± 0.1	0.5 ± 0.1	0.9 ± 0.2
$t\bar{t} \to \ell^\pm\tau^\mp/\tau^+\tau^-$	0.0 ± 0.0	0.0 ± 0.0	0.1 ± 0.1	0.2 ± 0.1
$t\bar{t} \to$ fake	0.0 ± 0.0	0.0 ± 0.0	0.0 ± 0.0	0.0 ± 0.0
DY	0.0 ± 0.0	0.0 ± 0.0	0.0 ± 0.0	0.0 ± 0.0
W^+W^-	0.0 ± 0.0	0.0 ± 0.0	0.0 ± 0.0	0.1 ± 0.0
$W^\pm Z^0$	0.0 ± 0.0	0.0 ± 0.0	0.0 ± 0.0	0.0 ± 0.0
Z^0Z^0	0.0 ± 0.0	0.0 ± 0.0	0.0 ± 0.0	0.0 ± 0.0
single top	0.0 ± 0.0	0.0 ± 0.0	0.0 ± 0.0	0.0 ± 0.0
$W +$ jets	0.0 ± 0.0	0.0 ± 0.0	0.0 ± 0.0	0.0 ± 0.0
tot SM MC	0.2 ± 0.1	0.4 ± 0.1	0.7 ± 0.2	1.3 ± 0.2
data	3	0	3	6
LM1	2.7 ± 0.2	3.2 ± 0.2	1.7 ± 0.1	7.6 ± 0.3
LM3	0.4 ± 0.0	0.5 ± 0.0	0.7 ± 0.1	1.7 ± 0.1

Table 7: High p_T dilepton trigger data and MC yields in the high H_T signal region. MC errors are statistical only.

Sample	ee	$\mu\mu$	$e\mu$	tot
$t\bar{t} \to \ell^+\ell^-$	0.1 ± 0.1	0.2 ± 0.1	0.2 ± 0.1	0.5 ± 0.1
$t\bar{t} \to \ell^\pm\tau^\mp/\tau^+\tau^-$	0.1 ± 0.1	0.1 ± 0.1	0.1 ± 0.1	0.2 ± 0.1
$t\bar{t} \to$ fake	0.0 ± 0.0	0.0 ± 0.0	0.0 ± 0.0	0.0 ± 0.0
DY	0.0 ± 0.0	0.0 ± 0.0	0.4 ± 0.4	0.4 ± 0.4
W^+W^-	0.0 ± 0.0	0.0 ± 0.0	0.0 ± 0.0	0.0 ± 0.0
$W^\pm Z^0$	0.0 ± 0.0	0.0 ± 0.0	0.0 ± 0.0	0.0 ± 0.0
Z^0Z^0	0.0 ± 0.0	0.0 ± 0.0	0.0 ± 0.0	0.0 ± 0.0
single top	0.0 ± 0.0	0.0 ± 0.0	0.0 ± 0.0	0.0 ± 0.0
$W +$ jets	0.0 ± 0.0	0.0 ± 0.0	0.0 ± 0.0	0.0 ± 0.0
tot SM MC	0.2 ± 0.1	0.3 ± 0.1	0.7 ± 0.4	1.2 ± 0.5
data	1	0	2	3
LM1	2.3 ± 0.1	2.7 ± 0.2	1.2 ± 0.1	6.2 ± 0.2
LM3	0.6 ± 0.0	0.6 ± 0.0	0.7 ± 0.1	1.9 ± 0.1

Table 8: Dilepton-$H_T$trigger data and MC yields in the 2010 signal region. MC errors are statistical only.

Sample	ee	$\mu\mu$	$e\mu$	tot
$t\bar{t} \to \ell^+\ell^-$	0.0 ± 0.0	0.1 ± 0.1	0.2 ± 0.1	0.3 ± 0.1
$t\bar{t} \to \ell^\pm\tau^\mp/\tau^+\tau^-$	0.0 ± 0.0	0.1 ± 0.1	0.0 ± 0.0	0.2 ± 0.1
$t\bar{t} \to$ fake	0.0 ± 0.0	0.0 ± 0.0	0.1 ± 0.0	0.1 ± 0.0
DY	0.0 ± 0.0	0.0 ± 0.0	0.0 ± 0.0	0.0 ± 0.0
W^+W^-	0.0 ± 0.0	0.0 ± 0.0	0.0 ± 0.0	0.0 ± 0.0
$W^\pm Z^0$	0.0 ± 0.0	0.0 ± 0.0	0.0 ± 0.0	0.0 ± 0.0
Z^0Z^0	0.0 ± 0.0	0.0 ± 0.0	0.0 ± 0.0	0.0 ± 0.0
single top	0.0 ± 0.0	0.0 ± 0.0	0.0 ± 0.0	0.0 ± 0.0
$W +$ jets	0.0 ± 0.0	0.0 ± 0.0	0.0 ± 0.0	0.0 ± 0.0
tot SM MC	0.0 ± 0.0	0.2 ± 0.1	0.3 ± 0.1	0.6 ± 0.1
data	0	1	0	1
LM1	0.2 ± 0.0	1.6 ± 0.1	1.3 ± 0.1	3.0 ± 0.2
LM3	0.0 ± 0.0	0.2 ± 0.0	0.1 ± 0.0	0.3 ± 0.0

Table 9: Dilepton-H_T trigger data and MC yields in the high y signal region. MC errors are statistical only.

Sample	ee	$\mu\mu$	$e\mu$	tot
$t\bar{t} \to \ell^+\ell^-$	0.0 ± 0.0	0.0 ± 0.0	0.0 ± 0.0	0.0 ± 0.0
$t\bar{t} \to \ell^\pm\tau^\mp/\tau^+\tau^-$	0.0 ± 0.0	0.0 ± 0.0	0.0 ± 0.0	0.0 ± 0.0
$t\bar{t} \to$ fake	0.0 ± 0.0	0.0 ± 0.0	0.0 ± 0.0	0.0 ± 0.0
DY	0.0 ± 0.0	0.0 ± 0.0	0.0 ± 0.0	0.0 ± 0.0
W^+W^-	0.0 ± 0.0	0.0 ± 0.0	0.0 ± 0.0	0.0 ± 0.0
$W^\pm Z^0$	0.0 ± 0.0	0.0 ± 0.0	0.0 ± 0.0	0.0 ± 0.0
Z^0Z^0	0.0 ± 0.0	0.0 ± 0.0	0.0 ± 0.0	0.0 ± 0.0
single top	0.0 ± 0.0	0.0 ± 0.0	0.0 ± 0.0	0.0 ± 0.0
$W +$ jets	0.0 ± 0.0	0.0 ± 0.0	0.0 ± 0.0	0.0 ± 0.0
tot SM MC	0.0 ± 0.0	0.0 ± 0.0	0.0 ± 0.0	0.0 ± 0.0
data	0	0	0	0
LM1	0.1 ± 0.0	0.7 ± 0.1	0.6 ± 0.1	1.3 ± 0.1
LM3	0.0 ± 0.0	0.1 ± 0.0	0.1 ± 0.0	0.1 ± 0.0

Table 10: Dilepton-H_T trigger data and MC yields in the high H_T signal region. MC errors are statistical only.

Sample	ee	$\mu\mu$	$e\mu$	tot
$t\bar{t} \to \ell^+\ell^-$	0.0 ± 0.0	0.0 ± 0.0	0.0 ± 0.0	0.0 ± 0.0
$t\bar{t} \to \ell^\pm\tau^\mp/\tau^+\tau^-$	0.0 ± 0.0	0.0 ± 0.0	0.0 ± 0.0	0.0 ± 0.0
$t\bar{t} \to$ fake	0.0 ± 0.0	0.0 ± 0.0	0.0 ± 0.0	0.0 ± 0.0
DY	0.0 ± 0.0	0.0 ± 0.0	0.0 ± 0.0	0.0 ± 0.0
W^+W^-	0.0 ± 0.0	0.0 ± 0.0	0.0 ± 0.0	0.0 ± 0.0
$W^\pm Z^0$	0.0 ± 0.0	0.0 ± 0.0	0.0 ± 0.0	0.0 ± 0.0
Z^0Z^0	0.0 ± 0.0	0.0 ± 0.0	0.0 ± 0.0	0.0 ± 0.0
single top	0.0 ± 0.0	0.0 ± 0.0	0.0 ± 0.0	0.0 ± 0.0
$W +$ jets	0.0 ± 0.0	0.0 ± 0.0	0.0 ± 0.0	0.0 ± 0.0
tot SM MC	0.0 ± 0.0	0.0 ± 0.0	0.0 ± 0.0	0.0 ± 0.0
data	0	0	0	0
LM1	0.1 ± 0.0	0.6 ± 0.1	0.4 ± 0.1	1.1 ± 0.1
LM3	0.0 ± 0.0	0.1 ± 0.0	0.0 ± 0.0	0.1 ± 0.0

These results are summarized as:

- High p_T dilepton trigger sample
  - 2010 signal region ($y > 8.5$ GeV$^{1/2}$, $H_T > 300$ GeV)
    - observed yield : 14
    - MC prediction : 8.6 ± 0.8
  - high y signal region ($y > 13$ GeV$^{1/2}$, $H_T > 300$ GeV)
    - observed yield : 6
    - MC prediction : 1.3 ± 0.2
  - high H_T signal region ($y > 8.5$ GeV$^{1/2}$, $H_T > 600$ GeV)
    - observed yield : 3
    - MC prediction : 1.2 ± 0.5
- Dilepton-H_T trigger sample
  - 2010 signal region ($y > 8.5$ GeV$^{1/2}$, $H_T > 300$ GeV)
    - observed yield : 1
    - MC prediction : 0.6 ± 0.1
  - high y signal region ($y > 13$ GeV$^{1/2}$, $H_T > 300$ GeV)
    - observed yield : 0
    - MC prediction : 0.0 ± 0.0
  - high H_T signal region ($y > 8.5$ GeV$^{1/2}$, $H_T > 600$ GeV)
    - observed yield : 0
    - MC prediction : 0.0 ± 0.0

For the high p_T dilepton trigger sample, in the 2010 signal region we observe 14 events, representing a slight excess with respect to the MC expectation. This excess is enhanced after moving to the high y signal region, where we find 6 events. In the high H_T region we observe 3 events, representing a slight excess. A data/MC comparison of the kinematic distributions of the 14 events passing the 2010 signal region selection is presented in App. D. For the dilepton-H_T trigger sample we observe 1 event in the 2010 signal region, consistent with MC expectations. We observe no events in either the high y or high H_T signal regions.

For all signal regions, we observe 0 events in the Z mass window, confirming the expectation from MC that the DY background is negligible. We also confirm the MC expectation that the contribution of fake leptons is small, using the data-driven fake rate method. For the high p_T dilepton trigger sample, We find 1 lepton + fakeable object in the 2010 signal region, giving a predicted contribution from fake leptons of 0.6 ± 0.6, consistent with MC expectations. For the high y and high H_T signal regions, we do not observe any lepton + fakeable object events and our data-driven prediction for the fake contributions in these regions is zero. For the dilepton-H_T trigger sample we observe 1 lepton + fakeable object event, leading to a predicted fake contribution of 0.4 ± 0.4, which falls in the high y signal region (but not in the high H_T signal region).

9 Data Driven Background Estimation Methods

For the high p_T dilepton trigger sample, we use 3 data-driven methods to estimate the background in the signal region. The first one exploits the fact that H_T and y are nearly uncorrelated for the $t\bar{t}$ background The second one is based on the fact that in $t\bar{t}$ the p_T of the dilepton pair is on average nearly the same as the p_T of the pair of neutrinos from W-decays, which is reconstructed as $\not{\mathrm{E}}_{\mathrm{T}}^{\mathrm{miss}}$ in the detector. The third method exploits the fact that in $t\bar{t}$ events the rates of same-flavor vs. opposite-flavor dilepton events are the same. For the low lepton p_T events collected by the dilepton-H_T triggers, we use the opposite-flavor subtraction technique.

We study the closure of these methods using our madgraph $t\bar{t}$ sample, as well as the powheg sample TTTo2L2Nu2B_7TeV-powheg-pythia6_Spring11-PU_S1_START311_V1G1-v1 which has approximately 10 times more events in the dilepton channel than the madgraph sample. We use these samples to estimate correction factors and systematic uncertainties for the background predictions. However, the final choice of correction factors and uncertainties will be extracted from the Summer11 $t\bar{t}$ madgraph sample which will have 50 times as many events as the current madgraph sample. For the studies presented in this section, we do not apply trigger efficiency corrections or reweighting for number of reconstructed vertices since are not comparing MC to data.

9.1 ABCD method

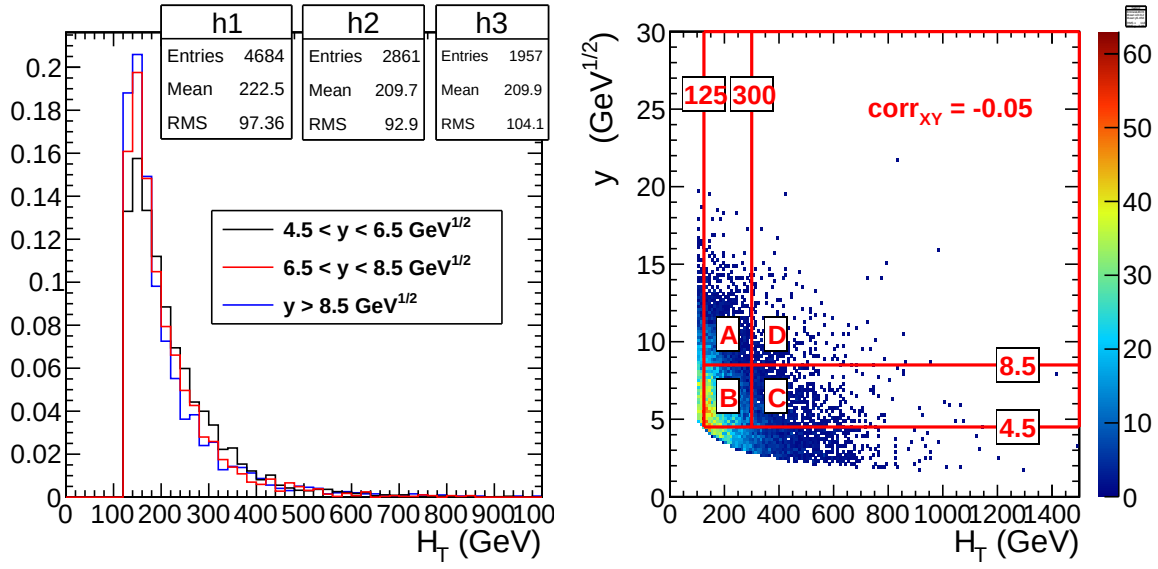

Figure 3: Left: distributions of H_T in MC $t\bar{t}$ events for different intervals of y. h1, h2, and h3 refer to the y intervals 4.5-6.5, 6.5-8.5 and >8.5, respectively. Right: Distributions of y vs. H_T for $t\bar{t}$ MC. Here we also show our choice of ABCD regions. The correlation coefficient $\mathrm{corr_{XY}}$ is computed for events falling in the ABCD regions.

We find that in $t\bar{t}$ events H_T and y are nearly uncorrelated, as demonstrated in Fig. 3 (left). Thus, we can use an ABCD method in the y vs. H_T plane to estimate the background in a data driven way. We define 4 regions in the plane of y vs. H_T, as shown in Fig. 3 (right). The region D is the signal region, and the regions A, B and C are control regions. The predicted background in region D is given by $N_A \times N_C/N_B$.

In Table 11, we quote the $t\bar{t}$ MC expected yields for 1 fb^{-1}. In general we find that the prediction agrees with the observed yield in the signal region within ∼30-50% for all signal regions. We also study the dependence of the ratio of observed to predicted signal yields, as a function of the y and H_T requirements used to define the signal region, shown in Fig. 4. Based on these results, we apply the scale factors and uncertainties summarized in Table 14 to the predicted background from the ABCD method.

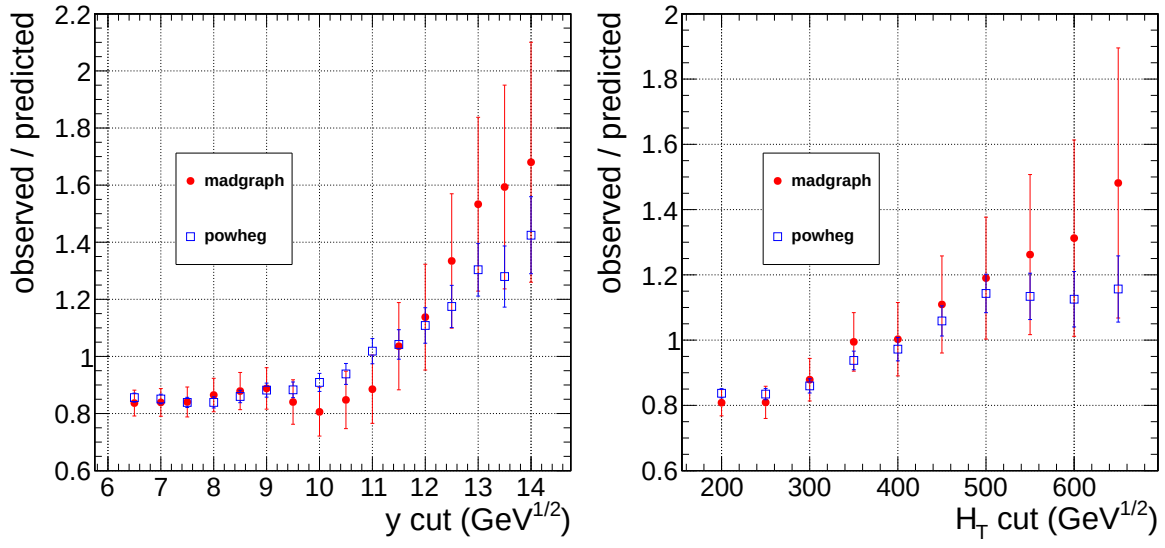

Figure 4: Variation of observed/predicted for the ABCD method as a function of the y and H_T cuts defining the signal region.

Table 11: Expected yields from $t\bar{t}$ MC in 1 fb^{-1} in the four ABCD regions for the signal regions depicted in Figs. 7-9, as well as the predicted yield in region D given by $N_A \times N_C/N_B$ and the ratio of the observed signal yield to the prediction. The quoted uncertainties are statistical only.

signal region	sample	A	B	C	D	$N_A \times N_C/N_B$	obs/pred
2010 signal region	madgraph	251.3 ± 6.1	951.5 ± 11.9	165.2 ± 4.9	38.3 ± 2.4	43.6 ± 1.8	0.88 ± 0.07
	powheg	231.7 ± 2.0	850.6 ± 3.7	157.8 ± 1.6	37.0 ± 0.8	43.0 ± 0.6	0.86 ± 0.02
high y signal region	madgraph	18.4 ± 1.6	951.5 ± 11.9	165.2 ± 4.9	4.9 ± 0.9	3.2 ± 0.3	1.53 ± 0.30
	powheg	17.3 ± 0.5	850.6 ± 3.7	157.8 ± 1.6	4.2 ± 0.3	3.2 ± 0.1	1.30 ± 0.09
high H_T signal region	madgraph	251.3 ± 6.1	951.5 ± 11.9	11.1 ± 1.3	3.8 ± 0.8	2.9 ± 0.3	1.31 ± 0.30
	powheg	231.7 ± 2.0	850.6 ± 3.7	12.5 ± 0.5	3.8 ± 0.3	3.4 ± 0.1	1.13 ± 0.08

9.2 Dilepton p_T method

This method is based on a suggestion by V. Pavlunin [9], and was investigated by our group in 2009 [10] and in our 2010 analysis [3]. The idea is that in dilepton $t\bar{t}$ events the lepton and neutrinos from W decays have the same p_T spectrum (modulo W polarization effects). One can then use the observed $p_T(\ell\ell)$ distribution to model the sum of neutrino p_T's which is identified with the $\not\!\!\mathrm{E}_{\mathrm{T}}^{\mathrm{miss}}$.

Then, in order to predict the $t\bar{t} \rightarrow$ dilepton contribution to a selection with $\not\!\!\mathrm{E}_{\mathrm{T}}^{\mathrm{miss}}$+X, one applies a cut on $p_T(\ell\ell)$+X instead. In practice one has to rescale the result of the $p_T(\ell\ell)$+X selection to account for the fact that any dilepton selection must include a moderate $\not\!\!\mathrm{E}_{\mathrm{T}}^{\mathrm{miss}}$ cut in order to reduce Drell Yan backgrounds. This is discussed in Section 5.3 of Reference [10]; for a $\not\!\!\mathrm{E}_{\mathrm{T}}^{\mathrm{miss}}$ cut of 50 GeV, the rescaling factor is obtained from the MC as

$$K = \frac{\int_0^\infty \mathcal{N}(p_T(\ell\ell))\ \ dp_T(\ell\ell)}{\int_{50}^\infty \mathcal{N}(p_T(\ell\ell))\ \ dp_T(\ell\ell)} = 1.5.$$

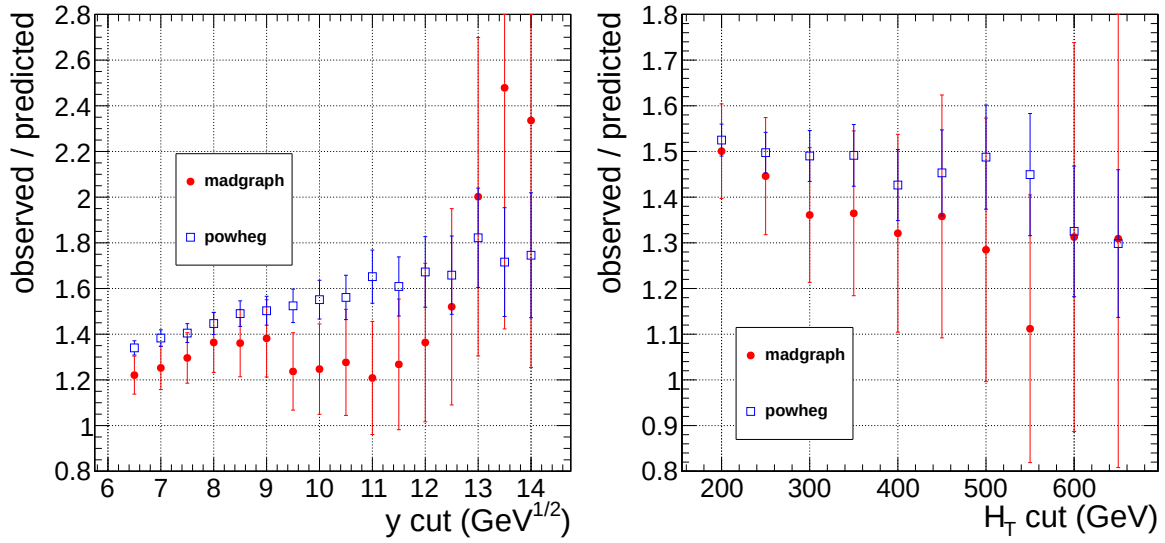

Figure 5: Variation of observed/predicted for the $p_T(\ell\ell)$ method as a function of the y and H_T cuts defining the signal region.

We summarize the expected results of the $p_T(\ell\ell)$ method in 1 fb^{-1} $t\bar{t}$ MC in Table 12, and we show the dependence of observed/predicted vs. the signal region requirements in Fig. 5. Based on these results, we apply the scale factors and uncertainties summarized in Table 14 to the predicted background from the $p_T(\ell\ell)$ method. In [2], we have studied extensively the origin of the excess of observed vs. predicted events from this method. We found that it is due mostly to the W polarization, which results in a harder p_T distribution for the W neutrinos than charged leptons.

Table 12: Expected observed and predicted yields in 1 fb^{-1} for $t\bar{t}$ MC for the $p_T(\ell\ell)$ method applied to the 3 signal regions, and the ratio of the observed signal yield to the prediction. The quoted uncertainties are statistical only.

signal region	sample	predicted	observed	obs/pred
2010 signal region	madgraph	28.2 ± 2.5	38.3 ± 2.4	1.36 ± 0.15
	powheg	24.8 ± 0.8	37.0 ± 0.8	1.49 ± 0.06
high y signal region	madgraph	2.4 ± 0.7	4.9 ± 0.9	2.00 ± 0.70
	powheg	2.3 ± 0.2	4.2 ± 0.3	1.82 ± 0.22
high H_T signal region	madgraph	2.9 ± 0.8	3.8 ± 0.8	1.31 ± 0.43
	powheg	2.9 ± 0.2	3.8 ± 0.3	1.33 ± 0.14

As a validation of the $p_T(\ell\ell)$ method, we also apply the background estimate to the H_T sideband region 125–300 GeV, where we expect the events to be dominated by background and where the higher event yields allow us to test the method with higher statistcal precision. The results of the $p_T(\ell\ell)$ method applied to $t\bar{t}$ MC in the H_T sideband region with the y requirements corresponding to the 2010 signal region ($y > 8.5$ GeV$^{1/2}$) and the high y region

Table 13: Expected observed and predicted yields in 1 fb^{-1} for $t\bar{t}$ MC for the $p_T(\ell\ell)$ method for the control regions in the H_T sideband region $125 < H_T < 300$ GeV, and the ratio of the observed signal yield to the prediction. The quoted uncertainties are statistical only, assuming Gaussian errors.

control region	sample	predicted	observed	obs/pred
$125 < H_T < 300$ GeV, $y > 8.5$ GeV$^{1/2}$	madgraph	35.8 ± 1.3	51.3 ± 1.2	1.43 ± 0.06
	powheg	33.4 ± 0.4	47.3 ± 0.4	1.42 ± 0.02
$125 < H_T < 300$ GeV,$y > 13$ GeV$^{1/2}$	madgraph	3.4 ± 0.4	4.4 ± 0.4	1.29 ± 0.19
	powheg	3.3 ± 0.1	4.1 ± 0.1	1.23 ± 0.06

($y > 13$ GeV$^{1/2}$) are given in Table 13. Based on these results we will apply a correction factor $K_C = 1.4 \pm 0.1$ ($K_C = 1.2 \pm 0.1$) to data for the loose (tight) y requirements in the H_T sideband region.

Table 14: Summary of correction factors and systematic uncertainties for the ABCD and $p_T(\ell\ell)$ methods in the 3 signal regions.

signal region	ABCD	$p_T(\ell\ell)$
2010 signal region	1.0 ± 0.2	1.4 ± 0.2
high y signal region	1.3 ± 0.3	1.7 ± 0.3
high H_T signal region	1.2 ± 0.2	1.3 ± 0.2

9.3 Opposite-Flavor Subtraction

The opposite-flavor subtraction technique exploits the fact that in $t\bar{t}$, the flavor of the 2 leptons from W decay are uncorrelated. Hence we expect equal rates of same-flavor (SF) ee or $\mu\mu$ vs. opposite-flavor (OF) $e\mu$ lepton pairs. In SUSY, the lepton flavors may be correlated, producing an excess of SF over OF events. We use the observed yield in the OF final state to predict the yields in the SF final state according to:

$$N(ee) = \frac{1}{2R_{\mu e}} N(e\mu) \text{ and } N(\mu\mu) = \frac{R_{\mu e}}{2} N(e\mu)$$

where $R_{\mu e}$ is the ratio of muon to electron selection efficiencies. This quantity is evaluated by taking the ratio of the number of observed $Z \to \mu^+\mu^-$ to $Z \to e^+e^-$ events, in the mass range 76-106 GeV with no jets or $\mathrm{E_T^{miss}}$ requirements (see Fig. 2). Alternatively, we can quantify the excess of SF vs. OF events with the quantity:

$$\Delta = R_{\mu e} N(ee) + \frac{1}{R_{\mu e}} N(\mu\mu) - N(e\mu), \quad (1)$$

which is predicted to be 0 for processes with uncorrelated lepton flavors. In order for this technique to work, the kinematic selection applied to events in all dilepton flavor channels must be the same, which is not the case for our default selection because the Z mass veto is applied only to same-flavor channels. Therefore when applying the OF subtraction technique we also apply the Z mass veto also to the $e\mu$ channel.

We will apply this technique to both the high p_T dilepton trigger and dilepton-H_T trigger data samples. In the following, we first apply the technique to $t\bar{t}$ MC with high p_T leptons, and then to $t\bar{t}$ MC with low p_T leptons.

9.3.1 OF subtraction: Application to high p_T lepton sample

We begin by applying the OF subtraction technique to $t\bar{t}$ MC with leptons passing $p_T > (20,10)$ GeV. Here we extract $R_{e\mu}$ by taking the ratio of $Z \to \mu^+\mu^-$ vs. $Z \to e^+e^-$ events in the window 76–106 GeV in DY MC. For data, we have verified that the contribution from fake leptons in the high lepton p_T signal regions is small using the data-driven fake rate method, hence we do not need to correct for fake leptons here. The results are summarized in Table 15, where we find values of Δ consistent with 0, as expected.

9.3.2 OF subtraction: Application to low p_T lepton sample

In this section, we apply the OF subtraction technique to $t\bar{t}$ MC with leptons passing $p_T > (10,5)$ GeV but not passing $p_T > (20,10)$ GeV (in order to remove overlap with the high lepton p_T sample). The OF subtraction in the low lepton p_T regime is complicated by 2 factors:

Table 15: Expected yields in 1 fb^{-1} $t\bar{t}$ MC for the OF subtraction method, and the quantity Δ, defined in Eq. 1. The quoted systematic uncertainty refers to that of $R_{\mu e}$.

region	sample	$N(ee)$	$N(\mu\mu)$	$N(e\mu)$	Δ
preselection region	madgraph	431.1 $\pm$ 8.0	531.3 $\pm$ 8.9	945.8 $\pm$ 11.8	11.8 $\pm$ 16.8 (stat) $\pm$ 1.1 (syst)
	powheg	383.1 $\pm$ 2.5	492.9 $\pm$ 2.9	876.2 $\pm$ 3.8	-7.0 $\pm$ 5.4 (stat) $\pm$ 0.8 (syst)
2010 signal region	madgraph	7.4 $\pm$ 1.0	10.7 $\pm$ 1.3	14.5 $\pm$ 1.5	3.3 $\pm$ 2.2 (stat) $\pm$ 0.04 (syst)
	powheg	7.2 $\pm$ 0.3	8.6 $\pm$ 0.4	16.8 $\pm$ 0.5	-1.1 $\pm$ 0.7 (stat) $\pm$ 0.03 (syst)

- The ratio of muon to electron selection efficiencies $R_{\mu e}$ increases significantly at low p_T, due to a drop in the electron selection efficiency.
- We reconstruct muons down to $p_T > 5$ GeV but electrons only to $p_T > 10$ GeV.

Our strategy is the following:

- Evaluate $R_{\mu e}$ from $t\bar{t}$ MC.
- Parameterize $R_{\mu e}$ as a function of lepton p_T. For now we split in 2 bins, $10 < p_T < 20$ GeV and $p_T > 20$ GeV.
- For data, we will apply to $R_{\mu e}$ a trigger efficiency correction and subtract the expected contribution from fake leptons from the data-driven fake rate method (but neither correction is performed for the MC studies in this section).
- We first apply the OF subtraction to the preselection region, and then to the signal region.

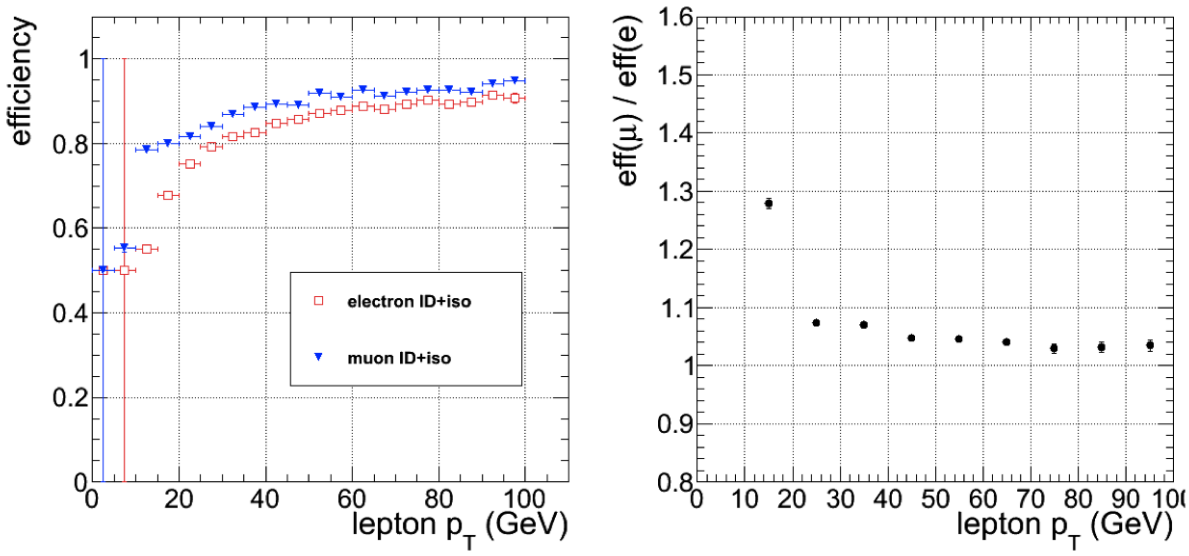

Figure 6: Left: the electron and muon selection efficiencies, as a function of lepton p_T, extracted from $t\bar{t}$ MC. Right: the ratio $R_{\mu e}$ of muon to electron selection efficiencies as a function of lepton p_T.

We begin by examining the dependence of $R_{\mu e}$ on lepton p_T, as shown in Fig. 6. We find that $R_{\mu e}$ increases in the region p_T 10–20 GeV, but is roughly constant for $p_T > 20$ GeV. Hence we take $R_{\mu e}^{10-20} = 1.28$ for p_T 10–20 GeV and $R_{\mu e}^{>20} = 1.08$ for $p_T > 20$ GeV, and assign a 5% systematic uncertainty.

Next, to take into account the fact the electrons and muons have a different p_T range, we split the low p_T sample into events with leptons passing $p_T >$ (10,10) GeV, denoted in the following as (10,10), and events with leptons passing $p_T >$ (10,5) GeV but not passing $p_T >$ (10,10) GeV, denoted in the following as (10,5). We find the following relations, expected for backgrounds with uncorrelated lepton flavors:

- $N(ee)(10,10) = 1/(2R_{\mu e}^{10-20})N(e\mu)(10,10)$
- $N(\mu\mu)(10,10) = (R_{\mu e}^{10-20}/2)N(e\mu)(10,10)$
- $N(\mu\mu)(10,5) = R_{\mu e}^{>20}N(e\mu)(10,5)$

Note that for (10,10) events, both leptons are in the range p_T 10–20 GeV, hence the relevant efficiency ratio is $R_{\mu e}^{10-20}$. For (10,5) events, both ee and $\mu\mu$ events have a muon with p_T 5–10 GeV and an additional lepton with $p_T > 10$ GeV. In most cases the leading lepton has $p_T > 20$ GeV, hence we use $R_{\mu e}^{>20}$ for these events.

In this case we find the following expression for Δ, quantifying the excess of SF vs. OF yields:

$$\Delta = R_{\mu e}^{10-20}N(ee)(10,10) + 1/R_{\mu e}^{10-20}N(\mu\mu)(10,10) + 1/R_{\mu e}^{>20}N(\mu\mu)(10,5) - N(e\mu)(10,10) - N(e\mu)(10,5) \quad (2)$$

In Table 16 we apply this technique to $t\bar{t}$ MC. As expected, we find Δ consistent with 0.

Table 16: Expected yields in 1 fb^{-1} $t\bar{t}$ MC for the OF subtraction method in the low lepton p_T regime, and the quantity Δ, defined in Eq. 2. The quoted systematic uncertainty refers to that of $R_{\mu e}$.

region	sample	$N(ee)(10,10)$	$N(\mu\mu)(10,10)$	$N(e\mu)(10,10)$	$N(\mu\mu)(10,5)$	$N(e\mu)(10,5)$	Δ
preselection region	madgraph	3.4 ± 0.7	4.9 ± 0.9	6.4 ± 1.0	22.9 ± 1.8	18.2 ± 1.6	4.8 ± 2.8 (stat) $\pm$ 1.0 (syst)
	powheg	2.5 ± 0.2	4.4 ± 0.3	7.0 ± 0.3	19.0 ± 0.6	16.6 ± 0.5	0.6 ± 0.9 (stat) $\pm$ 0.9 (syst)
2010 signal region	madgraph	0.0 ± 0.0	0.4 ± 0.3	0.6 ± 0.3	1.0 ± 0.4	0.7 ± 0.3	-0.0 $\pm$ 0.6 (stat) $\pm$ 0.1 (syst)
	powheg	0.1 ± 0.0	0.2 ± 0.1	0.4 ± 0.1	1.4 ± 0.2	1.1 ± 0.1	0.1 ± 0.2 (stat) $\pm$ 0.1 (syst)

10 Results

10.1 Background estimate from the ABCD method

The data yields in the four regions are summarized in Tables 17-19 for the 3 signal regions. The ABCD background prediction $N_A \times N_C/N_B$ is scaled by the correction factors determined in Sec. 9, as summarized in Table 14. The results of the ABCD predictions are summarized in Table 20.

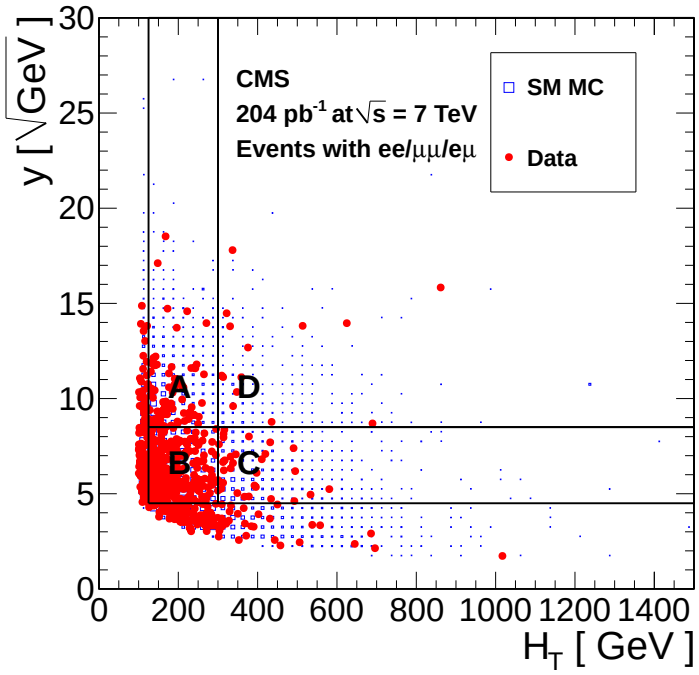

Figure 7: Distributions of y vs. H_T for SM Monte Carlo and data. The 2010 signal region boundaries are overlayed.

Table 17: Data yields in the four regions of Figure 7 for the 2010 signal region, as well as the predicted yield in region D given by A $\times$ C / B. The quoted uncertainty on the prediction in data is statistical only, assuming Gaussian errors. We also show the SM Monte Carlo expectations with statistical errors only.

sample	A	B	C	D	A $\times$ B / C
$t\bar{t}$	48.8 ± 1.4	184.1 ± 2.7	31.9 ± 1.1	7.3 ± 0.5	8.5 ± 0.4
DY	0.5 ± 0.4	8.2 ± 1.5	0.7 ± 0.5	1.0 ± 0.6	0.0 ± 0.0
W^+W^-	0.6 ± 0.1	1.6 ± 0.1	0.1 ± 0.0	0.2 ± 0.0	0.1 ± 0.0
$W^\pm Z^0$	0.1 ± 0.0	0.3 ± 0.0	0.0 ± 0.0	0.0 ± 0.0	0.0 ± 0.0
Z^0Z^0	0.0 ± 0.0	0.1 ± 0.0	0.0 ± 0.0	0.0 ± 0.0	0.0 ± 0.0
single top	1.9 ± 0.1	5.6 ± 0.2	0.2 ± 0.0	0.1 ± 0.0	0.1 ± 0.0
W + jets	0.6 ± 0.6	1.2 ± 0.6	0.0 ± 0.0	0.0 ± 0.0	0.0 ± 0.0
Total SM MC	52.6 ± 1.6	201.2 ± 3.2	33.1 ± 1.2	8.6 ± 0.8	8.6 ± 0.4
data	72	238	29	14	8.8 ± 2.0

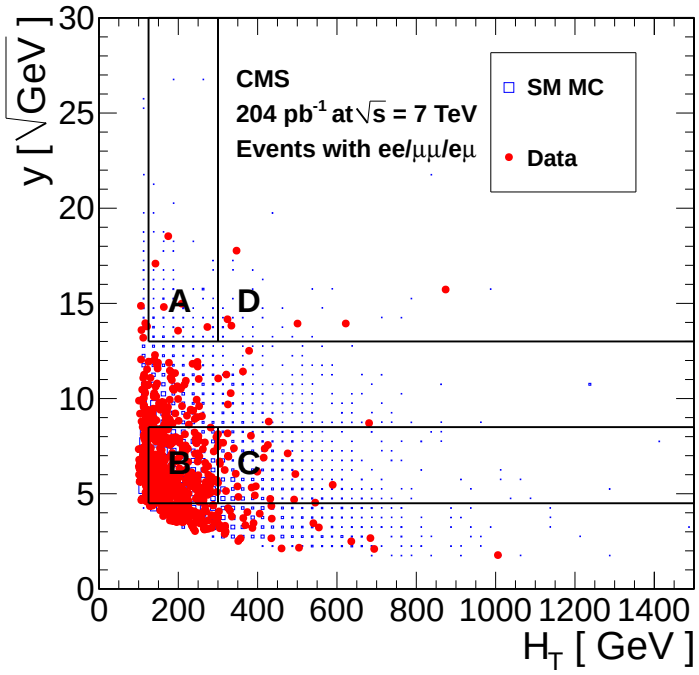

Figure 8: Distributions of y vs. H_T for SM Monte Carlo and data. The high y signal region boundaries are overlayed.

Table 18: Data yields in the four regions of Figure 8 for the high y signal region, as well as the predicted yield in region D given by A $\times$ C / B. The quoted uncertainty on the prediction in data is statistical only, assuming Gaussian errors. We also show the SM Monte Carlo expectations with statistical uncertainties.

sample	A	B	C	D	A $\times$ B / C
$t\bar{t}$	3.6 ± 0.4	184.1 ± 2.7	31.9 ± 1.1	1.2 ± 0.2	0.6 ± 0.1
DY	0.3 ± 0.3	8.2 ± 1.5	0.7 ± 0.5	0.0 ± 0.0	0.0 ± 0.0
W^+W^-	0.1 ± 0.0	1.6 ± 0.1	0.1 ± 0.0	0.1 ± 0.0	0.0 ± 0.0
$W^\pm Z^0$	0.0 ± 0.0	0.3 ± 0.0	0.0 ± 0.0	0.0 ± 0.0	0.0 ± 0.0
Z^0Z^0	0.0 ± 0.0	0.1 ± 0.0	0.0 ± 0.0	0.0 ± 0.0	0.0 ± 0.0
single top	0.2 ± 0.0	5.6 ± 0.2	0.2 ± 0.0	0.0 ± 0.0	0.0 ± 0.0
W + jets	0.0 ± 0.0	1.2 ± 0.6	0.0 ± 0.0	0.0 ± 0.0	0.0 ± 0.0
Total SM MC	4.1 ± 0.5	201.2 ± 3.2	33.1 ± 1.2	1.3 ± 0.2	0.7 ± 0.1
data	6	238	29	6	0.7 ± 0.3

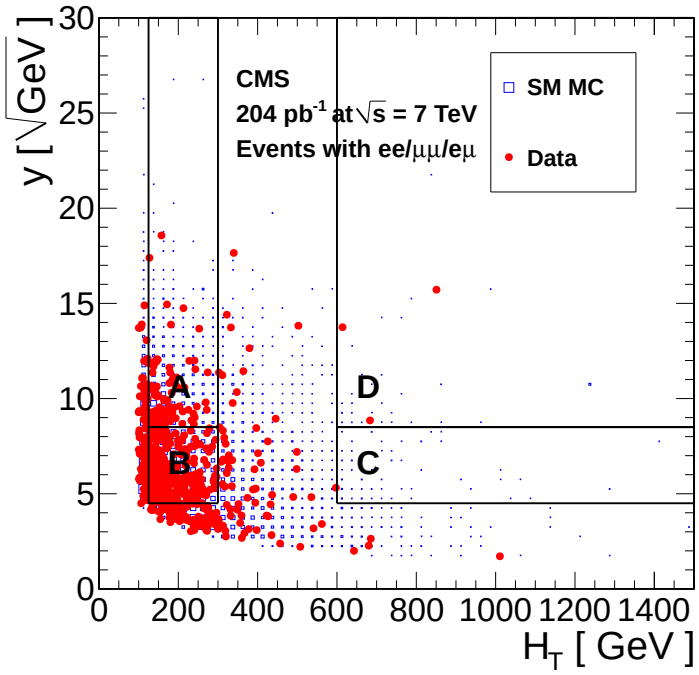

Figure 9: Distributions of y vs. H_T for SM Monte Carlo and data. The high H_T signal region boundaries are overlayed.

Table 19: Data yields in the four regions of Figure 9 for the high H_T signal region, as well as the predicted yield in region D given by A $\times$ C / B. The quoted uncertainty on the prediction in data is statistical only, assuming Gaussian errors. Since the yield in region C is 0, we assess as the uncertainty the prediction corresponding to 1 observed event in 1. We also show the SM Monte Carlo expectations with statistical uncertainties.

sample	A	B	C	D	A $\times$ B / C
ttall	48.8 ± 1.4	184.1 ± 2.7	2.2 ± 0.3	0.7 ± 0.2	0.6 ± 0.1
DY	0.5 ± 0.4	8.2 ± 1.5	0.0 ± 0.0	0.4 ± 0.4	0.0 ± 0.0
WW	0.6 ± 0.1	1.6 ± 0.1	0.0 ± 0.0	0.0 ± 0.0	0.0 ± 0.0
WZ	0.1 ± 0.0	0.3 ± 0.0	0.0 ± 0.0	0.0 ± 0.0	0.0 ± 0.0
ZZ	0.0 ± 0.0	0.1 ± 0.0	0.0 ± 0.0	0.0 ± 0.0	0.0 ± 0.0
t	1.9 ± 0.1	5.6 ± 0.2	0.0 ± 0.0	0.0 ± 0.0	0.0 ± 0.0
wjets	0.6 ± 0.6	1.2 ± 0.6	0.0 ± 0.0	0.0 ± 0.0	0.0 ± 0.0
Total SM MC	52.6 ± 1.6	201.2 ± 3.2	2.2 ± 0.3	1.2 ± 0.5	0.6 ± 0.1
data	72	238	0	3	0.0 ± 0.3

Table 20: Summary of results of the ABCD method, applied to the 3 signal regions.

Signal Region	$N_A \times N_C/N_B$	correction factor	prediction
2010 signal region	8.8 ± 2.0	1.0 ± 0.2	8.8 ± 2.0 (stat) $\pm$ 1.8 (syst)
high y signal region	0.7 ± 0.3	1.3 ± 0.2	0.9 ± 0.4 (stat) $\pm$ 0.2 (syst)
high H_T signal region	0.0 ± 0.3	1.2 ± 0.2	0.0 ± 0.4 (stat) $\pm$ 0.1 (syst)

10.2 Background estimate from the $P_T(\ell\ell)$ method

Table 21: Summary of results of the dilepton p_T template method applied to the 3 signal regions. The quantities indicated in the table are discussed in the text. The quoted statistical uncertainty in the prediction N_P is due to that of $N(D')$, the quoted systematic uncertainty includes that of $N(DY)$ and K_C.

Signal Region	$N(D')$	$N(DY)$	K	K_C	N_P
2010 signal region	3	0.4 ± 0.3	1.5	1.4 ± 0.2	5.5 ± 3.6 (stat) $\pm$ 1.0 (syst)
high y signal region	2	0.1 ± 0.1	1.5	1.7 ± 0.3	4.8 ± 3.6 (stat) $\pm$ 0.9 (syst)
high H_T signal region	0	0.0 ± 0.1	1.3	1.3 ± 0.2	0.0 ± 1.7 (stat) $\pm$ 0.3 (syst)

For each signal region D, we count the number of events falling in the region D', which is defined using the same requirements as D but switching the y requirement to a $p_T(\ell\ell)/\sqrt{H_T}$ requirement. We subtract off the expected DY contribution using the data-driven $R_{out/in}$ technique, using $R_{out/in} = 0.13 \pm 0.07$. We then scale this yield by 2 corrections factors: K, the $\mathrm{E_T^{miss}}$ acceptance correction factor, and K_C, the correction factor determined in Sec. 9. Our final prediction N_P is given by:

$$N_P = (N(D') - N(DY)) \times K \times K_C,$$

as summarized in Table 21, and displayed in Figs. 10-12. Note that we currently extract K from MC, and verify that it is consistent with the value extracted from data. We may instead use K extracted from data in the future, as the data sample increases and the statistical uncertainty in K decreases. We also perform the $p_T(\ell\ell)$ method in the H_T sideband region 125–300 GeV, as a validation of the technique in a high statistics sample which is expected to be dominated by background. The results are summarized in Table 22. For both the loose ($y > 8.5$ GeV$^{1/2}$) and tight ($y > 13$ GeV$^{1/2}$) control regions, the observed yields are consistent with the predictions from the $p_T(\ell\ell)$ method.

Table 22: Summary of results of the dilepton p_T template method applied to the H_T sideband control region 125–300 GeV. The quantities indicated in the table are discussed in the text. The quoted statistical uncertainty in the prediction N_P is due to that of $N(D')$, the quoted systematic uncertainty includes that of $N(DY)$ and K_C. The predictions are compare with the observed yield N_O.

Control Region	$N(D')$	$N(DY)$	K	K_C	N_P	N_O
$125 < H_T < 300$ GeV, $y > 8.5$ GeV$^{1/2}$	32	1.7 ± 0.9	1.7	1.4 ± 0.1	71 ± 13 (stat) $\pm$ 5.5 (syst)	72
$125 < H_T < 300$ GeV, $y > 13$ GeV$^{1/2}$	5	0.5 ± 0.3	1.7	1.2 ± 0.1	9.0 ± 4.5 (stat) $\pm$ 1.0 (syst)	6

10.3 Background estimate from OF subtraction

The results of the OF subtraction technique applied to the high p_T dilepton trigger sample are summarized in Table 23. We evaluate the quantity $\Delta = R_{\mu e}N(ee) + \frac{1}{R_{\mu e}}N(\mu\mu) - N(e\mu)$ with $R_{\mu e} = 1.12 \pm 0.05$ extracted from the ratio of $Z \to \mu^+\mu^-$ vs. $Z \to e^+e^-$ events in data. We perform the OF subtraction first in the preselection region, and find Δ consistent with 0, as expected. We then perform the OF subtraction in all 3 signal regions, and do not observe any excess of same-flavor vs. opposite-flavor events.

For the dilepton-H_T trigger sample, we observe only 1 event in the 2010 signal region, consistent with MC expectations, and no events in either the high y or high H_T signal regions. In the case of an excess of events at low lepton p_T, we will perform the OF subtraction technique of Sec. 9.3.2.

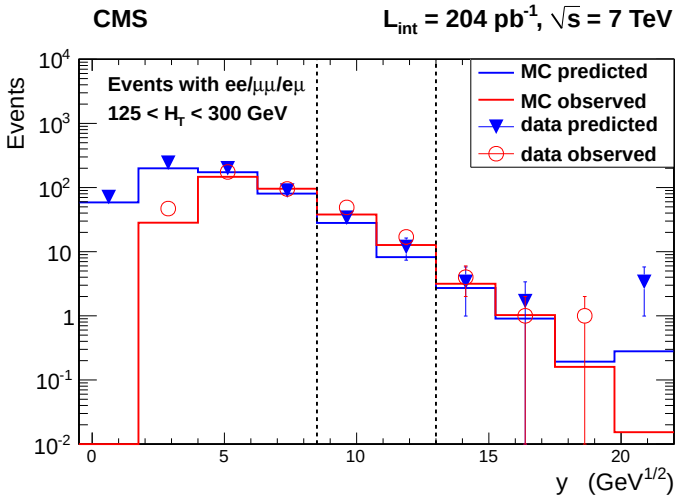

Figure 10: Distributions of $p_T(\ell\ell)/\sqrt{H_T}$ (predicted) and y (observed) for SM MC and data, for the H_T sideband region 125–300 GeV. The vertical dashed lines indicate the loose ($y > 8.5$ GeV$^{1/2}$) and tight ($y > 13$ GeV$^{1/2}$) control regions.

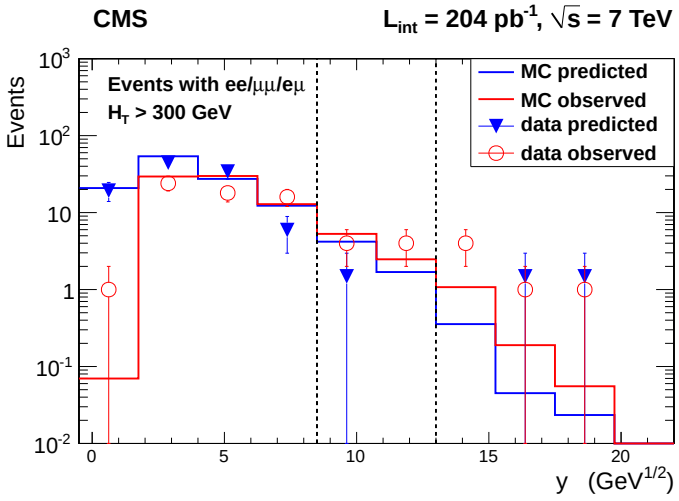

Figure 11: Distributions of $p_T(\ell\ell)/\sqrt{H_T}$ (predicted) and y (observed) for SM MC and data, for the region $H_T>$ 300 GeV. The vertical dashed lines indicate the 2010 signal region ($y > 8.5$ GeV$^{1/2}$) and high y signal region ($y > 13$ GeV$^{1/2}$).

10.4 Summary of results

A summary of our results is presented in Table 24. We observe a slight excess of events with respect to MC and data-driven predictions in our loose 2010 signal region. The excess with respect to MC and ABCD predictions is enhanced after tightening the y requirement, but the observed yield shows no significant excess with respect to the $p_T(\ell\ell)$ method prediction. There is also a slight excess of events with respect to MC and data-driven predictions for the high H_T signal region. We do not observe any excess of same-flavor vs. opposite-flavor events.

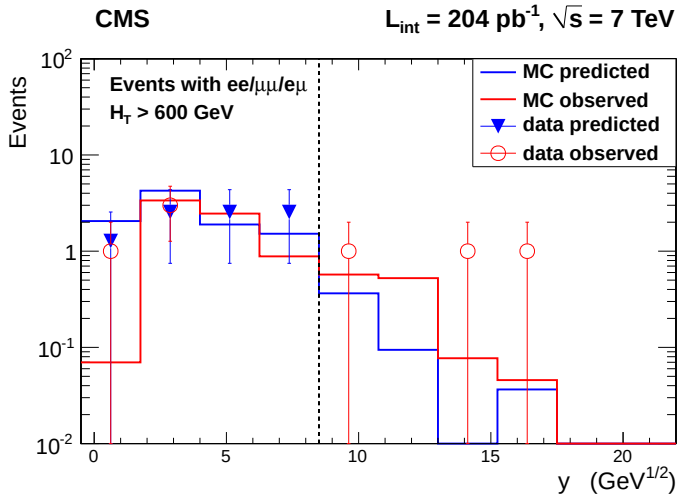

Figure 12: Distributions of $p_T(\ell\ell)/\sqrt{H_T}$ (predicted) and y (observed) for SM MC and data, for the region $H_T >$ 600 GeV. The vertical dashed line indicates the high H_T signal region.

Table 23: Summary of results for the OF subtraction technique. The quantity $\Delta = R_{\mu e}N(ee) + \frac{1}{R_{\mu e}}N(\mu\mu) - N(e\mu)$ is quoted with $R_{\mu e} = 1.12 \pm 0.05$. The quoted systematic uncertainty corresponds to that of $R_{\mu e}$. The $e\mu$ yields differ from those previously quoted because the Z mass veto is included here.

region	$N(ee)$	$N(\mu\mu)$	$N(e\mu)$	Δ
preselection region	113	122	258	-22.5 $\pm$ 22.3 (stat) $\pm$ 0.8 (syst)
2010 signal region	4	3	5	2.2 $\pm$ 3.5 (stat) $\pm$ 0.1 (syst)
high y signal region	3	0	2	1.4 $\pm$ 2.4 (stat) $\pm$ 0.1 (syst)
high H_T signal region	1	0	1	0.1 $\pm$ 1.5 (stat) $\pm$ 0.0 (syst)

Table 24: Summary of the observed and predicted yields in the 3 signal regions. MC errors are statistical only. The systematic uncertainty on the ABCD and $p_T(\ell\ell)$ method is from the scaling factors from MC closure only. For the OF subtraction, the quantity $\Delta = R_{\mu e}N(ee) + \frac{1}{R_{\mu e}}N(\mu\mu) - N(e\mu)$ is quoted; the systematic uncertainty here is from the ratio of muon to electron selection efficiencies.

	2010 signal region	high y signal region	high H_T signal region
Observed yield	14	6	3
MC prediction	8.6 $\pm$ 0.8	1.3 $\pm$ 0.2	1.2 $\pm$ 0.5
ABCD prediction	8.8 $\pm$ 2.0 (stat) $\pm$ 1.8 (syst)	0.9 $\pm$ 0.4 (stat) $\pm$ 0.2 (syst)	0.0 $\pm$ 0.4 (stat) $\pm$ 0.1 (syst)
$p_T(\ell\ell)$ prediction	5.5 $\pm$ 3.6 (stat) $\pm$ 1.0 (syst)	4.8 $\pm$ 3.6 (stat) $\pm$ 0.9 (syst)	0.0 $\pm$ 1.7 (stat) $\pm$ 0.3 (syst)
OF subtraction (Δ)	2.2 $\pm$ 3.5 (stat) $\pm$ 0.1 (syst)	1.4 $\pm$ 2.4 (stat) $\pm$ 0.1 (syst)	0.1 $\pm$ 1.5 (stat) $\pm$ 0.0 (syst)

References

[1] ADD REF TO MET TEMPLATES NOTE, WHEN AVAILABLE

[2] CMS AN-2010/370

[3] arXiv:1103.1348v1 [hep-ex], "Search for Physics Beyond the Standard Model in Opposite-Sign Dilepton Events at $\sqrt{s} = 7$ TeV."

[4] Phys.Lett.B695:424-443,2011

[5] https://twiki.cern.ch/twiki/bin/viewauth/CMS/SimpleCutBasedEleID

[6] D. Barge *at al.*, AN-CMS2009/159.

[7] CMS AN-2011/155

[8] https://twiki.cern.ch/twiki/bin/view/CMS/ProductionReProcessingSpring10

[9] V. Pavlunin, Phys. Rev. **D81**, 035005 (2010).

[10] D. Barge *at al.*, AN-CMS2009/130.

[11] W. Andrews *et al.*, AN-CMS2009/023.

[12] D. Barge *at al.*, AN-CMS2010/257.

[13] W. Andrews *et al.*, AN-CMS2010/274.

[14] J. Conway, `http://www-cdf.fnal.gov/physics/statistics/code/bayes.f`.

[15] G. Landsberg, `https://twiki.cern.ch/twiki/pub/CMS/EXOTICA/cl95cms.c`

[16] `https://hypernews.cern.ch/HyperNews/CMS/get/susy/617/2/1.html`

[17] `https://twiki.cern.ch/twiki/bin/view/CMS/SUSY38XSUSYScan`

[18] arXiv:hep-ph/0605240v2

[19] `CleanExclusion.cc` available at `https://twiki.cern.ch/twiki/bin/viewauth/CMS/SUSYLimitTools`

[20] R. Cousins, `http://www.physics.ucla.edu/c̃ousins/stats/cousins_lognormal_prior.pdf`

[21] S. Harper, private communication (relayed to us by M. Chiorboli.).

[22] A. Barr *at al.*, J.Phys.G29:2343-2363,2003; Cheng, H.C., Han, arXiv:hep-ph/0810.5178v2.
`http://indico.cern.ch/contributionDisplay.py?contribId=3&confId=66410`

[23] `http://indico.cern.ch/contributionDisplay.py?contribId=5&confId=93837`

[24] M. Narain *et al.*, CMS AN-2010/259; we thank the Brown group for providing their code to us.

Appendix A Fakeable Object Definitions

We estimate the contributions from leptons not originating from W/Z decay (fake leptons) using the data-driven fake rate method [4]. We define the following 'fakeable object' selections, by taking the electron and muon requirements listed in Sec. 3 and loosening the following requirements:

- electrons
  - $d_0 < 0.2$ cm
  - $Iso \equiv E_T^{\rm iso}/p_T < 0.4$, $E_T^{\rm iso}$ is defined as the sum of transverse energy/momentum deposits in ecal, hcal, and tracker, in a cone of 0.3 A 1 GeV pedestal is subtracted from the ecal energy deposition in the EB, however the ecal energy is never allowed to go negative.
- muons
  - $d_0 < 0.2$ cm
  - χ^2/ndof of global fit < 50
  - $Iso \equiv E_T^{\rm iso}/p_T < 0.4$, $E_T^{\rm iso}$ is defined as the sum of transverse energy/momentum deposits in ecal, hcal, and tracker, in a cone of 0.3

Appendix B The ABCD' Technique

We have developed a novel technique, based on the ABCD technique which we perform in the plane of y vs. H_T, which allows us to estimate the background in a signal region defined in the $\mathrm{E_T^{miss}}$ vs. H_T plane. We refer to this as the ABCD' technique.

First, we extract the y and H_T distributions $f(y)$ and $g(H_T)$ from data, using events from control regions which we expect to be dominated by background. Under the assumption that y and H_T are weakly-correlated (the same assumption which allows the use of the ABCD technique), we can predict the distribution of events in the y vs. H_T plane as:

$$\frac{\partial^2 N}{\partial y \partial H_T} = f(y)g(H_T) \tag{3}$$

Once the distribution of events in the y vs. H_T plane is known, the number of events falling in any region of this plane can be deduced. In particular, we can deduce the number of events falling in a region defined by requirements on $\mathrm{E_T^{miss}}$ and H_T.

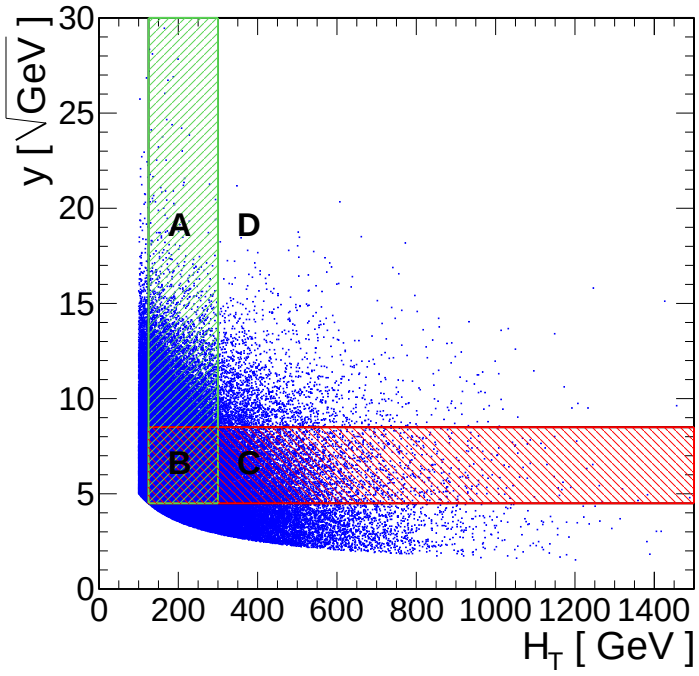

Figure 13: Distributions of y vs. H_T for $t\bar{t}$ MC. The $f(y)$ and $g(H_T)$ functions are measured using events in the green and red shaded areas, respectively.

In this section, we study the ABCD' technique by applying it to $t\bar{t}$ MC (we use the powheg sample which has 10 times the number of dilepton events as the madgraph sample). As a cross-check, we first use the ABCD' technique to estimate the background in the 2010 signal region defined as $y > 8.5$ GeV$^{1/2}$ and $H_T > 300$ GeV, which may be compared to the prediction of the standard ABCD technique. We measure the $f(y)$ and $g(H_T)$ distributions using events in the regions indicated in Fig. 13, yielding the distributions shown in Fig. 14. Next, we randomly sample values of y and H_T from these distributions; each pair of y and H_T values is a pseudo-event. We generate 1 million pseudo-events, and find the ratio $R_{S/C}$, the ratio of the number of pseudo-events falling in the 2010 signal region (ie. region D) to the number of pseudo-events falling in a control region, defined as the OR of the A, B and C regions. We then multiply this ratio by the number of $t\bar{t}$ MC events which fall in the control region to get the predicted yield, ie. $N_{pred} = R_{S/C} \times N(\mathrm{control})$. The results are summarized in Table 25, which show that the prediction of the ABCD' method is consistent with that of the ABCD method within the statistical uncertainty.

We next apply the ABCD' technique to estimate the background in the regions:

- SR1: $\mathrm{E_T^{miss}} > 275$ GeV, $H_T > 300$ GeV

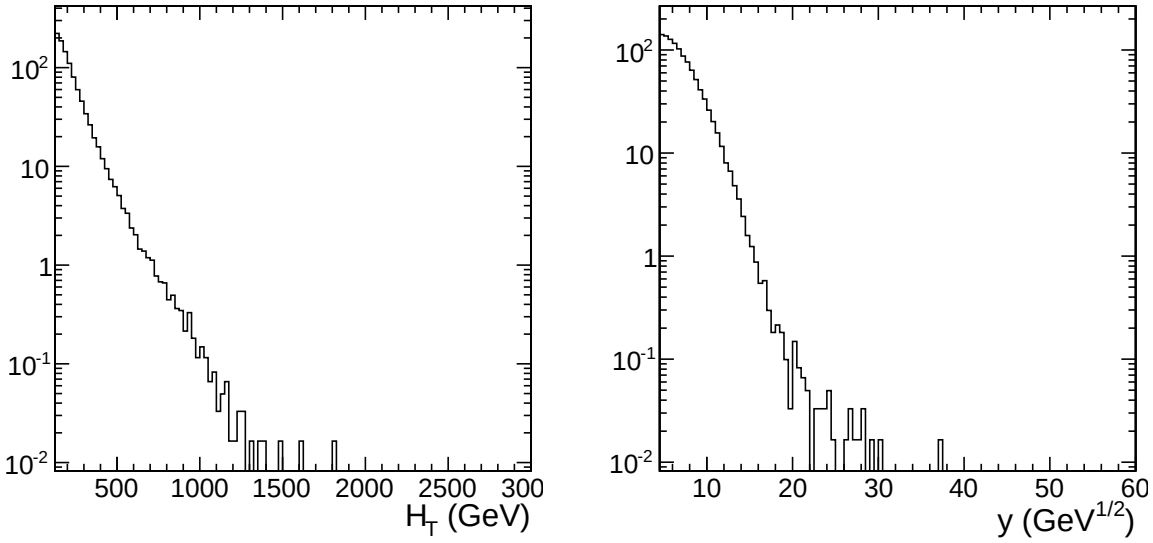

Figure 14: The distributions $f(y)$ and $g(H_T)$ extracted from $t\bar{t}$ MC.

- SR2: $\mathrm{E_T^{miss}} > 200$ GeV, $H_T > 600$ GeV.

Note that we are unable to predict the yield in this region using the standard ABCD technique, since $\mathrm{E_T^{miss}}$ and H_T are not weakly correlated. The signal regions are shown in Fig. 15. There is a sizable overlap between SR2 and region C, hence when estimating the background for this signal region we restrict the control region used to measure $g(H_T)$ and to determine $N(\mathrm{control})$ to $4.5 < y < 6.5$ GeV$^{1/2}$. As summarized in Table 25, we find agreement between the observed and predicted yields in these signal regions within $(25 \pm 8)\%$ and $(3 \pm 5)\%$ for SR1 and SR2, respectively.

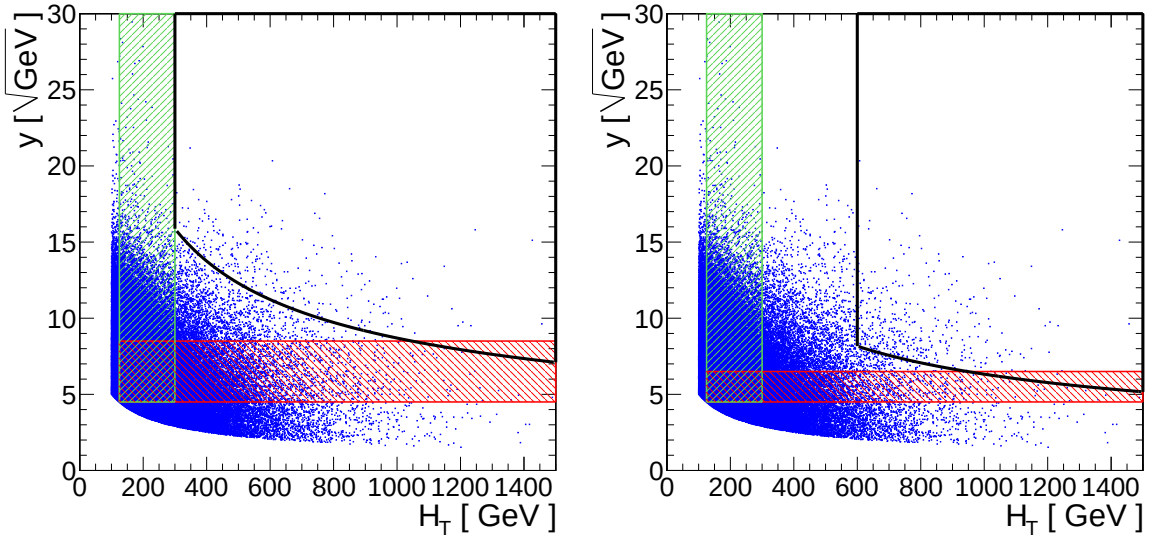

Figure 15: Distributions of y vs. H_T for $t\bar{t}$ MC. The signal regions $\mathrm{E_T^{miss}} > 275$ GeV, $H_T > 300$ GeV (left) and $\mathrm{E_T^{miss}} > 200$ GeV, $H_T > 600$ GeV (right) are indicated with thick black lines. The $f(y)$ and $g(H_T)$ functions are measured using events in the green and red shaded areas, respectively.

Table 25: Summary of results expected results of the ABCD' method for 1 fb^{-1} using $t\bar{t}$ MC. The quantities $R_{S/C}$ and $N(\mathrm{control})$ are discussed in the text. The prediction of the ABCD' technique (ABCD' pred) is compared with the observed signal yield (observed) and where applicable, with the prediction of the ABCD technique (ABCD pred). The errors in ABCD' pred and observed/ABCD' pred include only the statistical uncertainty in the observed yield. **will update after doing stat uncertainty for prediction**

	2010 signal region	$\mathrm{E_T^{miss}} > 275$ GeV, $H_T > 300$ GeV	$\mathrm{E_T^{miss}} > 200$ GeV, $H_T > 600$ GeV
$R_{S/C}$	3.5×10^{-2}	2.9×10^{-3}	5.1×10^{-3}
$N(\mathrm{control})$	1239	1239	1187
ABCD' pred	43.4	3.6	6.0
observed	37.0 ± 0.8	4.5 ± 0.3	6.2 ± 0.3
observed/ABCD' pred	0.85 ± 0.02	1.25 ± 0.08	1.03 ± 0.05
ABCD pred	43.0 ± 0.6	N/A	N/A

Appendix C Data/MC Comparison: Preselection Region

Here we compare data and MC distributions for data passing the preselection requirements. The high p_T dilepton trigger data is used.

The meaning of most of the variables plotted in the following figures should be obvious. There are some exceptions that we exlain below:

The $t\bar{t} \rightarrow \mathrm{fake}$ and $W + \mathrm{jets}$ samples are scaled here by 3.8, which is the ratio of the predicted contribution from fake leptons from the fake rate method to the MC expectation. All MC samples are scaled by an overall factor 1.10, the ratio of the observed data yield in the preselection region to the prediction from MC augmented by the data-driven fake lepton prediction. For illustration purposes, we overlay the distributions from the LM1 SUSY benchmakr point.

- $MT2$ is a kinematical quantity built from the two leptons and the $\mathrm{E_T^{miss}}$. For events with two $W \rightarrow \ell$ decays it should have a sharp kinematical cutoff at W mass. For more details, see Reference [22].
- $MT2J$ is very much like $MT2$ but it is built out of the leptons, the $\mathrm{E_T^{miss}}$ and the two jets. For $t\bar{t}$ events it has a kinematical cutoff at M_{top}, with tails due to the fact that occasionally one of the b-jets is not found and is replaced by a gluon jet from ISR or FSR. For more details, see Reference [23].

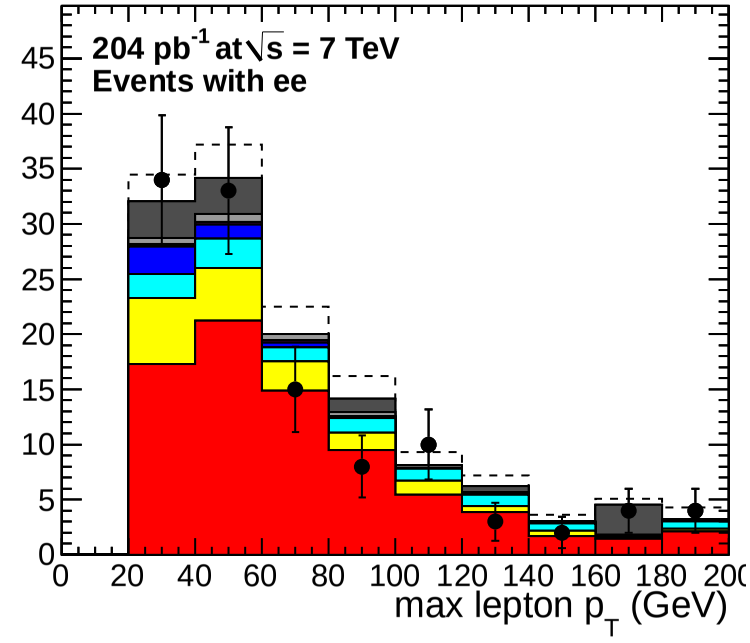
204 pb-1 at √s = 7 TeV
Events with ee
max lepton pT (GeV)

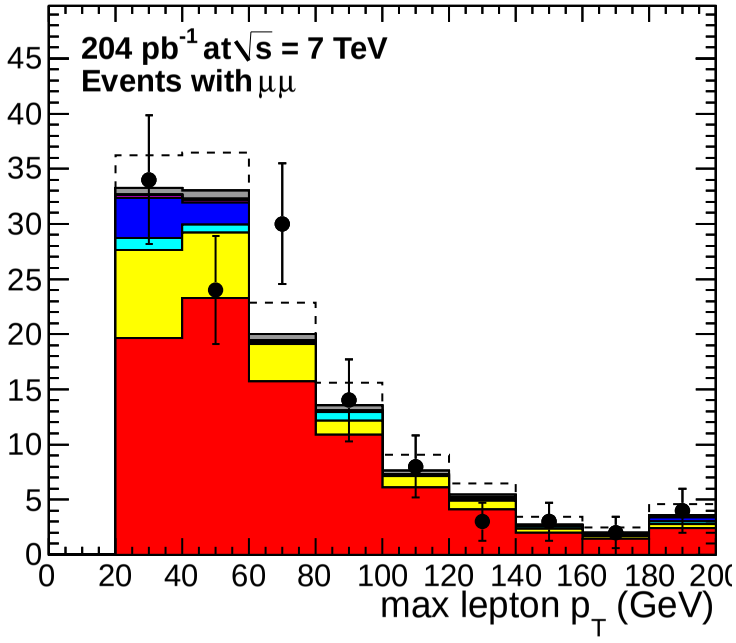
204 pb-1 at √s = 7 TeV
Events with μμ
max lepton pT (GeV)

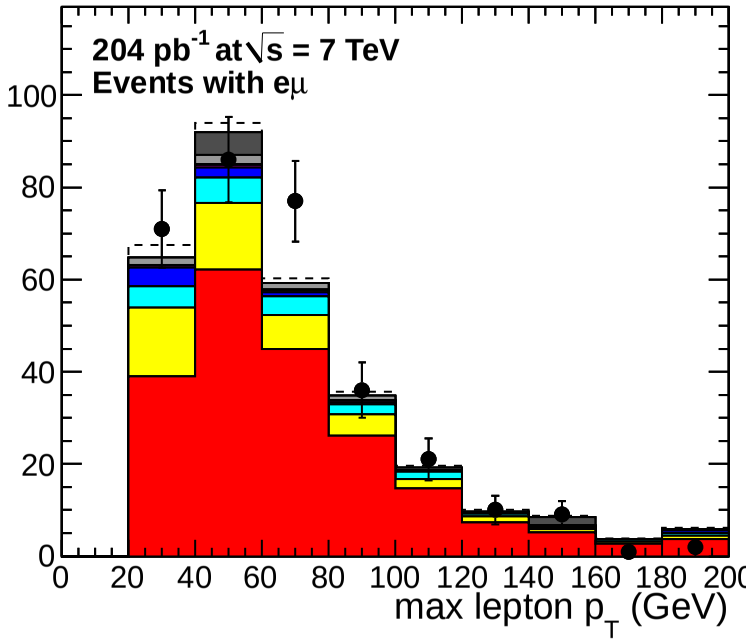
204 pb-1 at √s = 7 TeV
Events with eμ
max lepton pT (GeV)

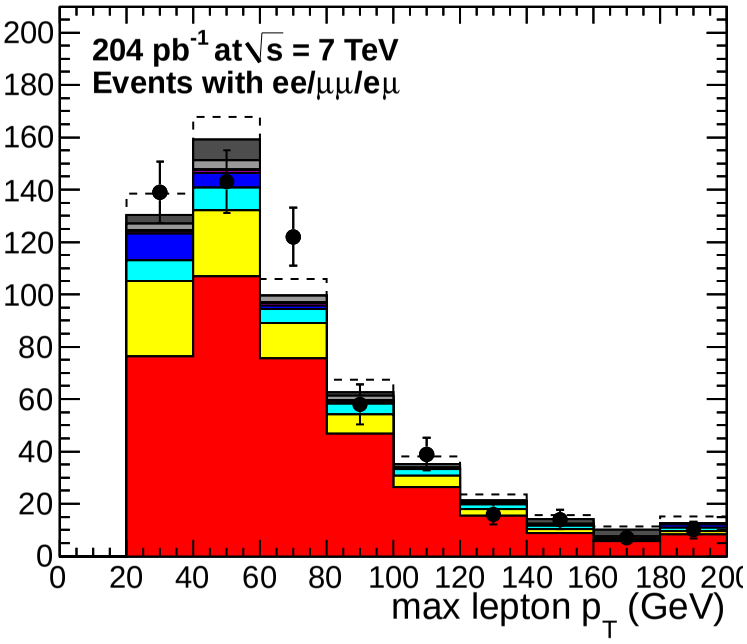
204 pb-1 at √s = 7 TeV
Events with ee/μμ/eμ
max lepton pT (GeV)

data
ttll
tttau
ttfake
DY
WW
WZ
ZZ
t
wjets
LM1

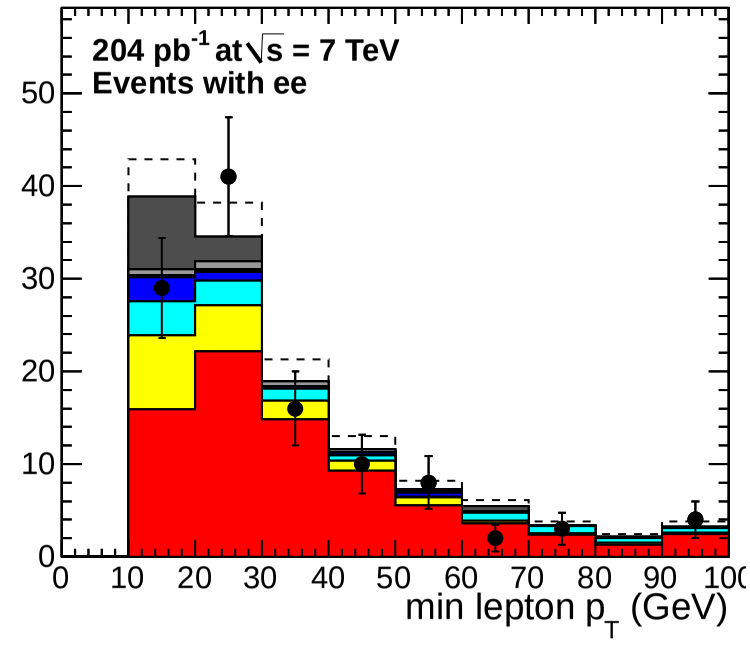
204 pb-1 at √s = 7 TeV
Events with ee
min lepton pT (GeV)

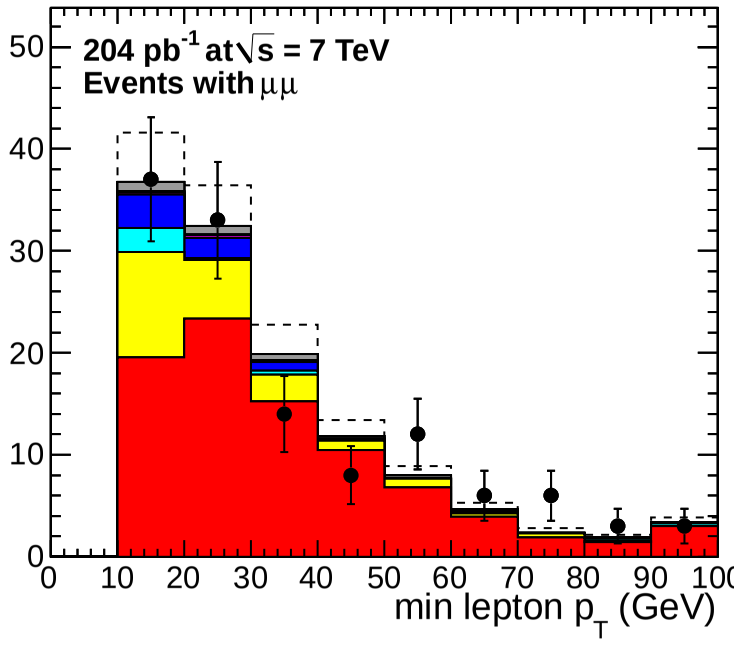
204 pb-1 at √s = 7 TeV
Events with μμ
min lepton pT (GeV)

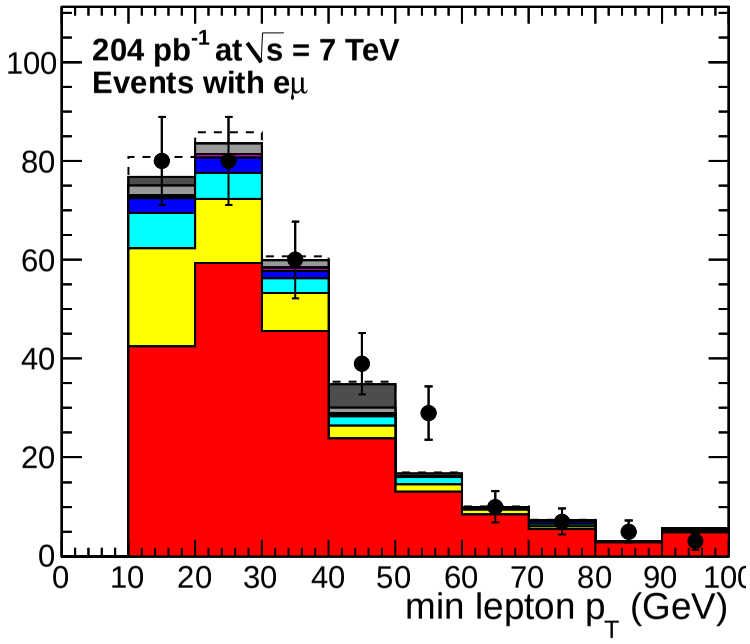
204 pb-1 at √s = 7 TeV
Events with eμ
min lepton pT (GeV)

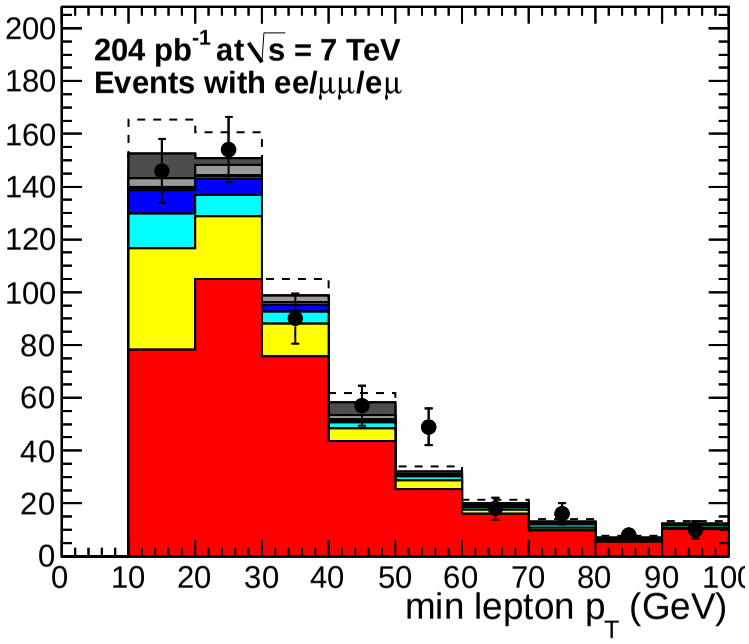
204 pb-1 at √s = 7 TeV
Events with ee/μμ/eμ
min lepton pT (GeV)

data
ttll
tttau
ttfake
DY
WW
WZ
ZZ
t
wjets
LM1

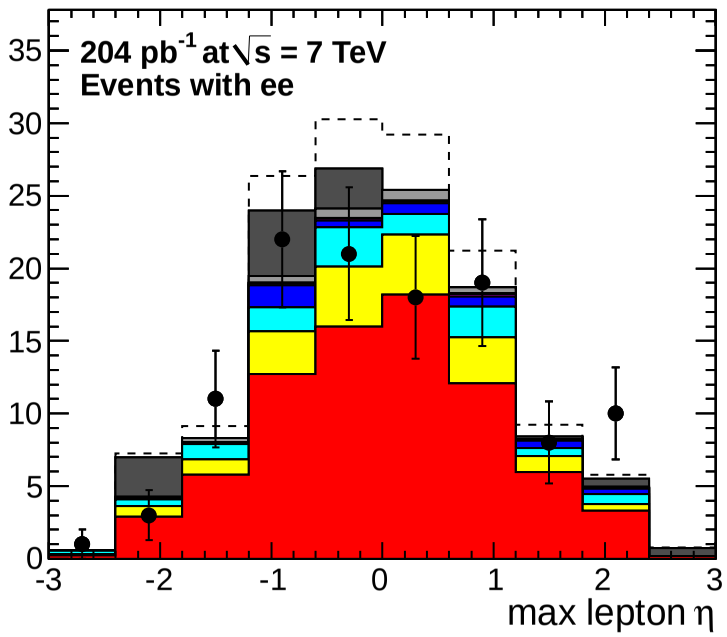
204 pb-1 at √s = 7 TeV
Events with ee
max lepton η

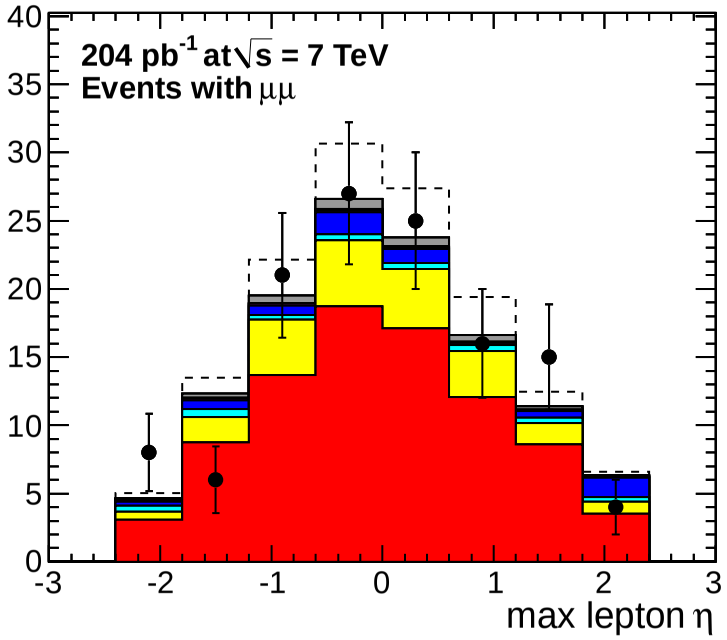
204 pb-1 at √s = 7 TeV
Events with μμ
max lepton η

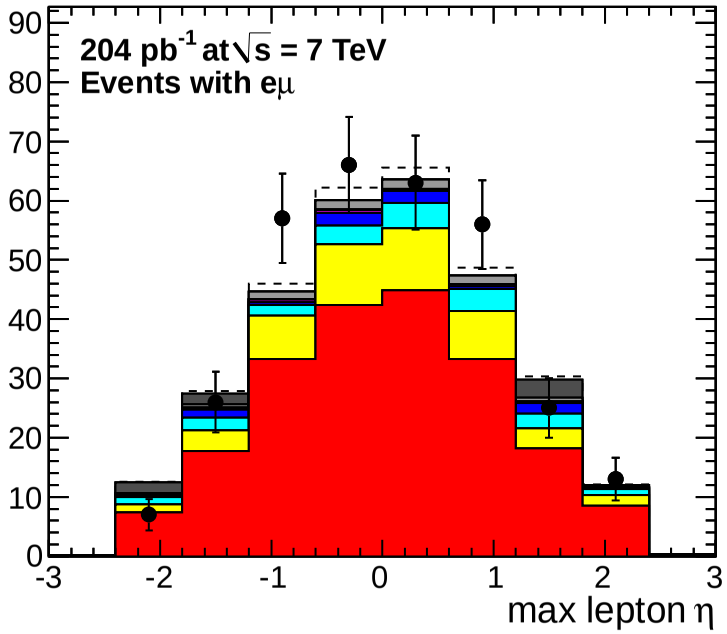
204 pb-1 at √s = 7 TeV
Events with eμ
max lepton η

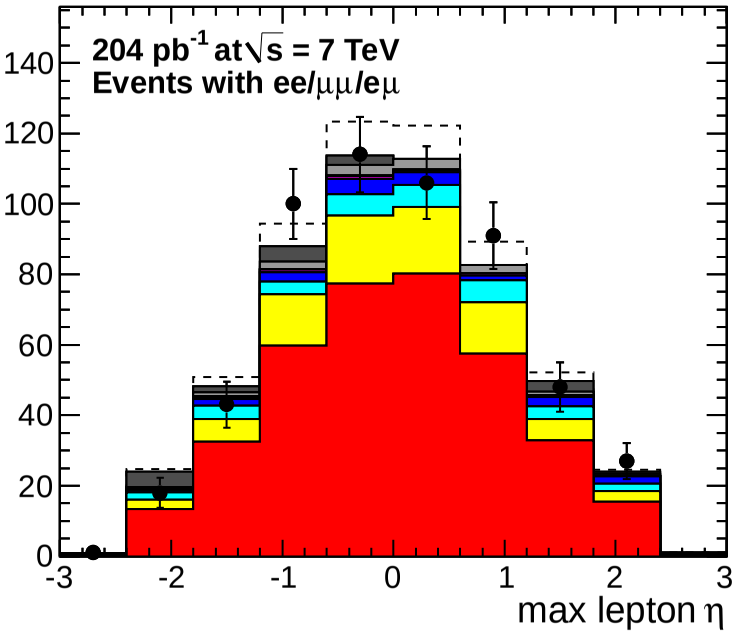
204 pb-1 at √s = 7 TeV
Events with ee/μμ/eμ
max lepton η

data
ttll
tttau
ttfake
DY
WW
WZ
ZZ
t
wjets
LM1

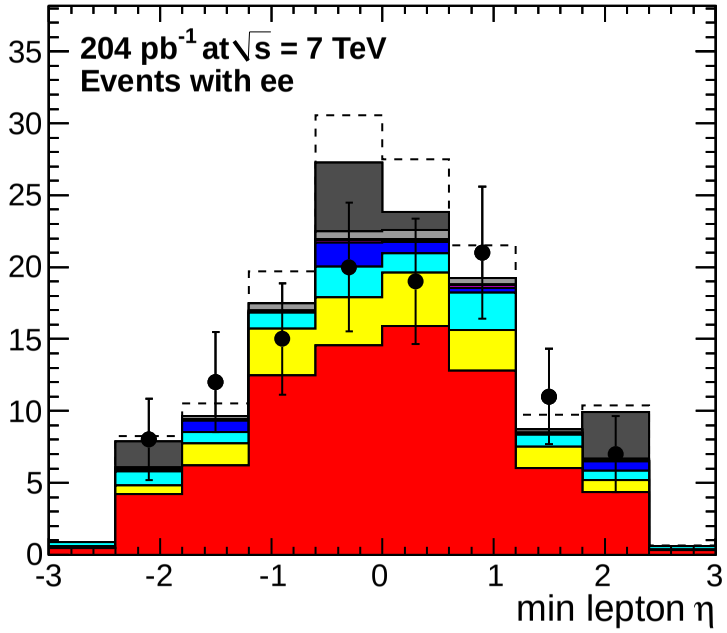
204 pb-1 at √s = 7 TeV
Events with ee
min lepton η

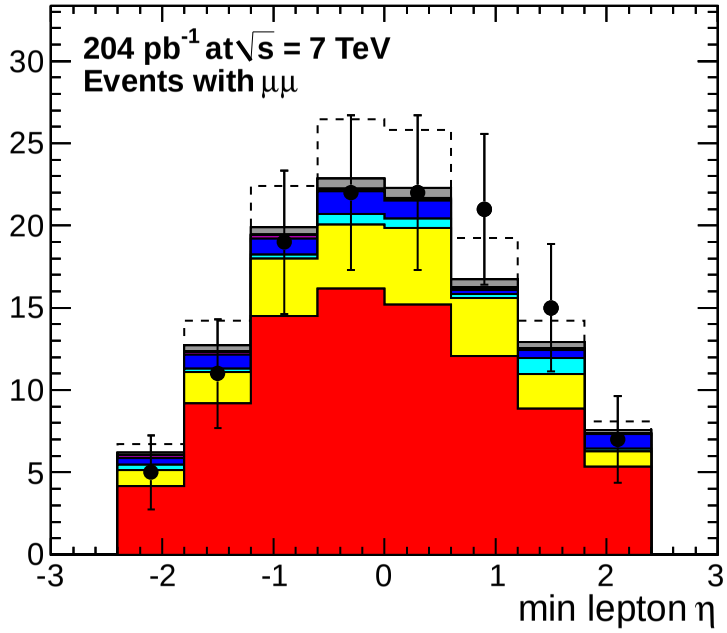
204 pb-1 at √s = 7 TeV
Events with μμ
min lepton η

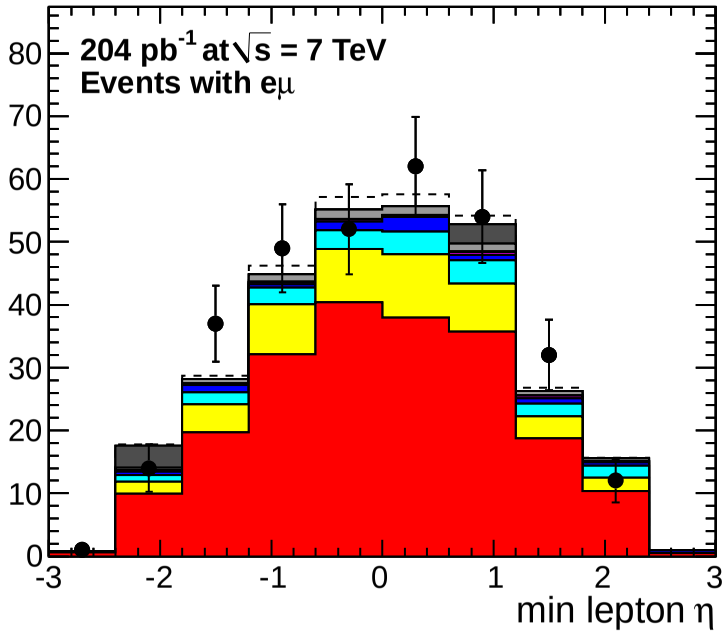
204 pb-1 at √s = 7 TeV
Events with eμ
min lepton η

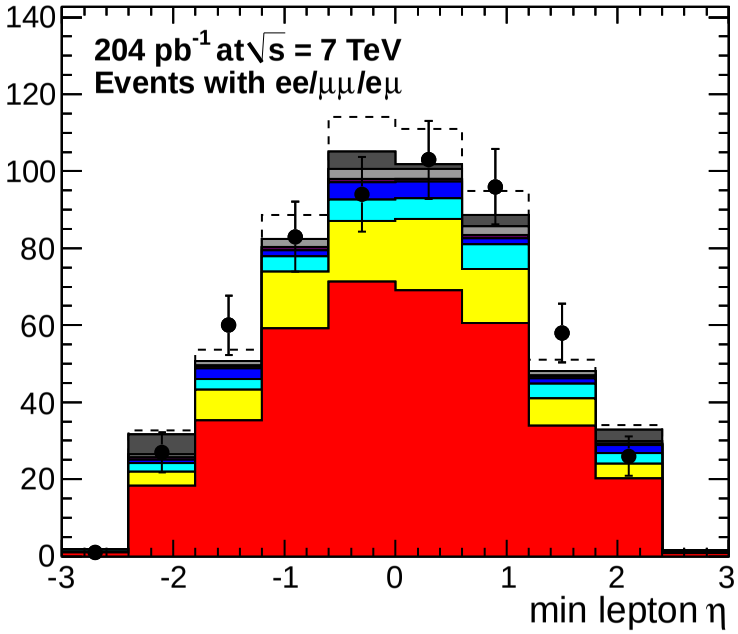
204 pb-1 at √s = 7 TeV
Events with ee/μμ/eμ
min lepton η

data
ttll
tttau
ttfake
DY
WW
WZ
ZZ
t
wjets
LM1

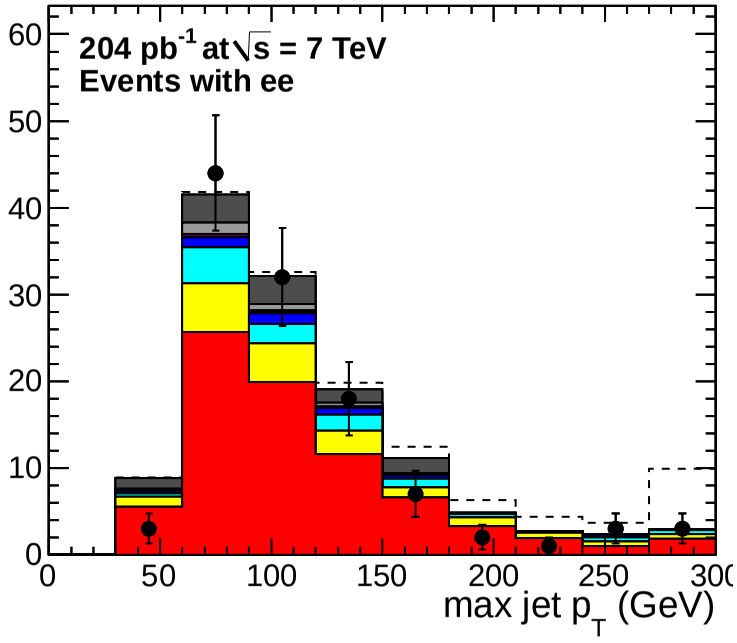
204 pb-1 at √s = 7 TeV
Events with ee
max jet pT (GeV)

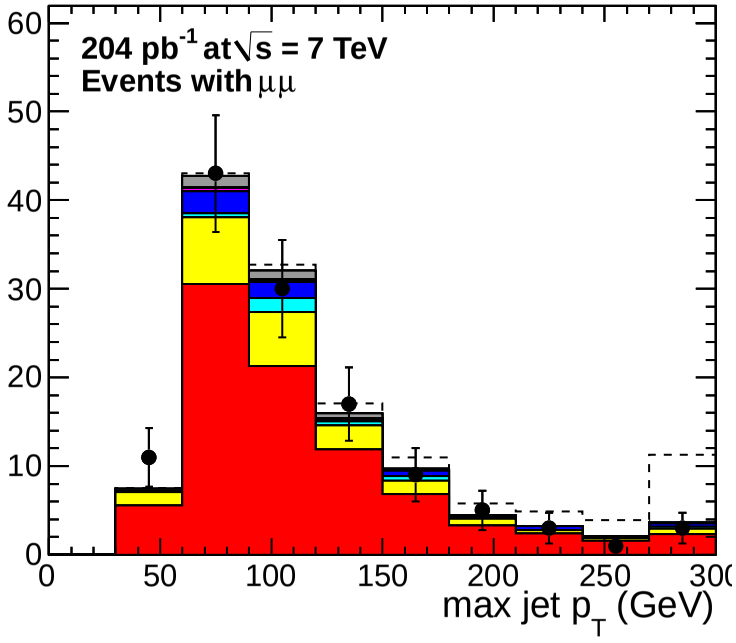
204 pb-1 at √s = 7 TeV
Events with μμ
max jet pT (GeV)

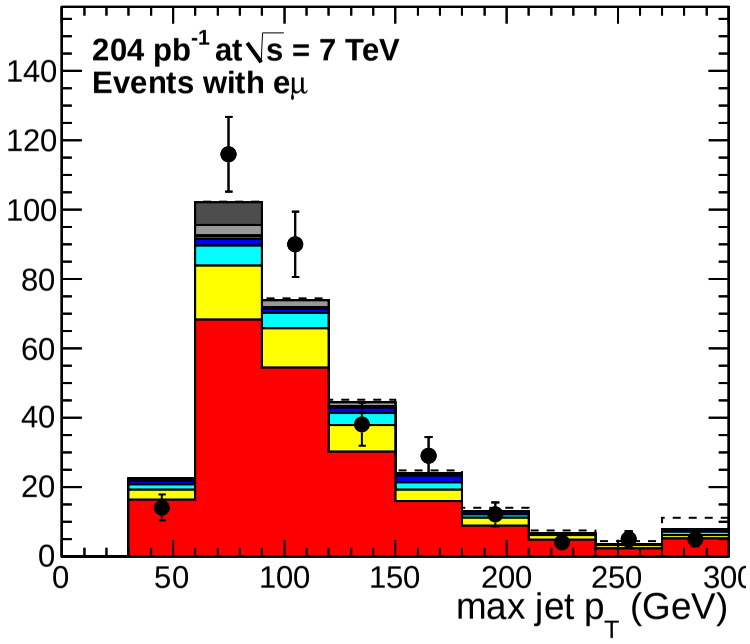
204 pb-1 at √s = 7 TeV
Events with eμ
max jet pT (GeV)

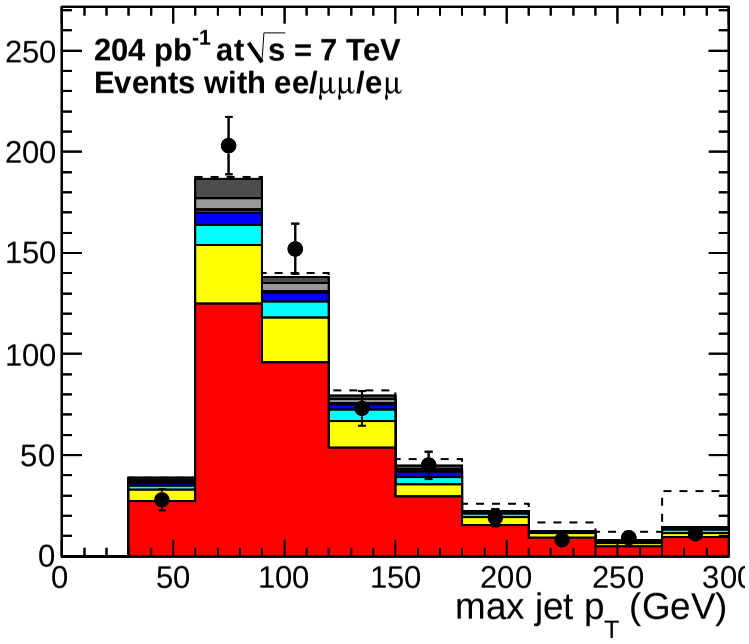
204 pb-1 at √s = 7 TeV
Events with ee/μμ/eμ
max jet pT (GeV)

data
ttll
tttau
ttfake
DY
WW
WZ
ZZ
t
wjets
LM1

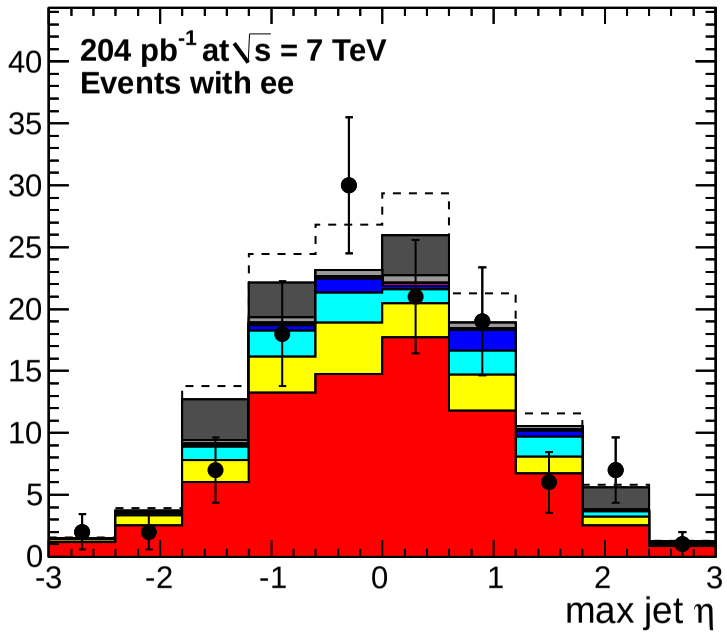
204 pb-1 at √s = 7 TeV
Events with ee
max jet η

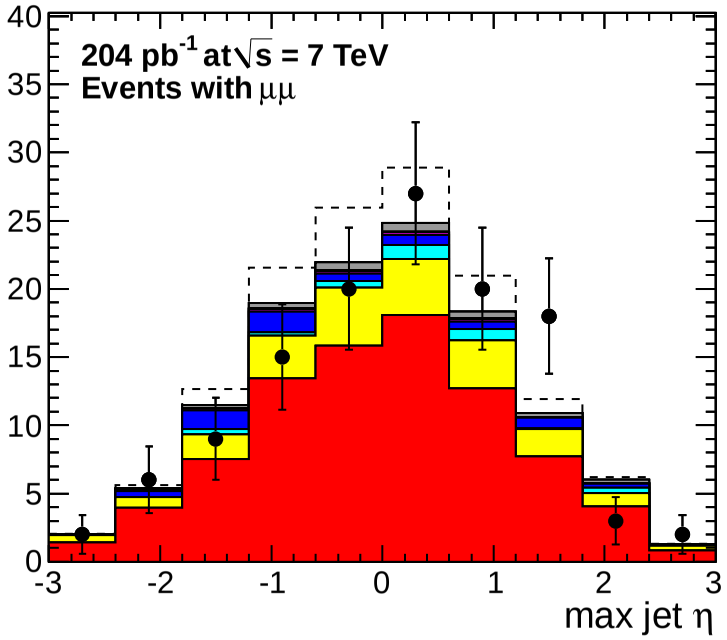
204 pb-1 at √s = 7 TeV
Events with μμ
max jet η

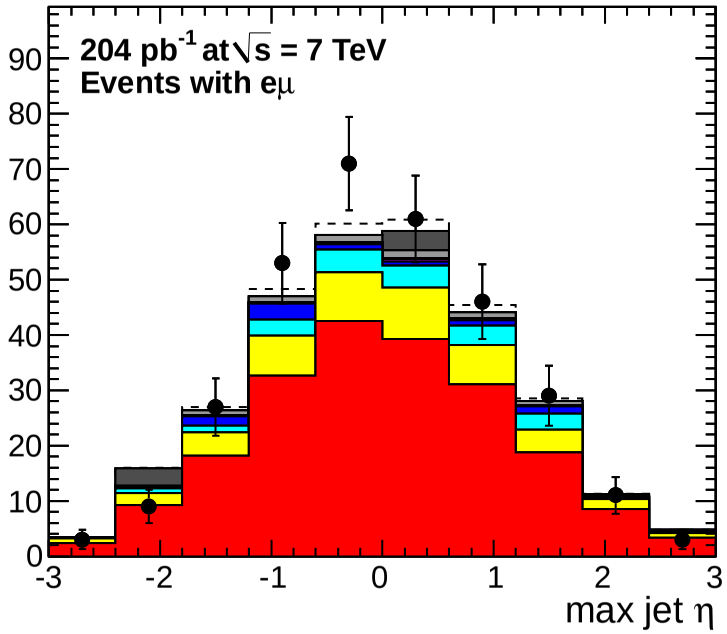
204 pb-1 at √s = 7 TeV
Events with eμ
max jet η

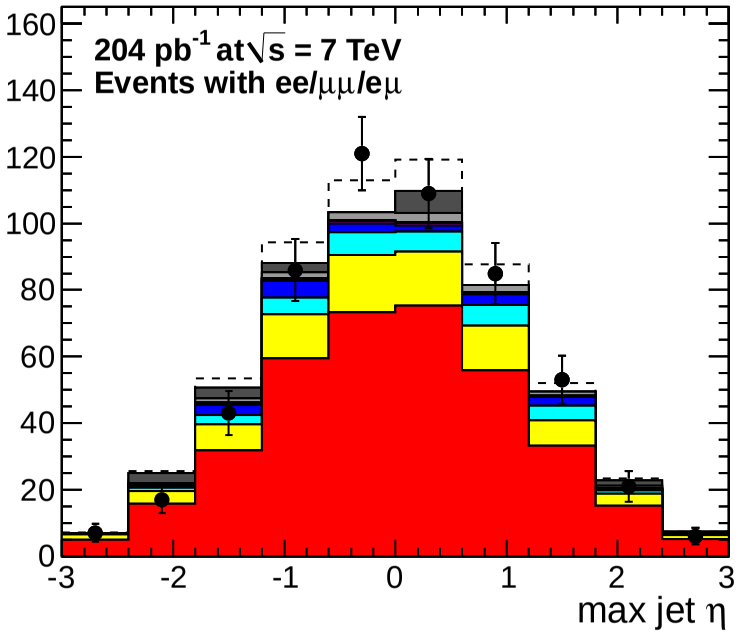
204 pb-1 at √s = 7 TeV
Events with ee/μμ/eμ
max jet η

data
ttll
tttau
ttfake
DY
WW
WZ
ZZ
t
wjets
LM1

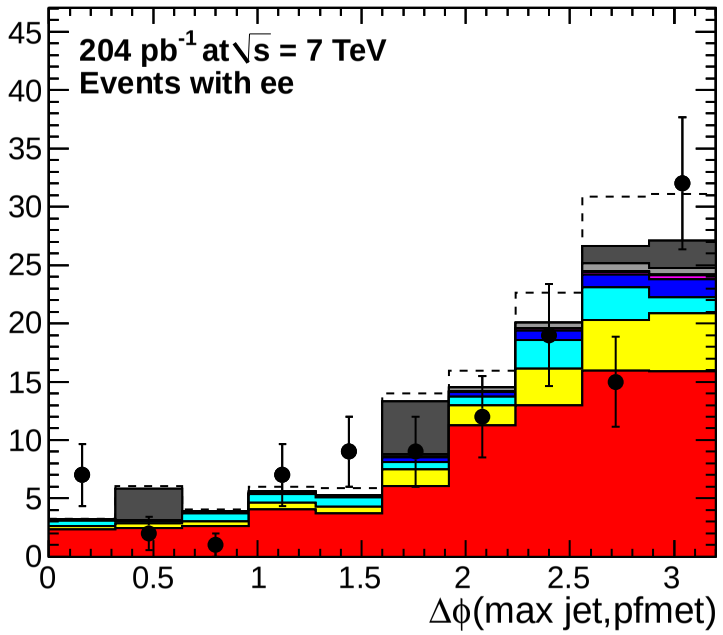
204 pb-1 at √s = 7 TeV
Events with ee
Δφ(max jet,pfmet)

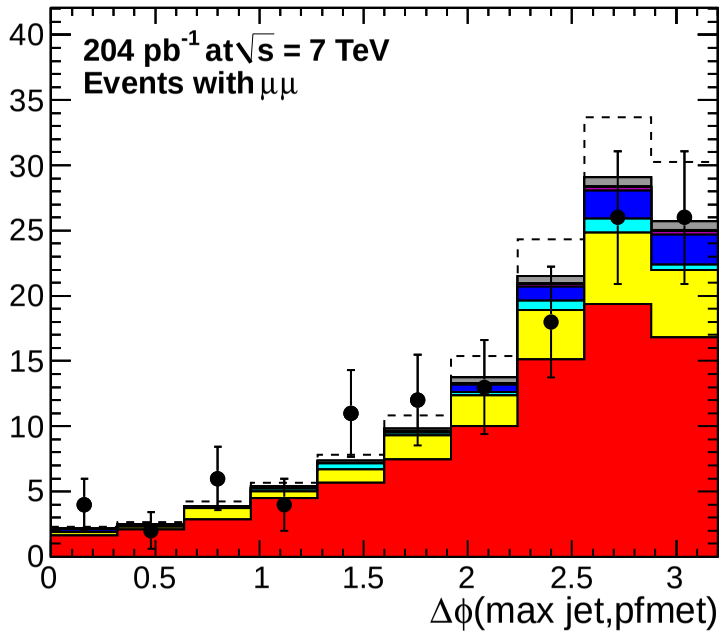
204 pb-1 at √s = 7 TeV
Events with μμ
Δφ(max jet,pfmet)

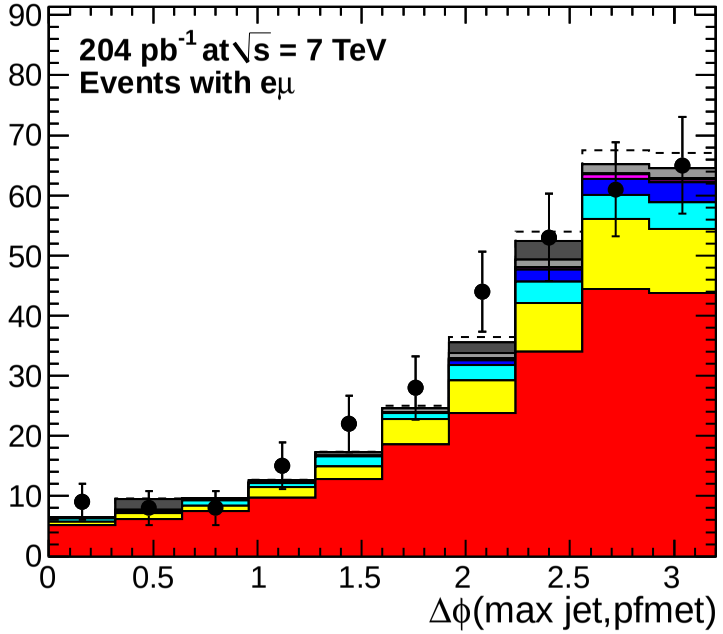
204 pb-1 at √s = 7 TeV
Events with eμ
Δφ(max jet,pfmet)

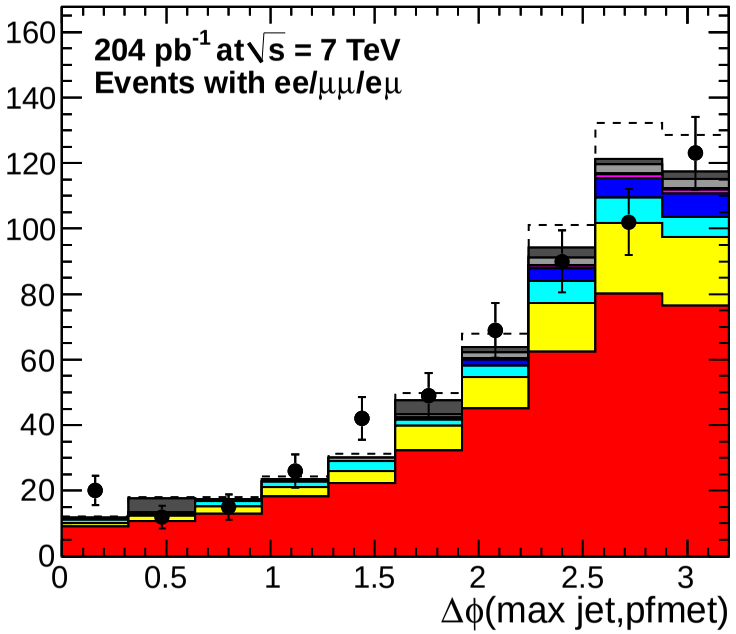
204 pb-1 at √s = 7 TeV
Events with ee/μμ/eμ
Δφ(max jet,pfmet)

data
ttll
tttau
ttfake
DY
WW
WZ
ZZ
t
wjets
LM1

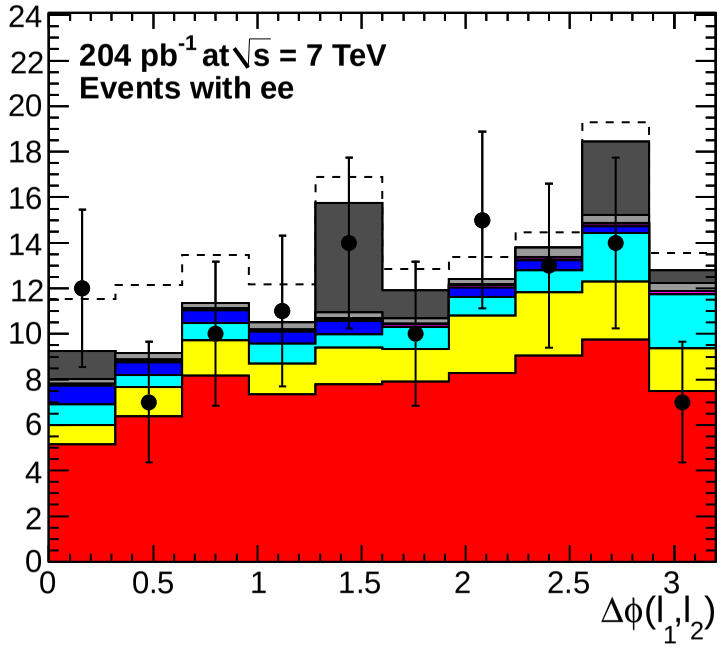
204 pb-1 at √s = 7 TeV
Events with ee
Δφ(l1,l2)

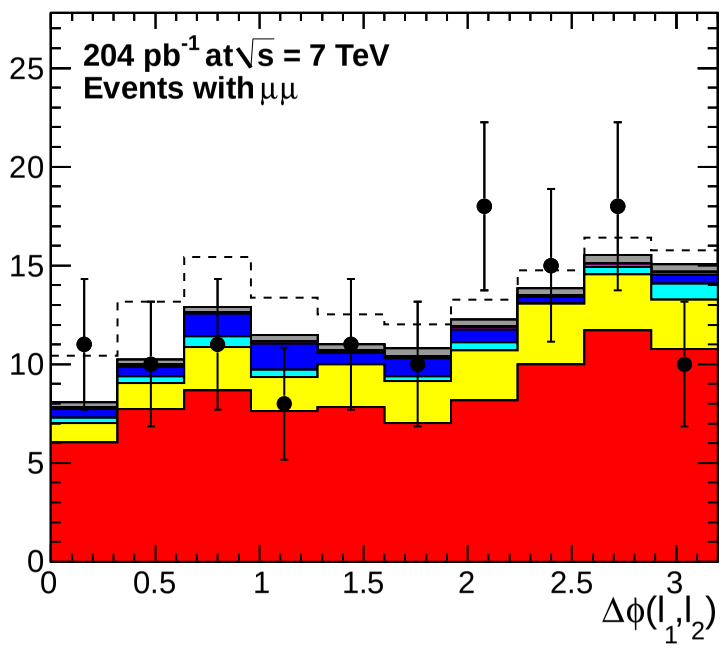
204 pb-1 at √s = 7 TeV
Events with μμ
Δφ(l1,l2)

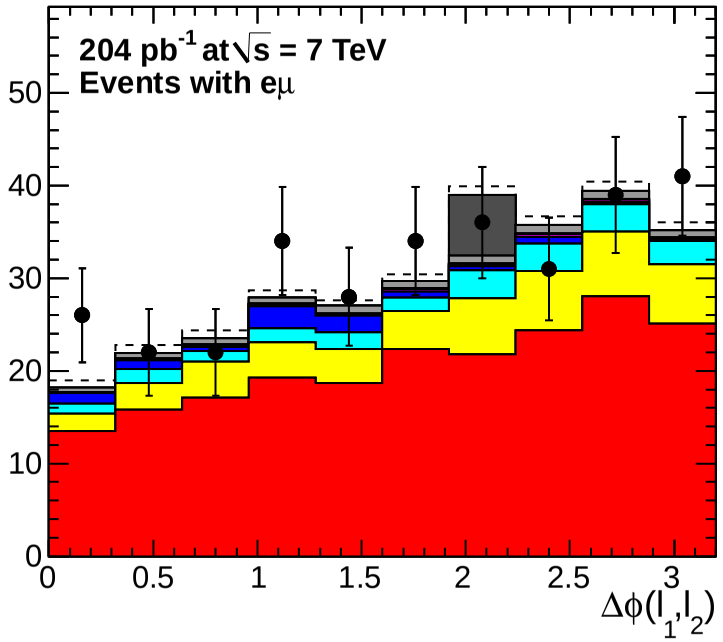
204 pb-1 at √s = 7 TeV
Events with eμ
Δφ(l1,l2)

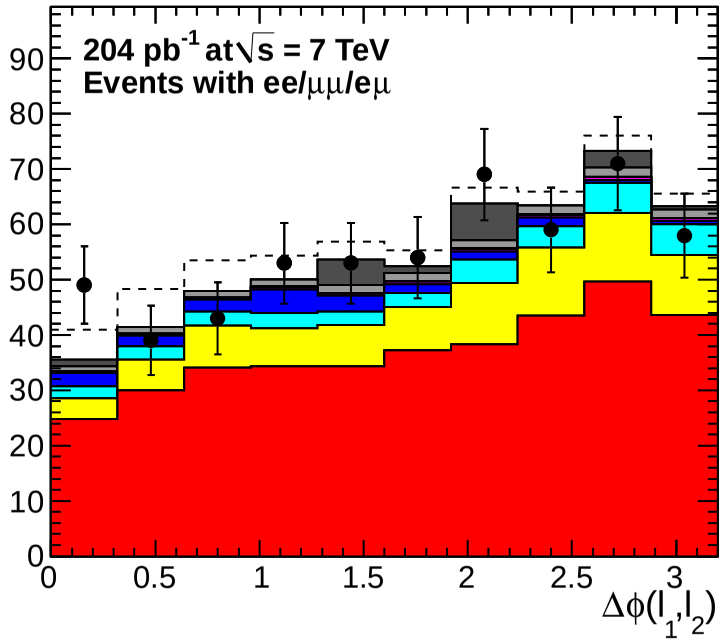
204 pb-1 at √s = 7 TeV
Events with ee/μμ/eμ
Δφ(l1,l2)

data
ttll
tttau
ttfake
DY
WW
WZ
ZZ
t
wjets
LM1

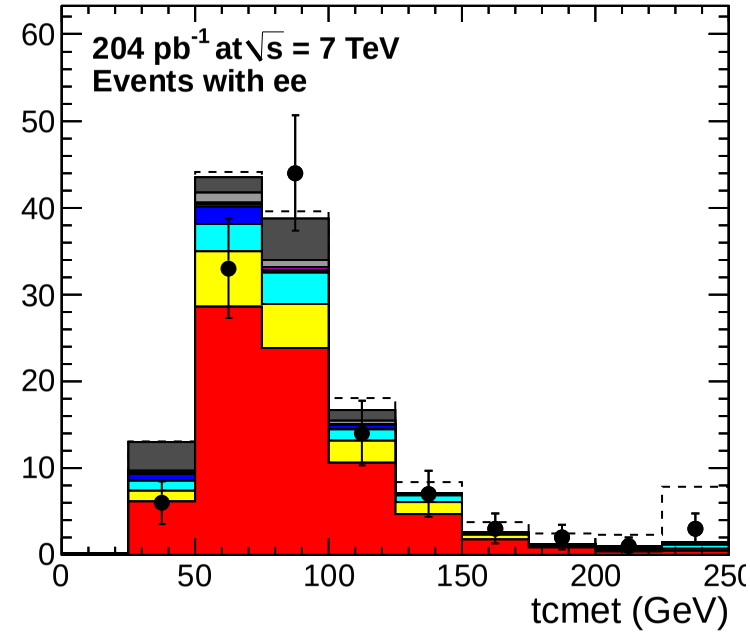
204 pb-1 at √s = 7 TeV
Events with ee
tcmet (GeV)

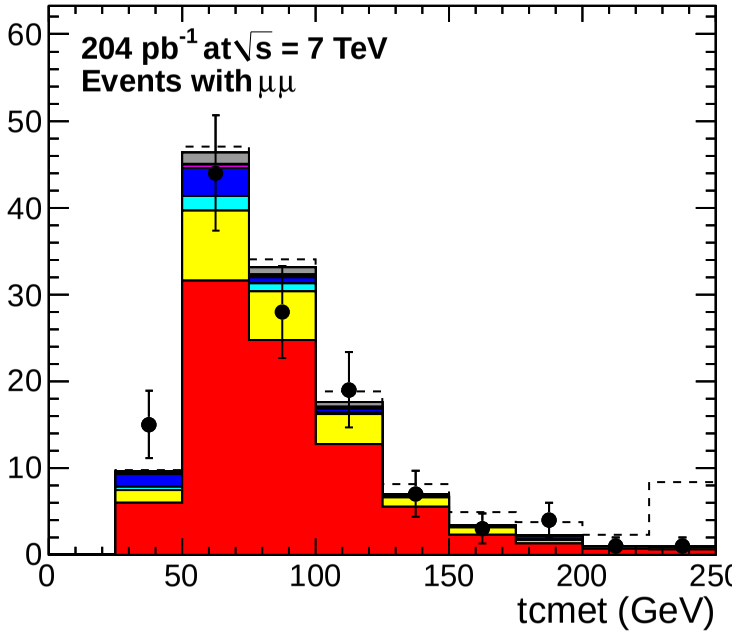
204 pb-1 at √s = 7 TeV
Events with μμ
tcmet (GeV)

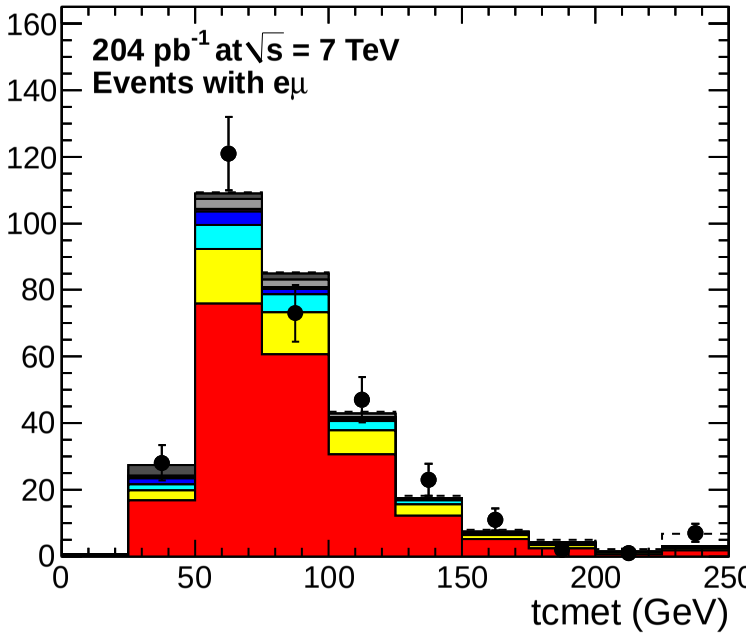
204 pb-1 at √s = 7 TeV
Events with eμ
tcmet (GeV)

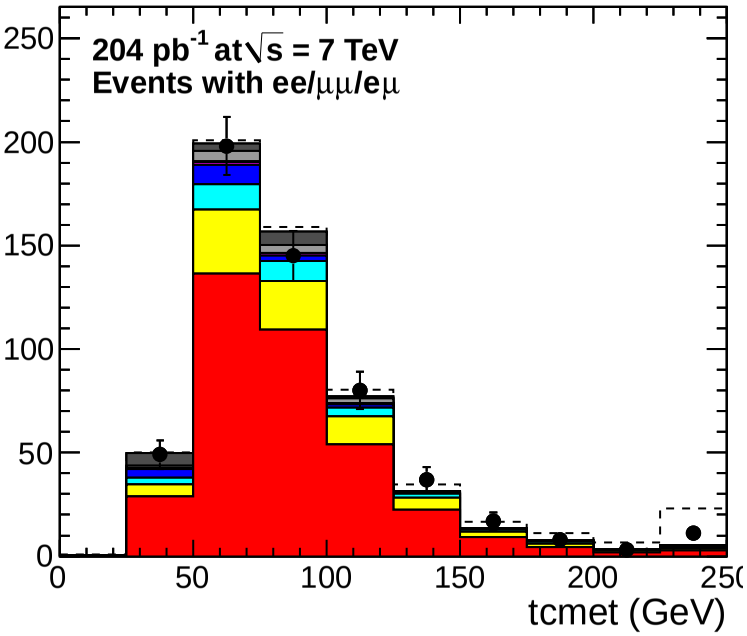
204 pb-1 at √s = 7 TeV
Events with ee/μμ/eμ
tcmet (GeV)

data
ttll
tttau
ttfake
DY
WW
WZ
ZZ
t
wjets
LM1

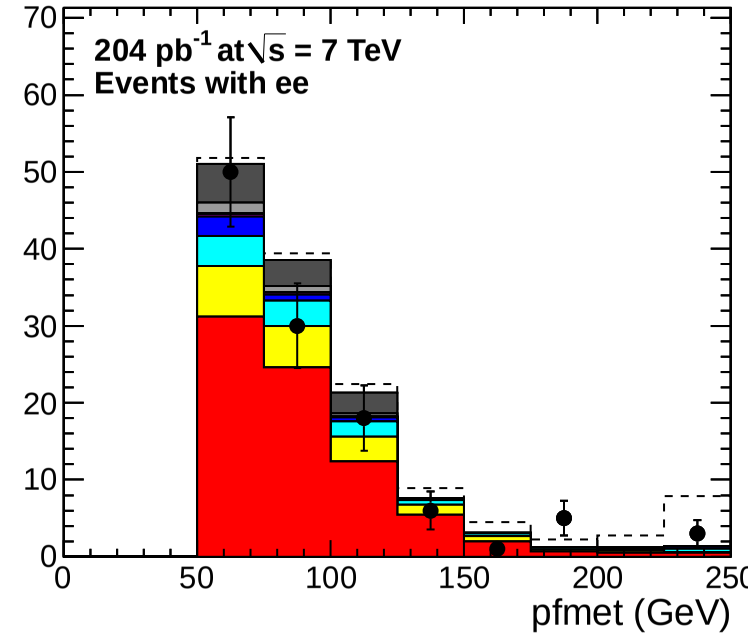
204 pb-1 at √s = 7 TeV
Events with ee
pfmet (GeV)

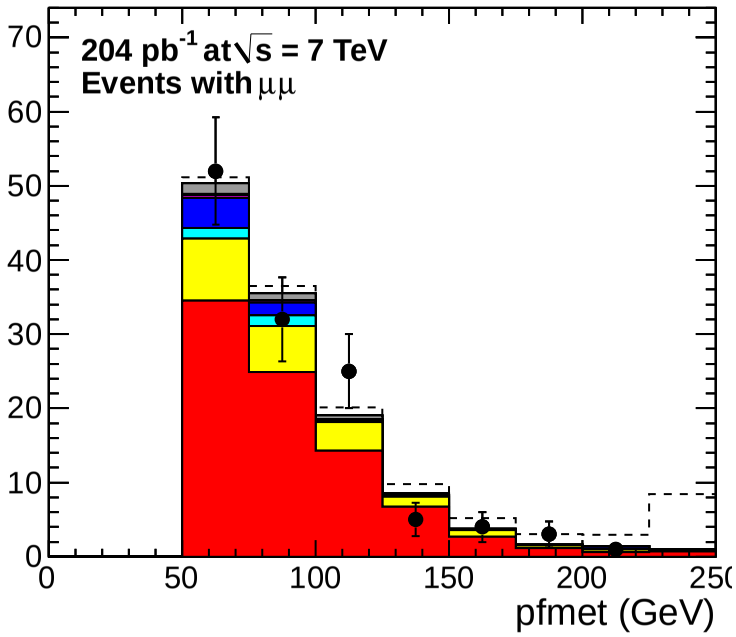
204 pb-1 at √s = 7 TeV
Events with μμ
pfmet (GeV)

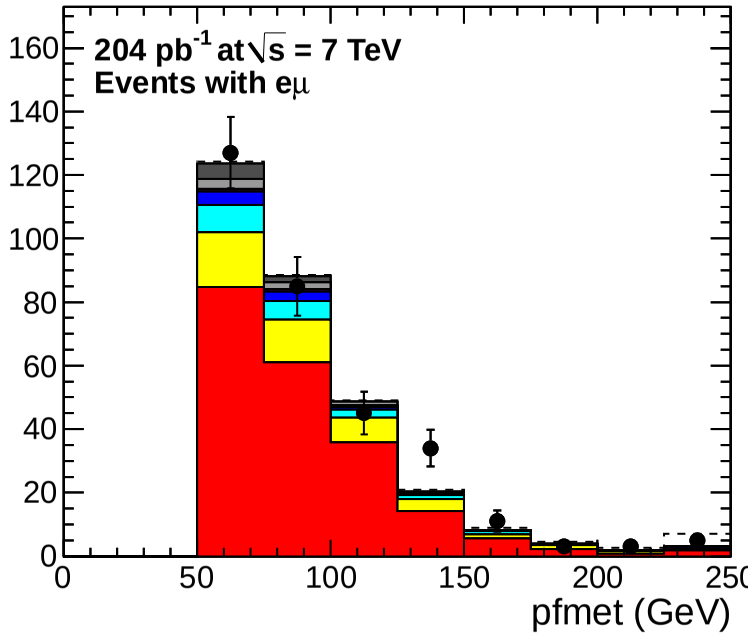
204 pb-1 at √s = 7 TeV
Events with eμ
pfmet (GeV)

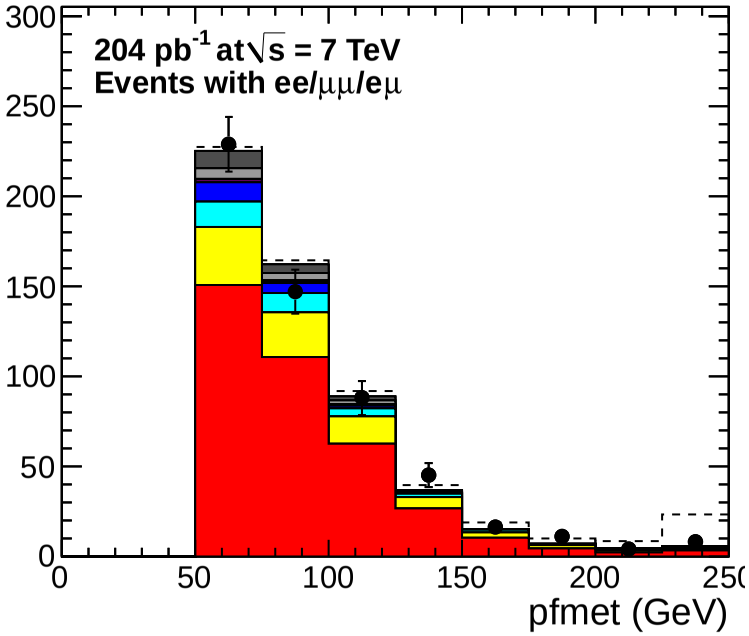
204 pb-1 at √s = 7 TeV
Events with ee/μμ/eμ
pfmet (GeV)

data
ttll
tttau
ttfake
DY
WW
WZ
ZZ
t
wjets
LM1

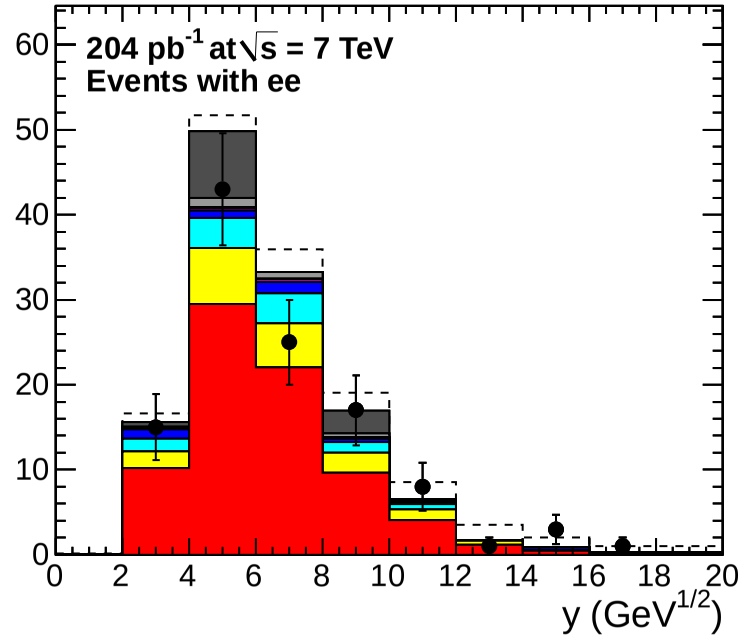
204 pb-1 at √s = 7 TeV
Events with ee
y (GeV1/2)

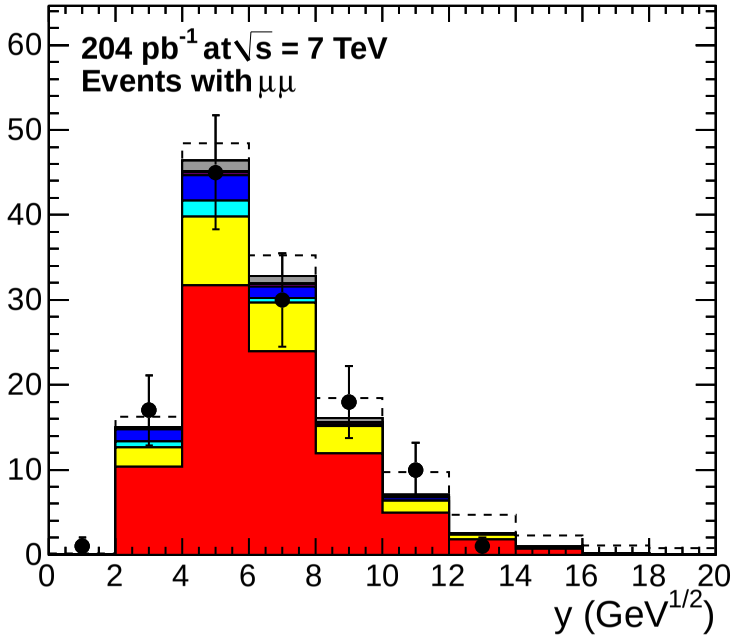
204 pb-1 at √s = 7 TeV
Events with μμ
y (GeV1/2)

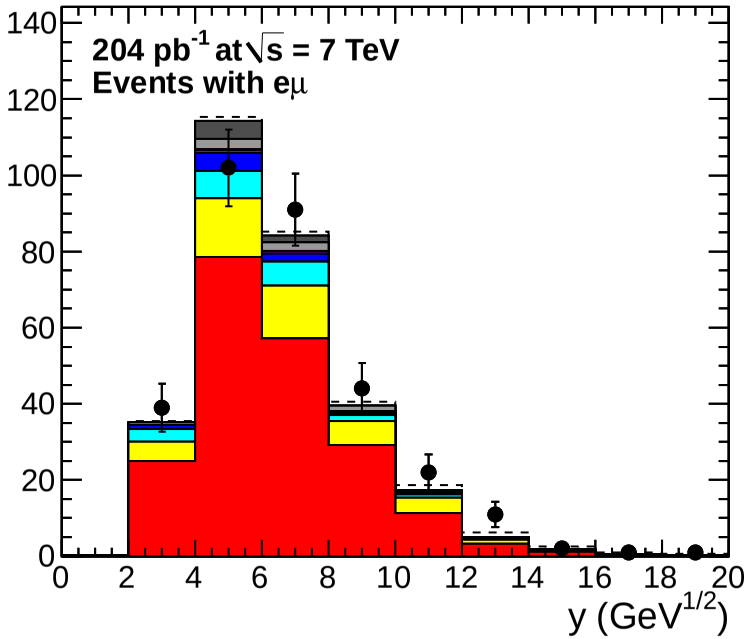
204 pb-1 at √s = 7 TeV
Events with eμ
y (GeV1/2)

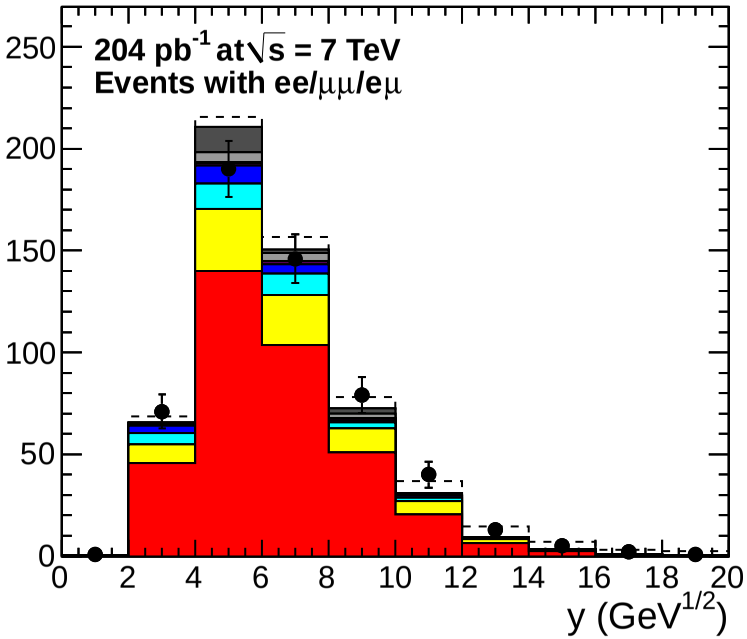
204 pb-1 at √s = 7 TeV
Events with ee/μμ/eμ
y (GeV1/2)

data
ttll
tttau
ttfake
DY
WW
WZ
ZZ
t
wjets
LM1

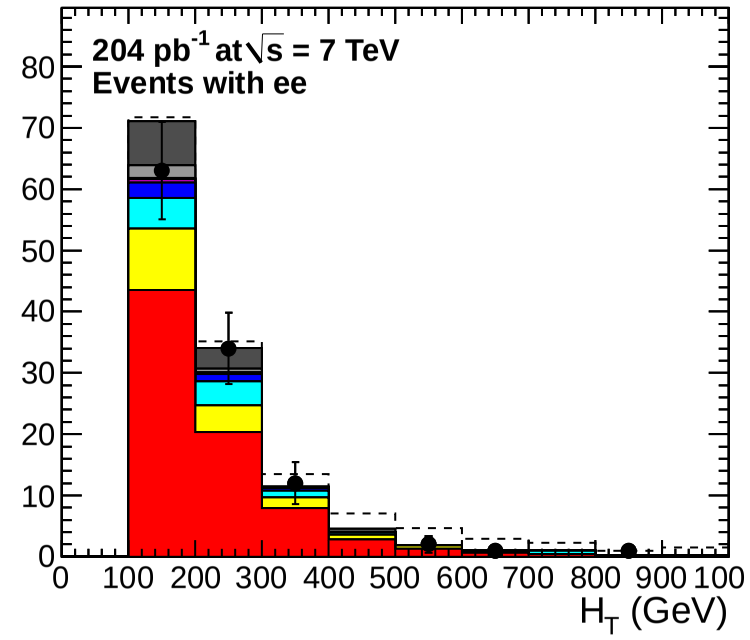
204 pb-1 at √s = 7 TeV
Events with ee
HT (GeV)

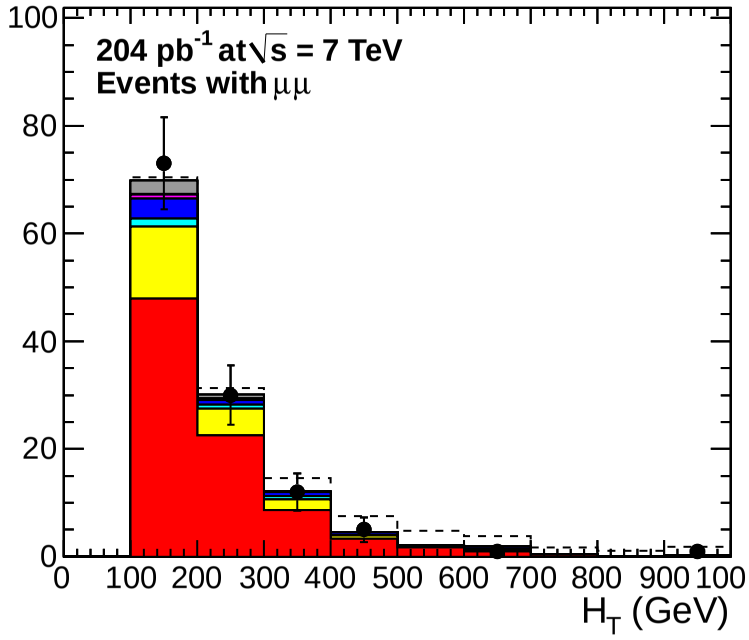
204 pb-1 at √s = 7 TeV
Events with μμ
HT (GeV)

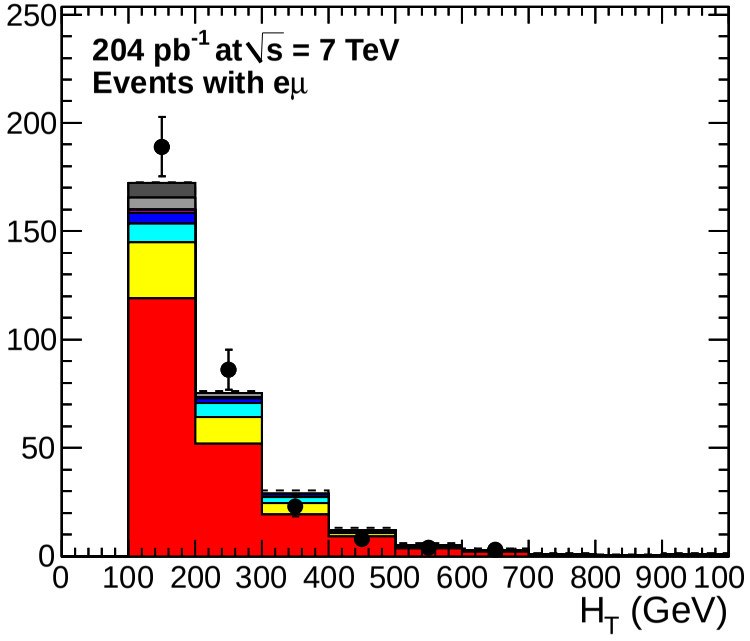
204 pb-1 at √s = 7 TeV
Events with eμ
HT (GeV)

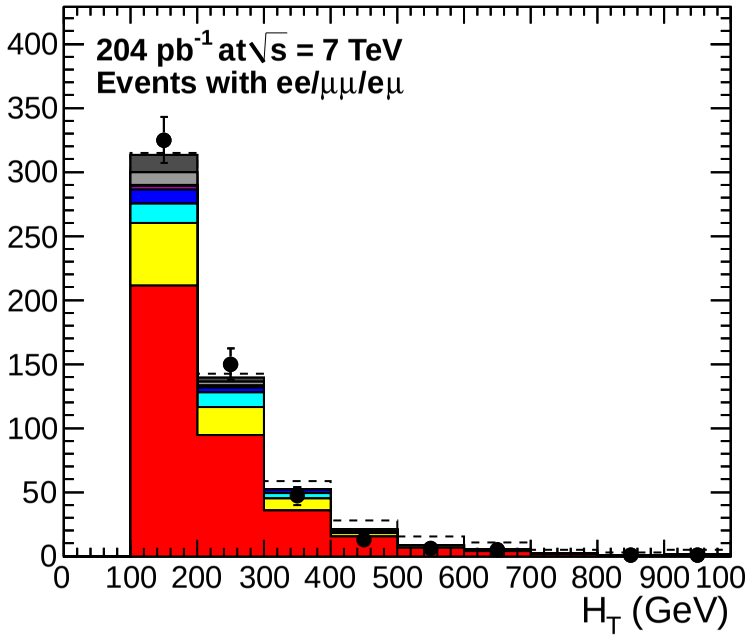
204 pb-1 at √s = 7 TeV
Events with ee/μμ/eμ
HT (GeV)

data
ttll
tttau
ttfake
DY
WW
WZ
ZZ
t
wjets
LM1

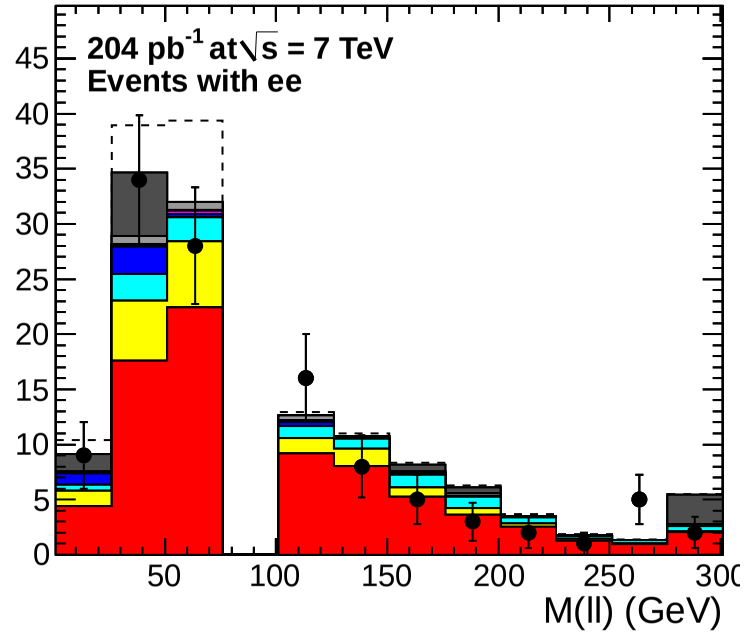
204 pb-1 at√s = 7 TeV
Events with ee
M(ll) (GeV)

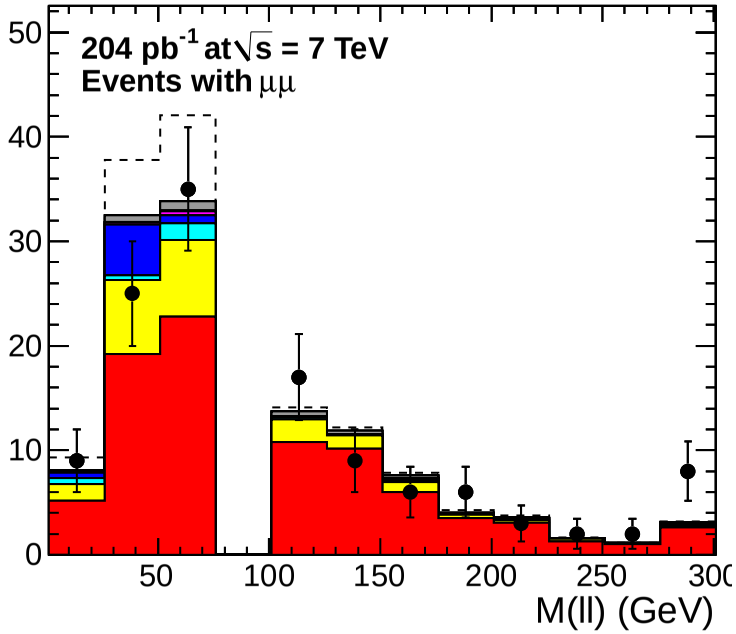
204 pb-1 at√s = 7 TeV
Events with μμ
M(ll) (GeV)

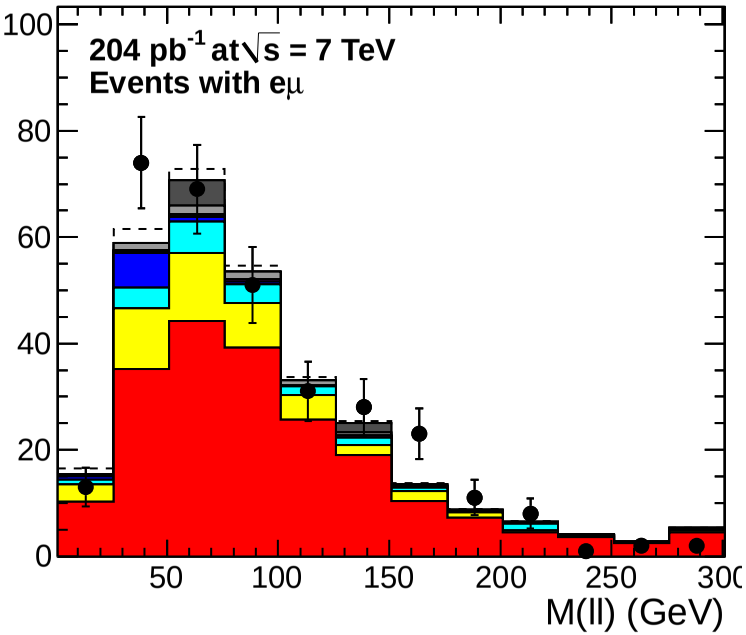
204 pb-1 at√s = 7 TeV
Events with eμ
M(ll) (GeV)

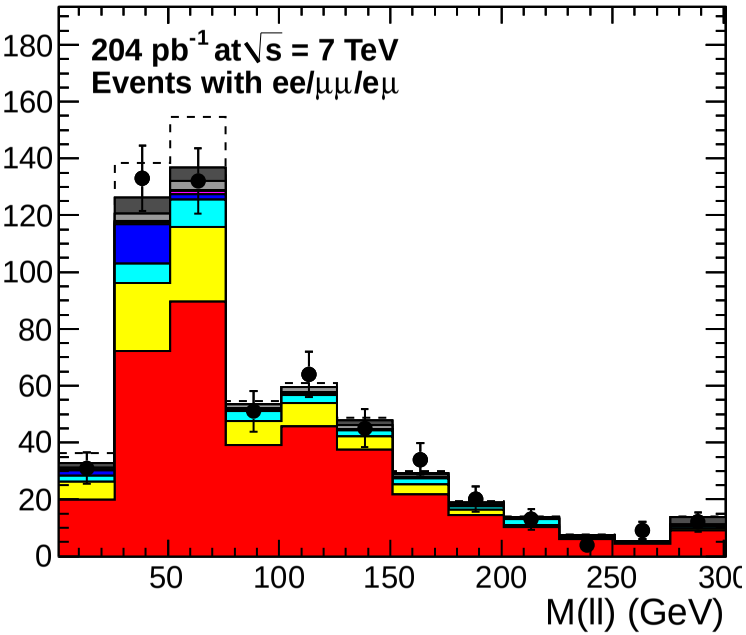
204 pb-1 at√s = 7 TeV
Events with ee/μμ/eμ
M(ll) (GeV)

data
ttll
tttau
ttfake
DY
WW
WZ
ZZ
t
wjets
LM1

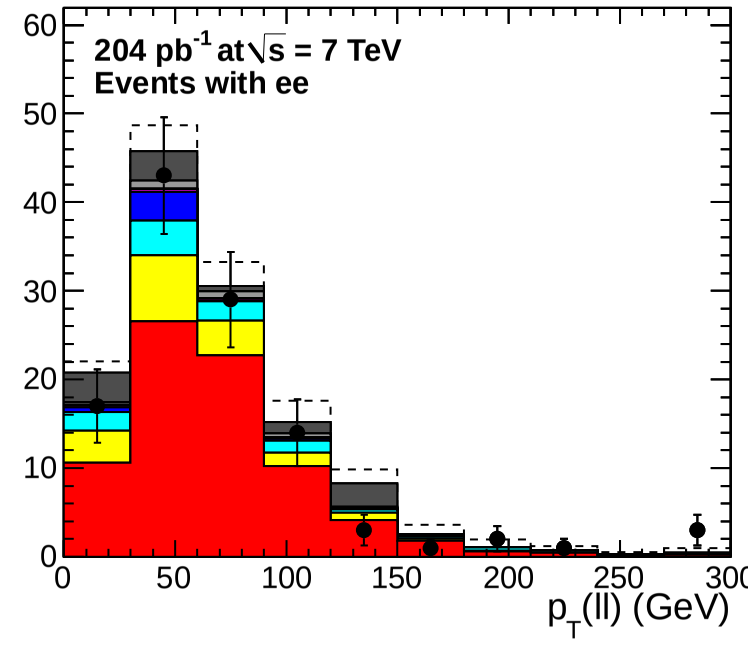
204 pb-1 at √s = 7 TeV
Events with ee
pT(ll) (GeV)

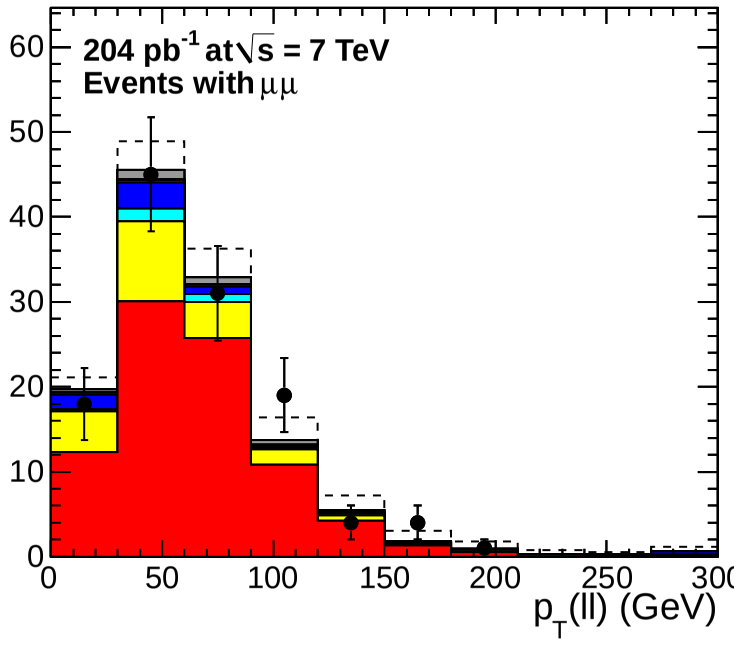
204 pb-1 at √s = 7 TeV
Events with μμ
pT(ll) (GeV)

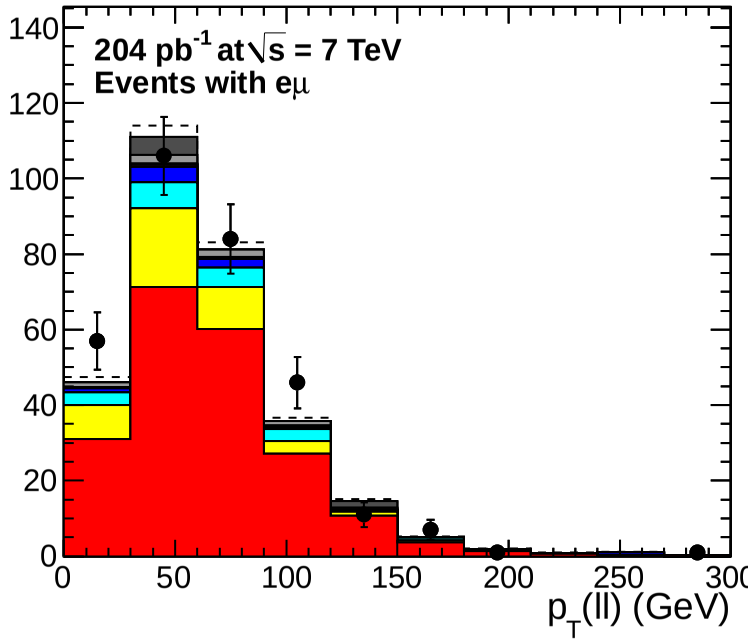
204 pb-1 at √s = 7 TeV
Events with eμ
pT(ll) (GeV)

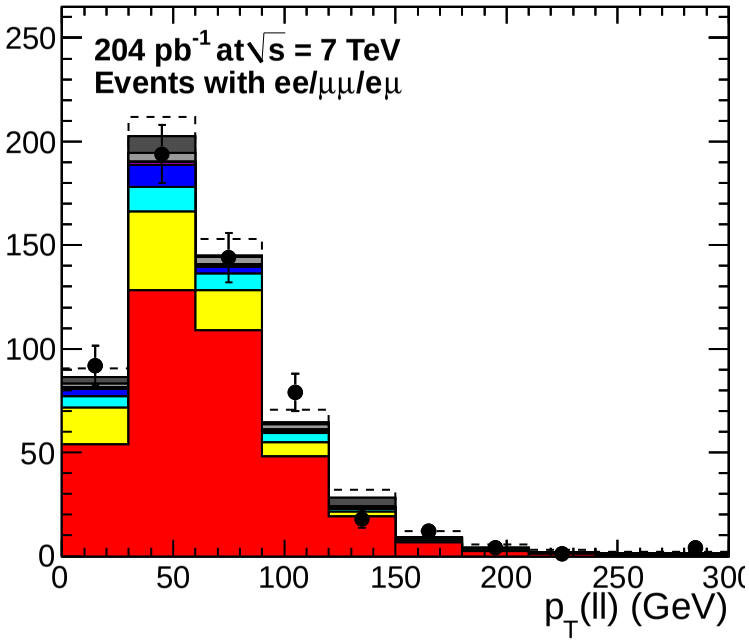
204 pb-1 at √s = 7 TeV
Events with ee/μμ/eμ
pT(ll) (GeV)

data
ttll
tttau
ttfake
DY
WW
WZ
ZZ
t
wjets
LM1

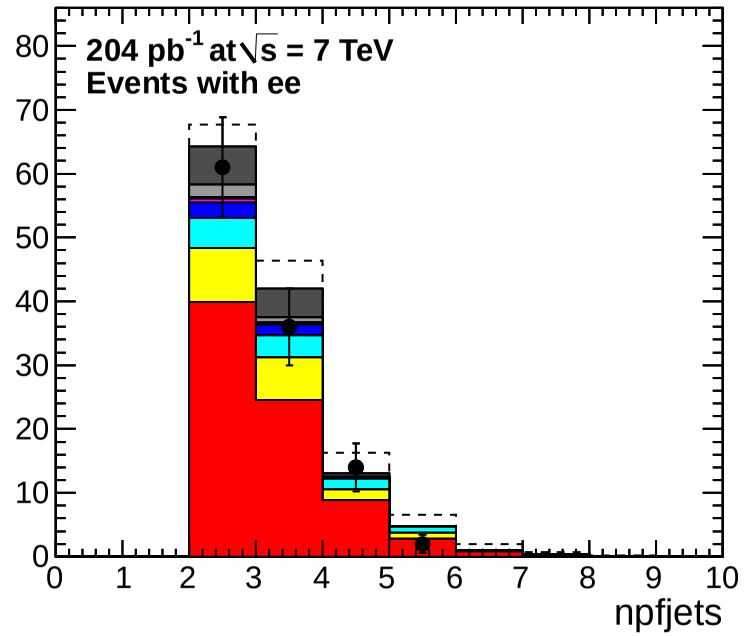
204 pb-1 at √s = 7 TeV
Events with ee
npfjets

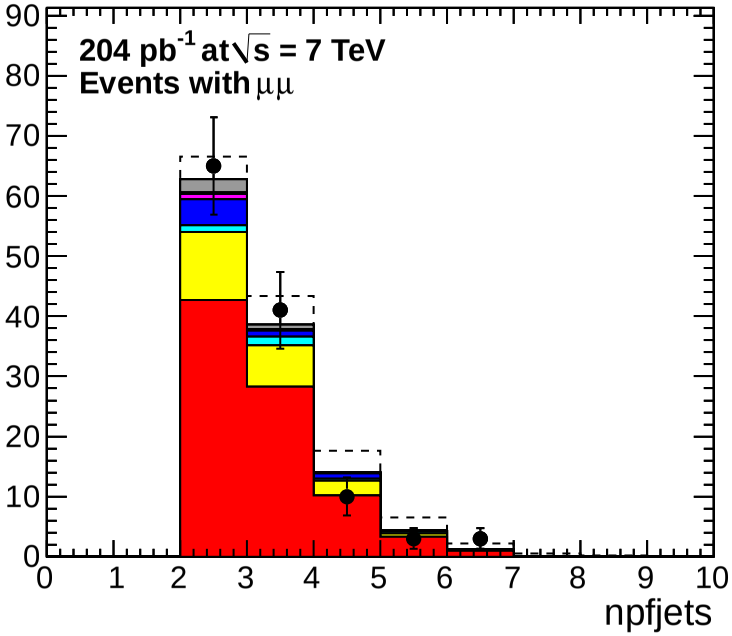
204 pb-1 at √s = 7 TeV
Events with μμ
npfjets

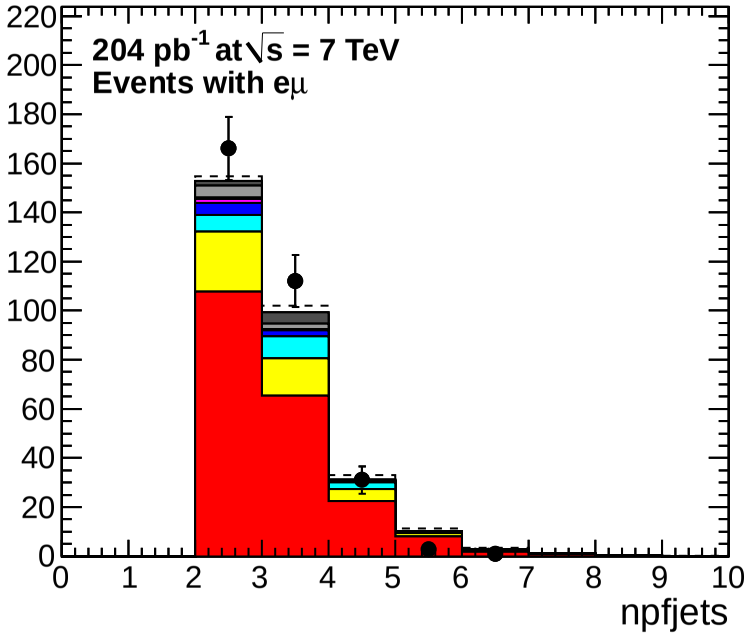
204 pb-1 at √s = 7 TeV
Events with eμ
npfjets

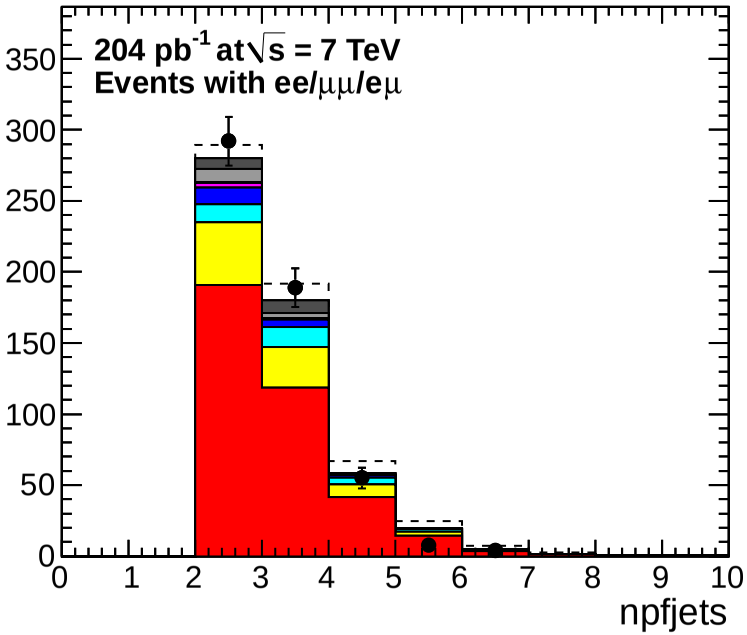
204 pb-1 at √s = 7 TeV
Events with ee/μμ/eμ
npfjets

data
ttll
tttau
ttfake
DY
WW
WZ
ZZ
t
wjets
LM1

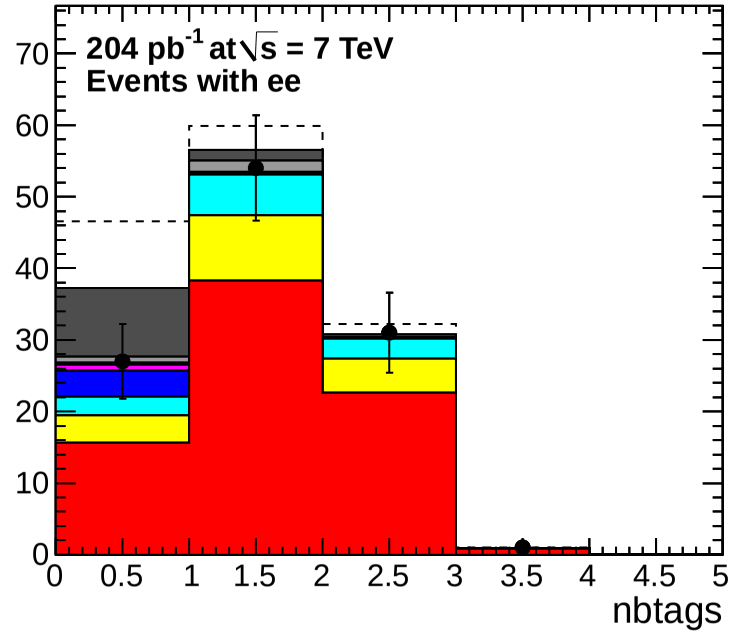
204 pb-1 at √s = 7 TeV
Events with ee
nbtags

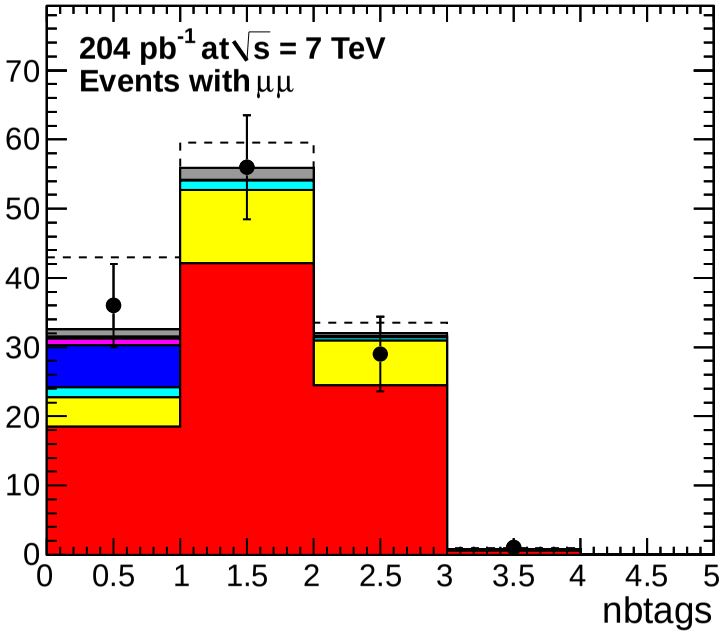
204 pb-1 at √s = 7 TeV
Events with μμ
nbtags

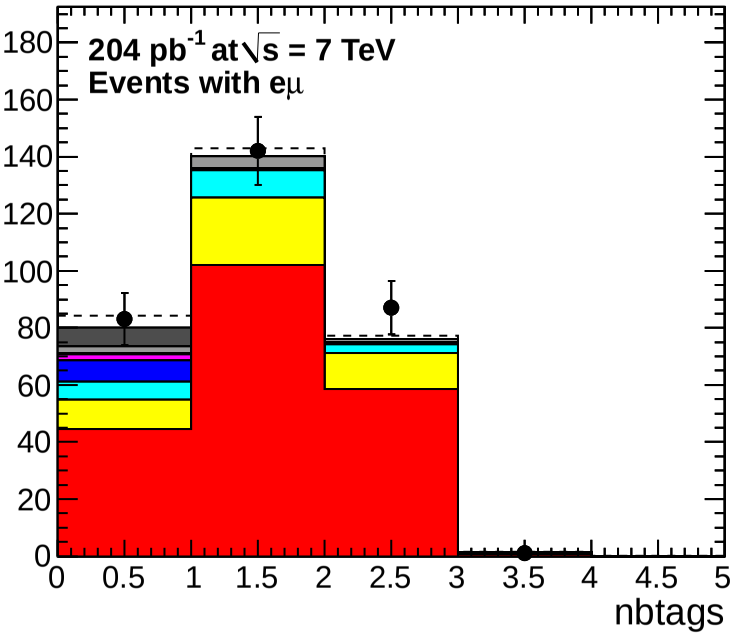
204 pb-1 at √s = 7 TeV
Events with eμ
nbtags

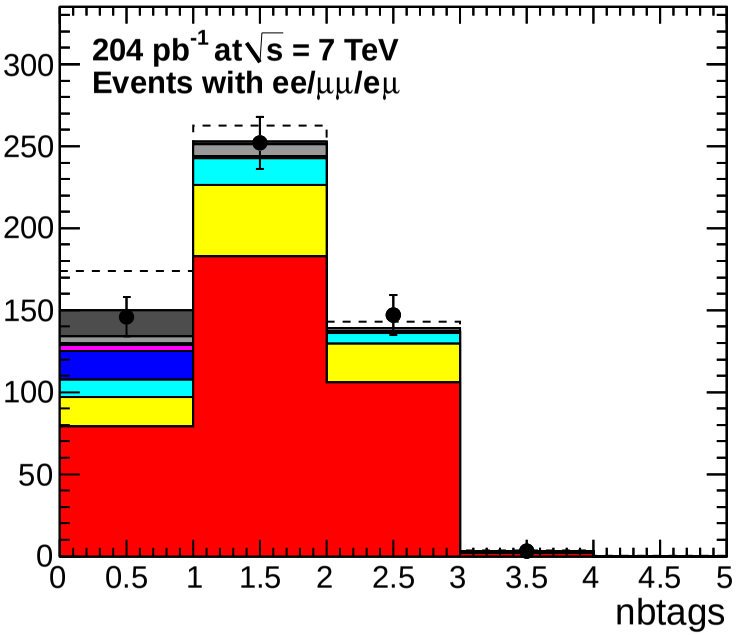
204 pb-1 at √s = 7 TeV
Events with ee/μμ/eμ
nbtags

data
ttll
tttau
ttfake
DY
WW
WZ
ZZ
t
wjets
LM1

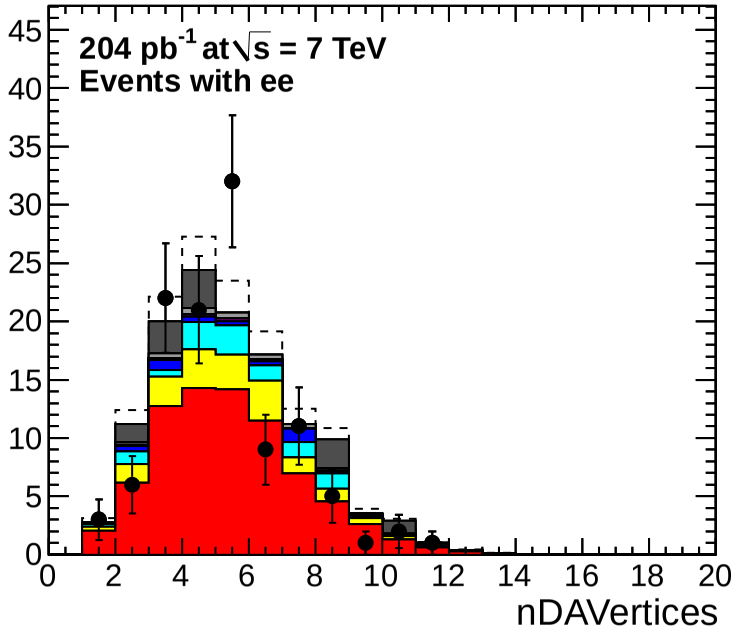
204 pb-1 at √s = 7 TeV
Events with ee
nDAVertices

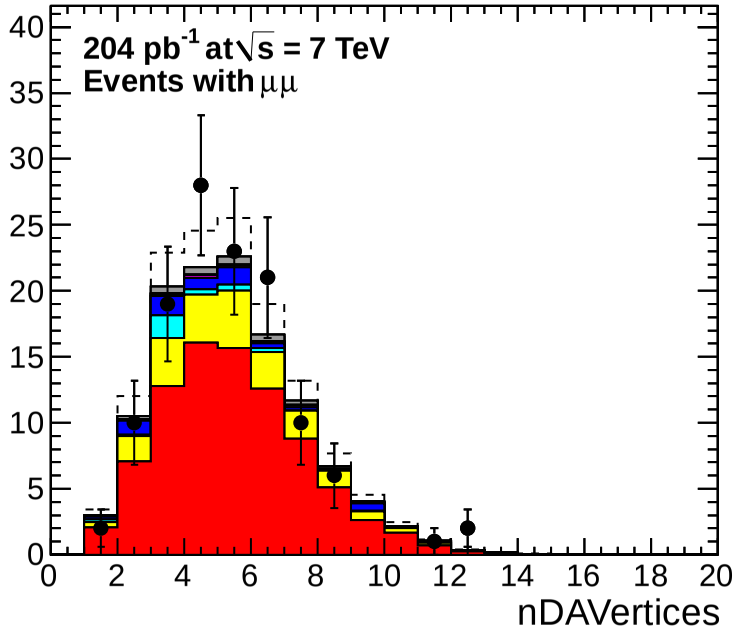
204 pb-1 at √s = 7 TeV
Events with μμ
nDAVertices

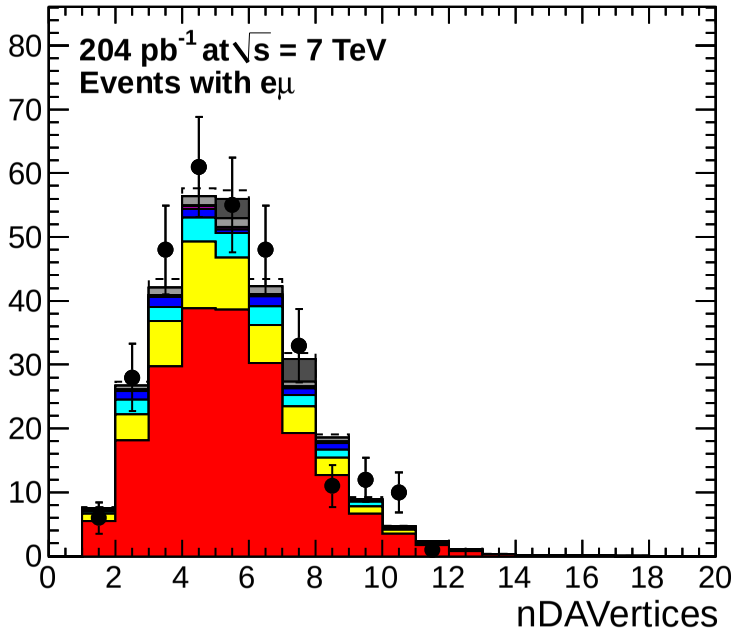
204 pb-1 at √s = 7 TeV
Events with eμ
nDAVertices

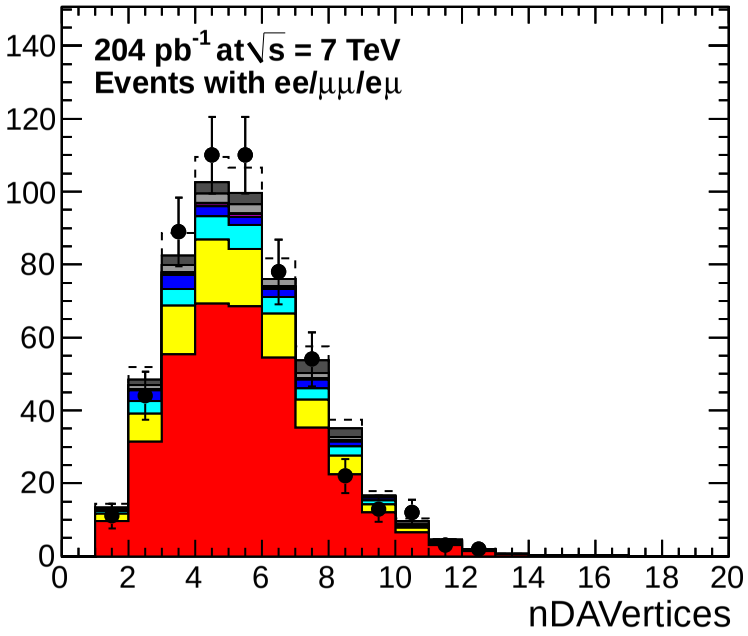
204 pb-1 at √s = 7 TeV
Events with ee/μμ/eμ
nDAVertices

data
ttll
tttau
ttfake
DY
WW
WZ
ZZ
t
wjets
LM1

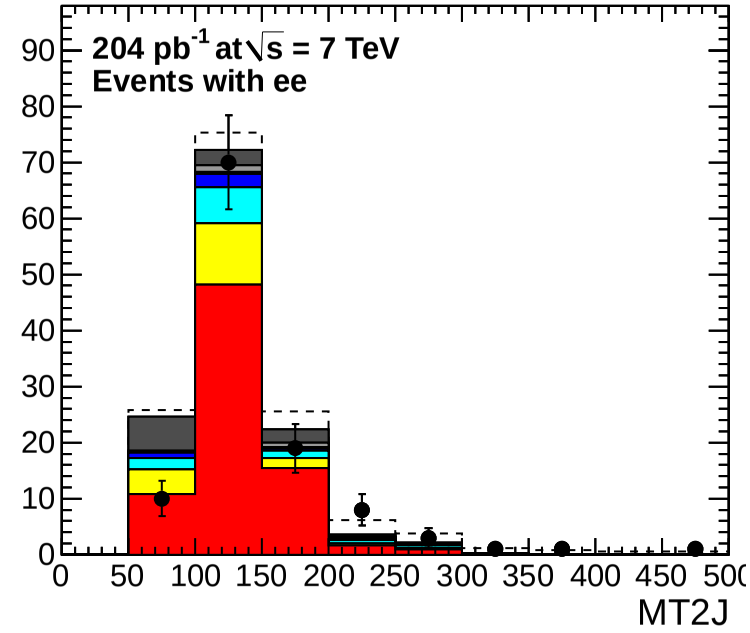
204 pb-1 at √s = 7 TeV
Events with ee
MT2J

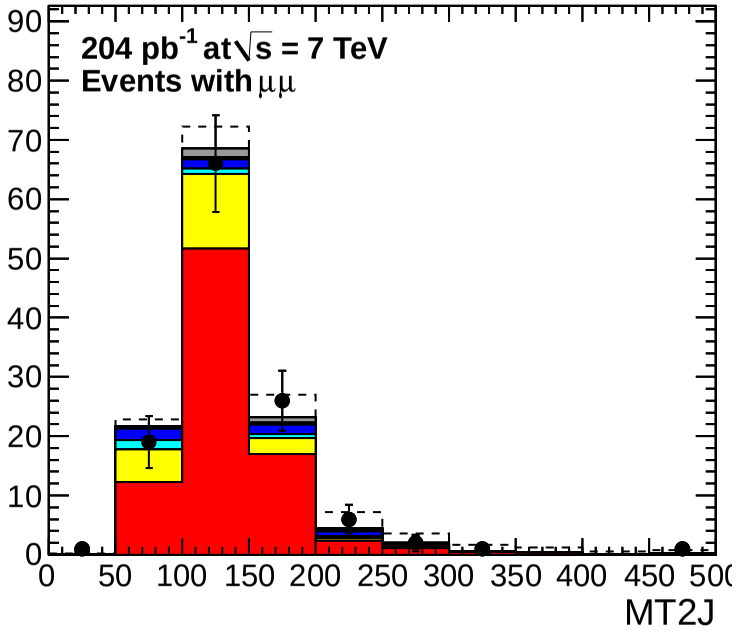
204 pb-1 at √s = 7 TeV
Events with μμ
MT2J

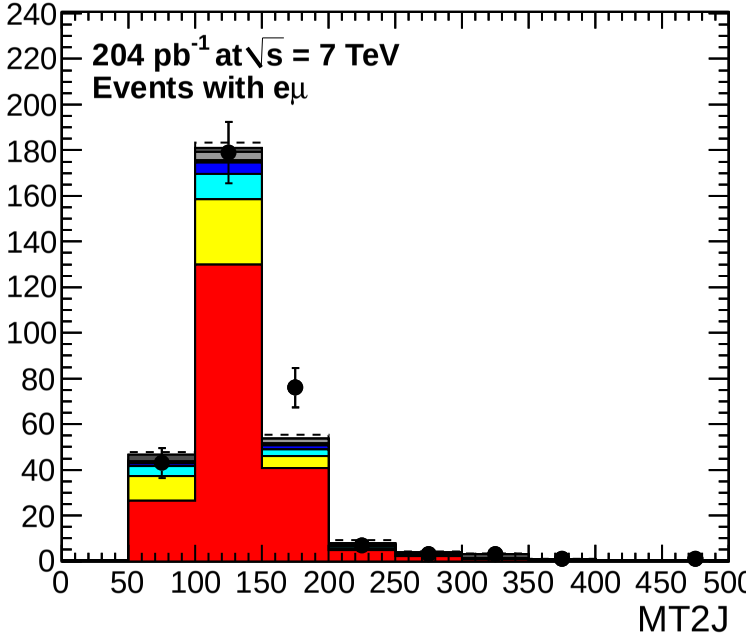
204 pb-1 at √s = 7 TeV
Events with eμ
MT2J

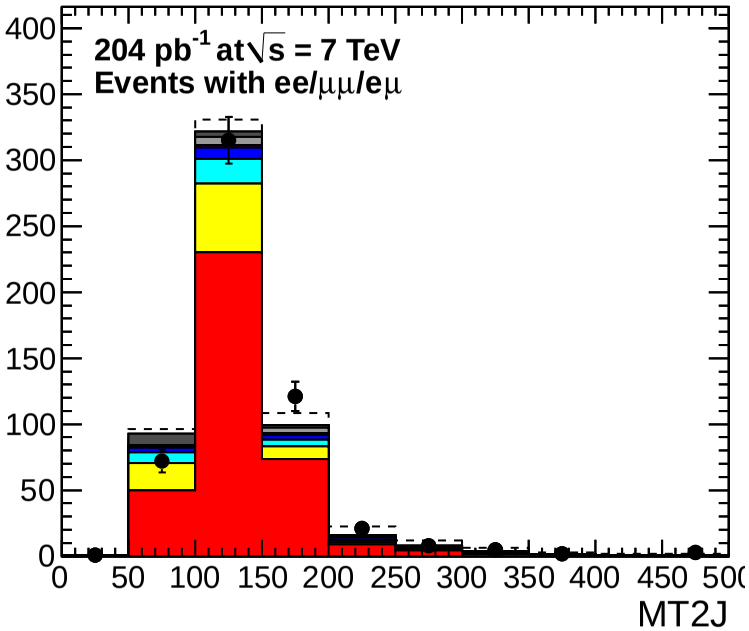
204 pb-1 at √s = 7 TeV
Events with ee/μμ/eμ
MT2J

data
ttll
tttau
ttfake
DY
WW
WZ
ZZ
t
wjets
LM1

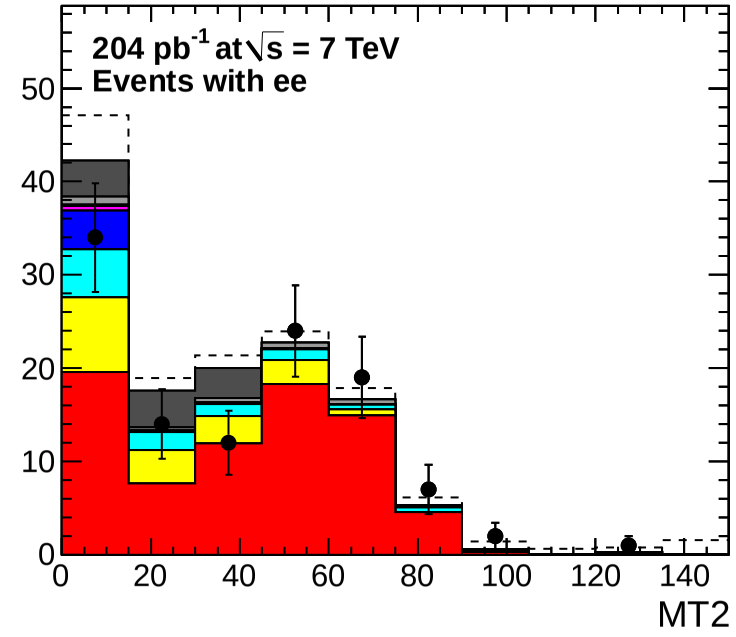
204 pb-1 at √s = 7 TeV
Events with ee
MT2

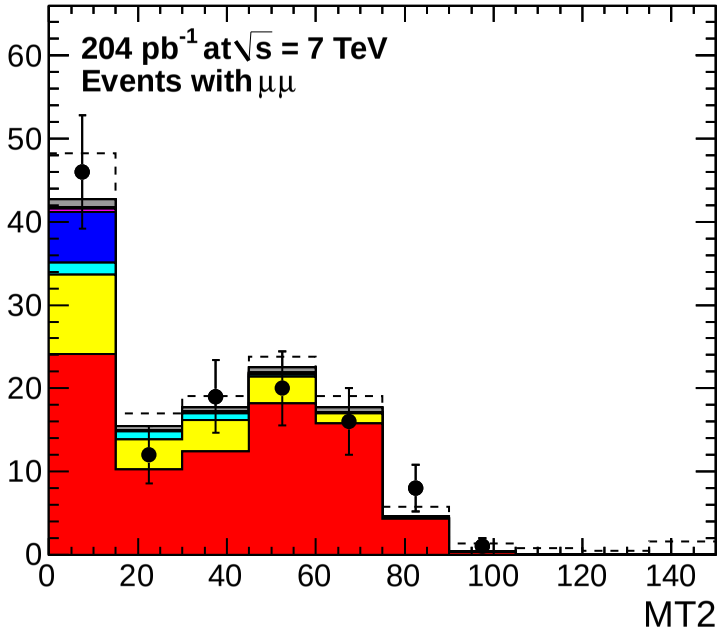
204 pb-1 at √s = 7 TeV
Events with μμ
MT2

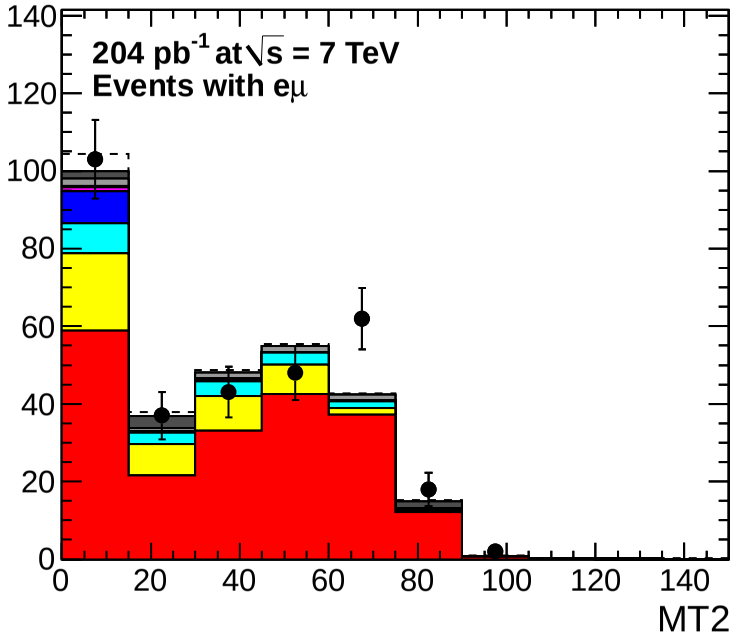
204 pb-1 at √s = 7 TeV
Events with eμ
MT2

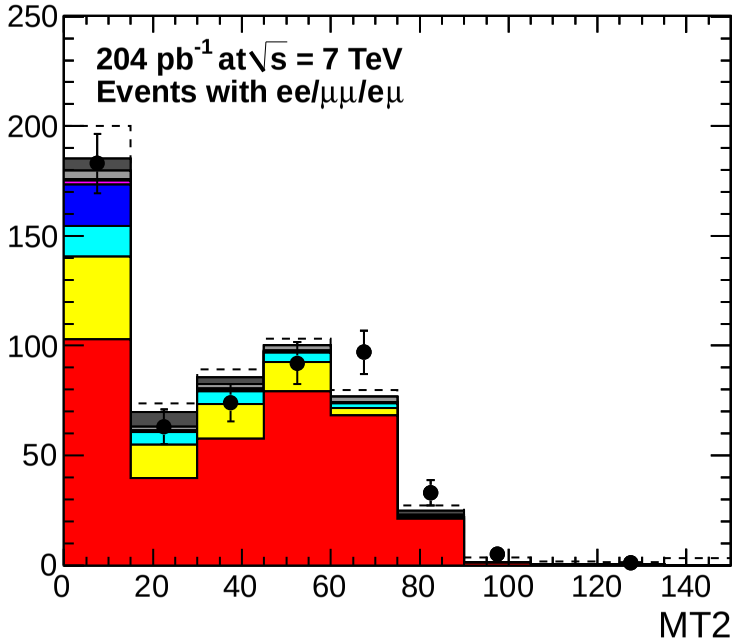
204 pb-1 at √s = 7 TeV
Events with ee/μμ/eμ
MT2

data
ttll
tttau
ttfake
DY
WW
WZ
ZZ
t
wjets
LM1

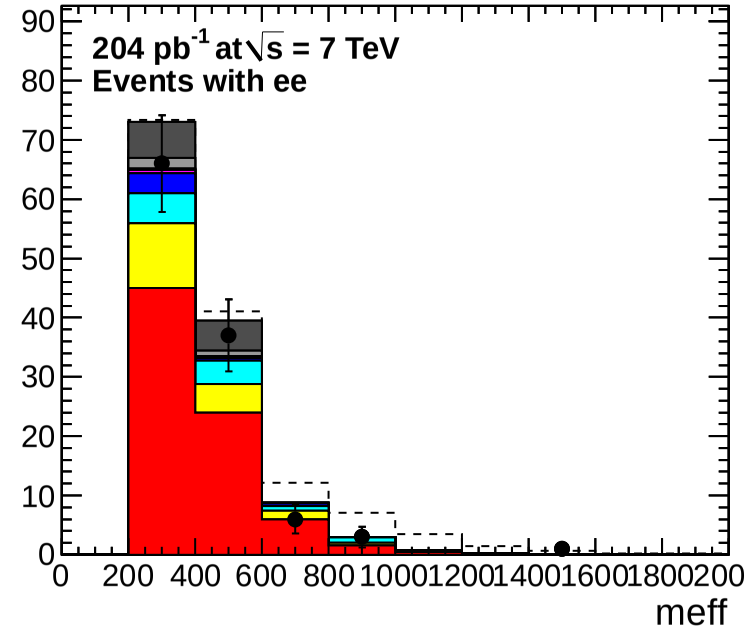
204 pb-1 at √s = 7 TeV
Events with ee
meff

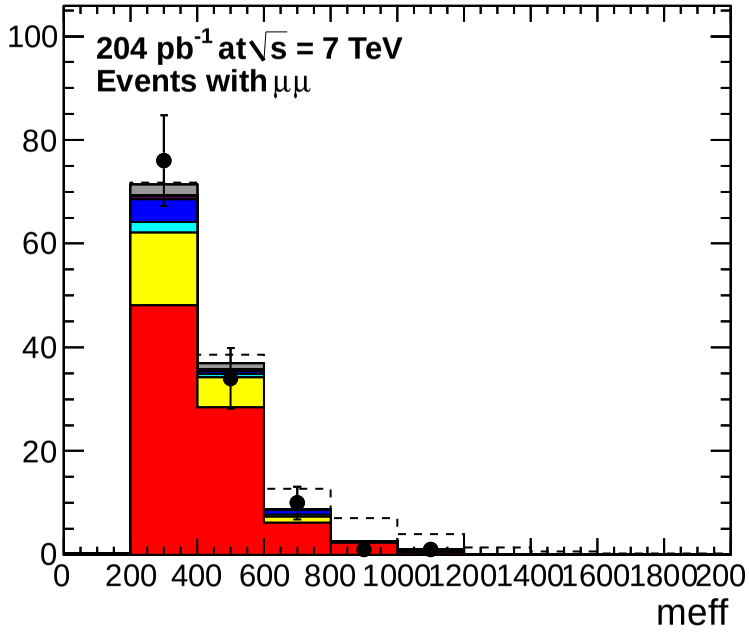
204 pb-1 at √s = 7 TeV
Events with μμ
meff

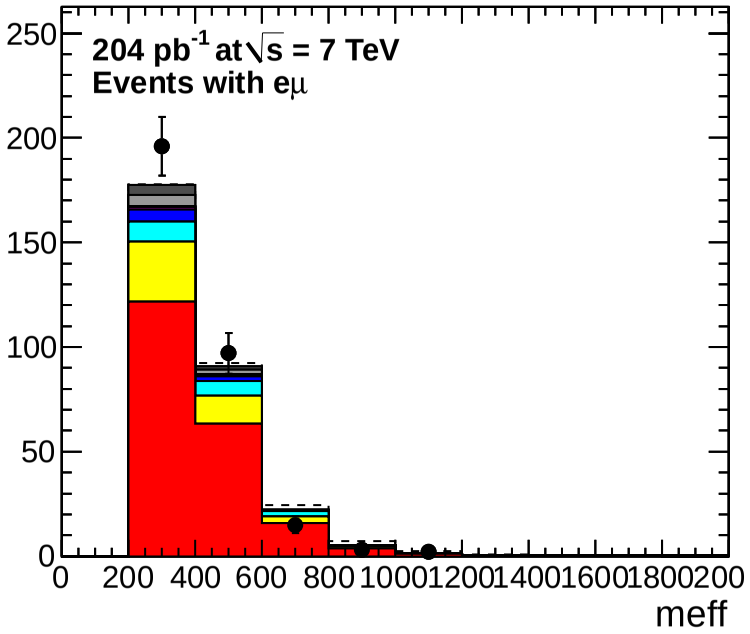
204 pb-1 at √s = 7 TeV
Events with eμ
meff

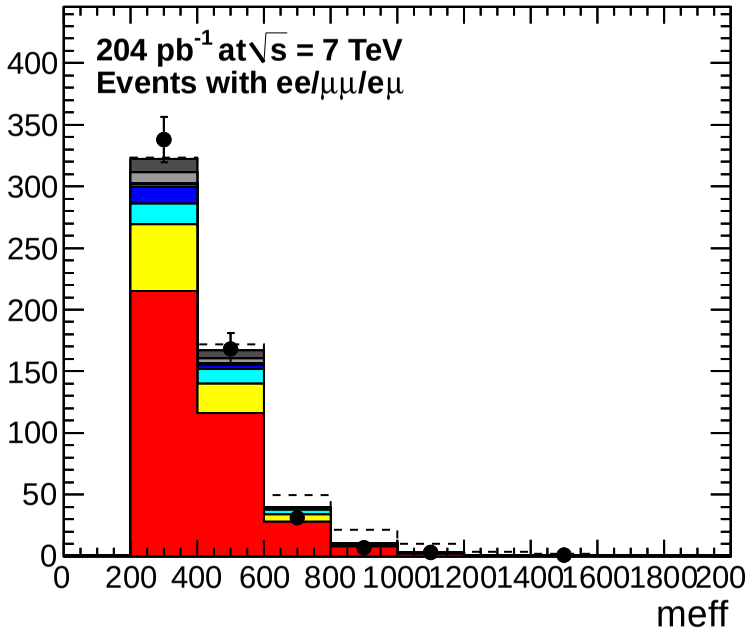
204 pb-1 at √s = 7 TeV
Events with ee/μμ/eμ
meff

data
ttll
tttau
ttfake
DY
WW
WZ
ZZ
t
wjets
LM1

Appendix D Data/MC Comparison: 2010 Signal Region

Here we compare data and MC distributions for data passing the 2010 signal region requirements (preselection + $y > 8.5$ GeV$^{1/2}$ + $H_T > 300$ GeV. The high p_T dilepton trigger data is used. We observe 14 events in this region.

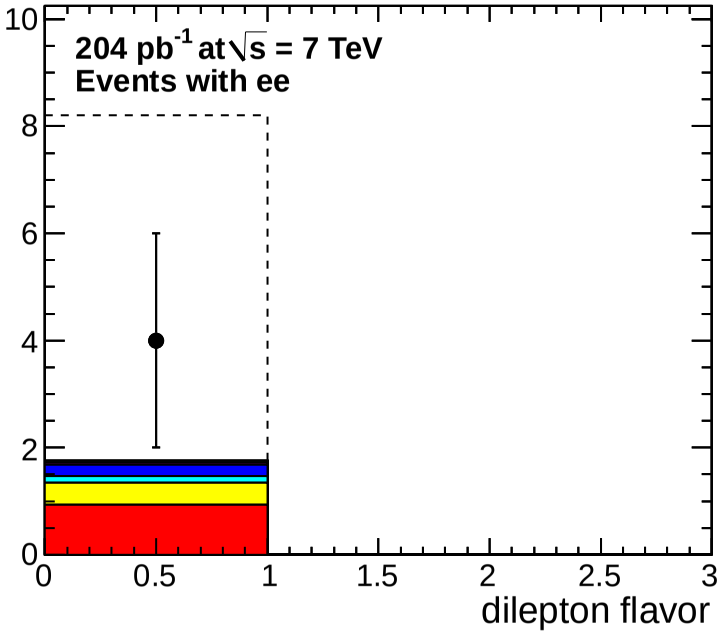
204 pb-1 at √s = 7 TeV
Events with ee
dilepton flavor

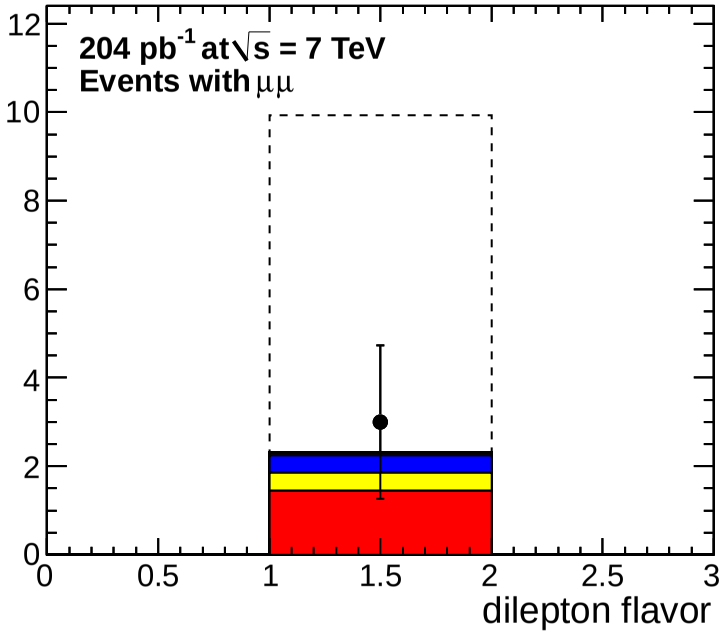
204 pb-1 at √s = 7 TeV
Events with μμ
dilepton flavor

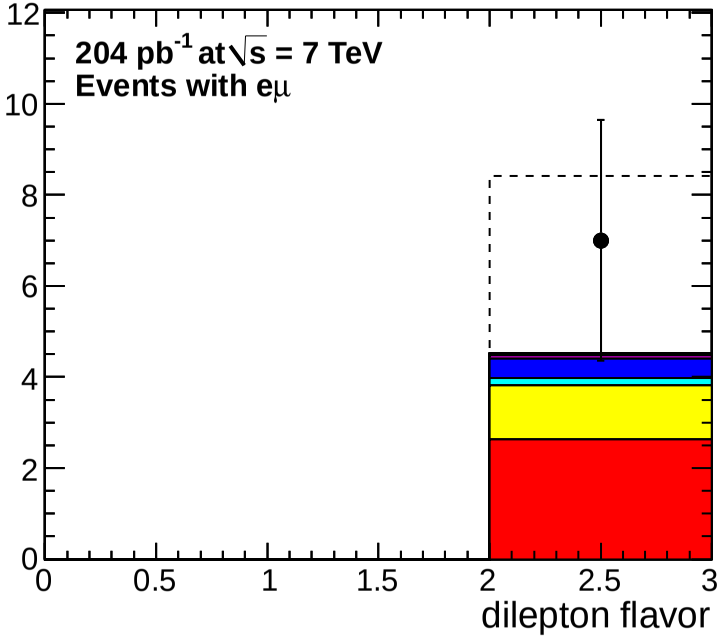
204 pb-1 at √s = 7 TeV
Events with eμ
dilepton flavor

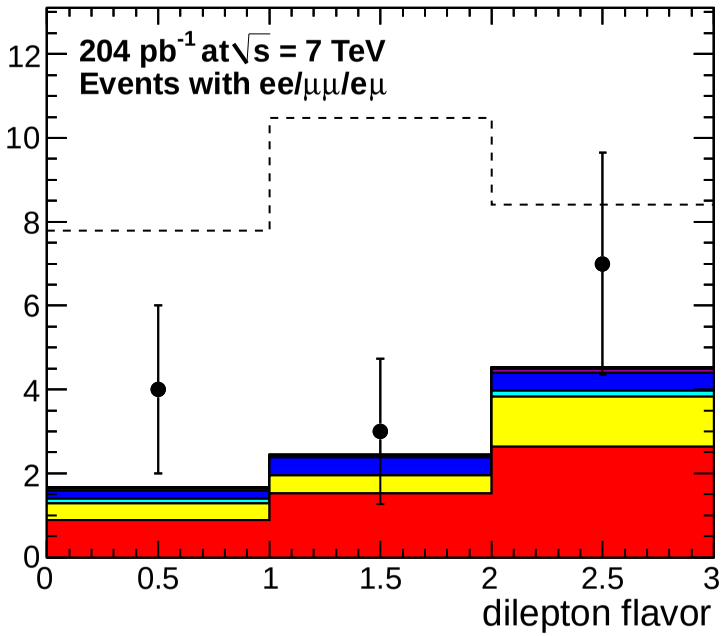
204 pb-1 at √s = 7 TeV
Events with ee/μμ/eμ
dilepton flavor

data
ttll
tttau
ttfake
DY
WW
WZ
ZZ
t
wjets
LM1

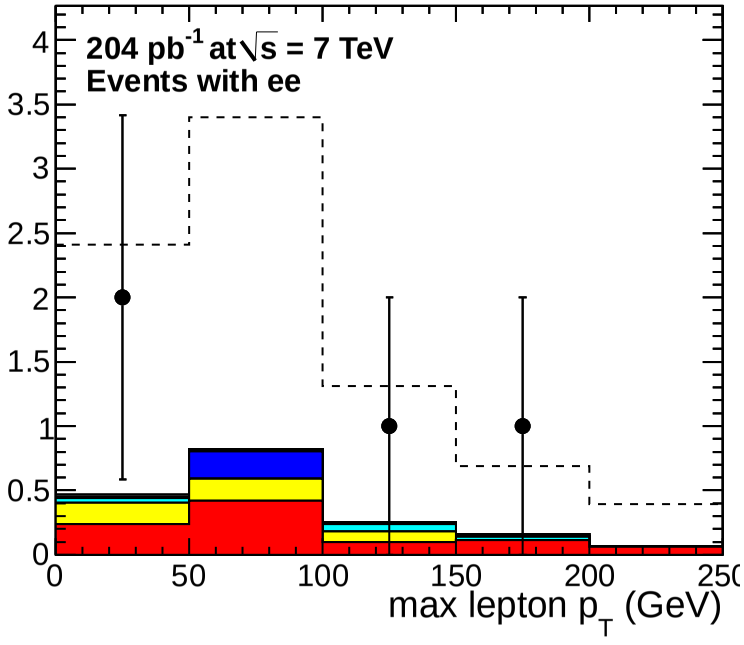
204 pb-1 at √s = 7 TeV
Events with ee
max lepton pT (GeV)

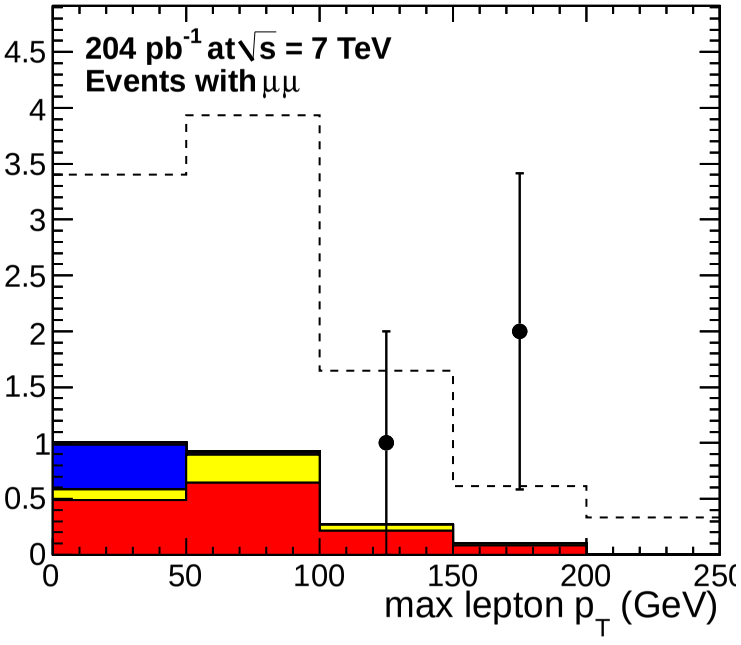
204 pb-1 at √s = 7 TeV
Events with μμ
max lepton pT (GeV)

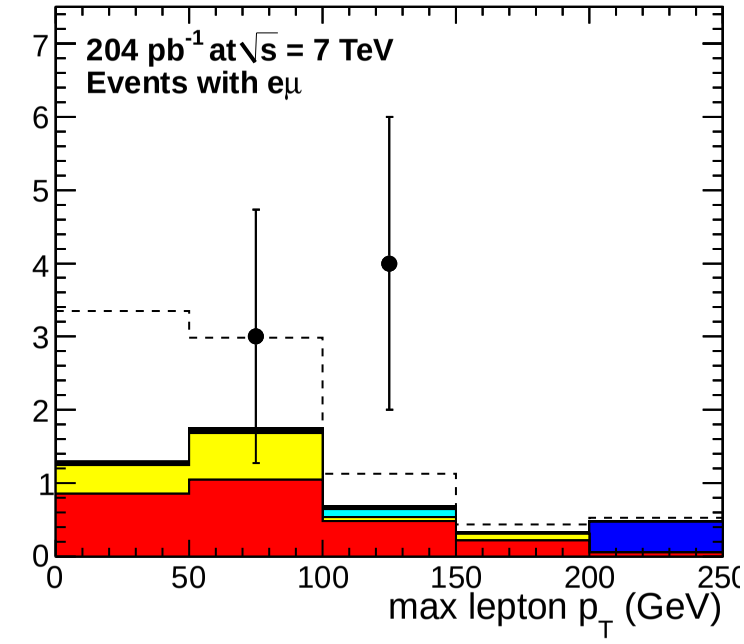
204 pb-1 at √s = 7 TeV
Events with eμ
max lepton pT (GeV)

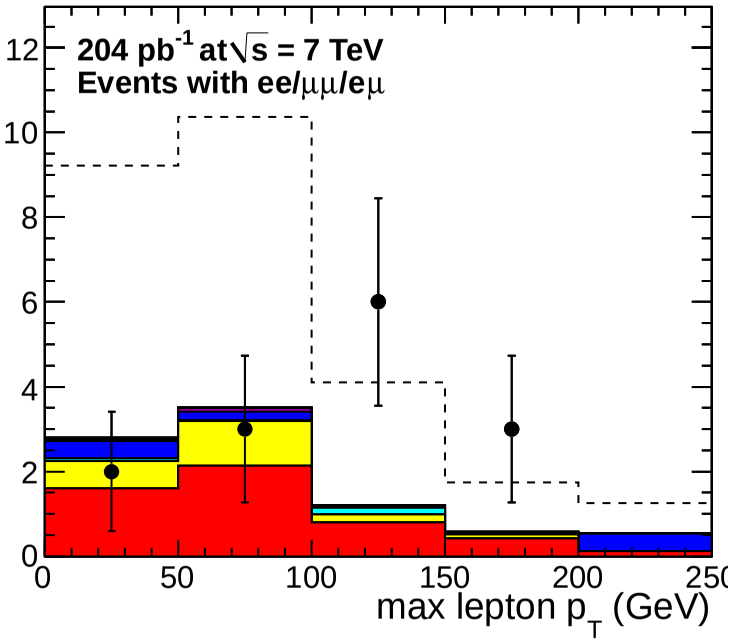
204 pb-1 at √s = 7 TeV
Events with ee/μμ/eμ
max lepton pT (GeV)

data
ttll
tttau
ttfake
DY
WW
WZ
ZZ
t
wjets
LM1

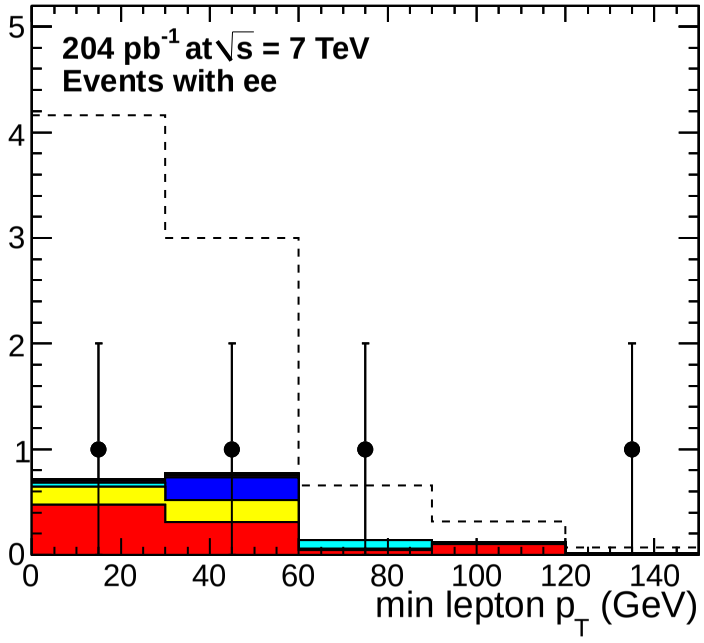
204 pb-1 at √s = 7 TeV
Events with ee
min lepton pT (GeV)

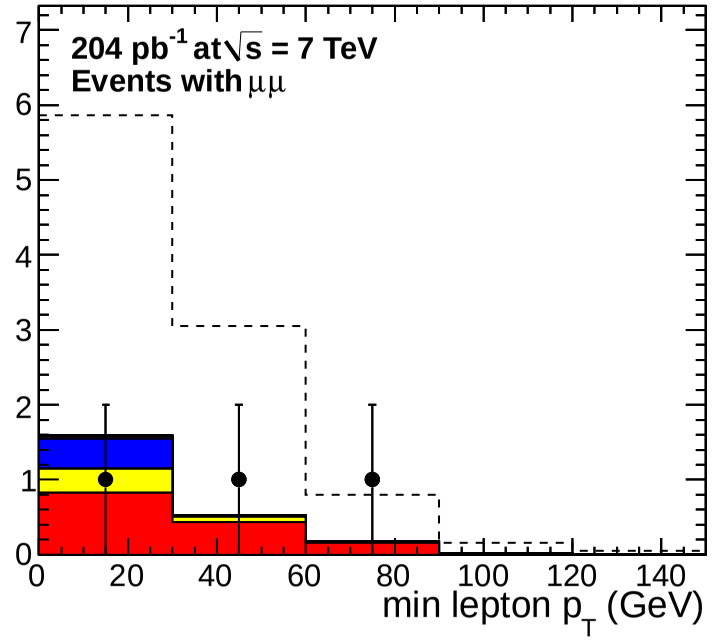
204 pb-1 at √s = 7 TeV
Events with μμ
min lepton pT (GeV)

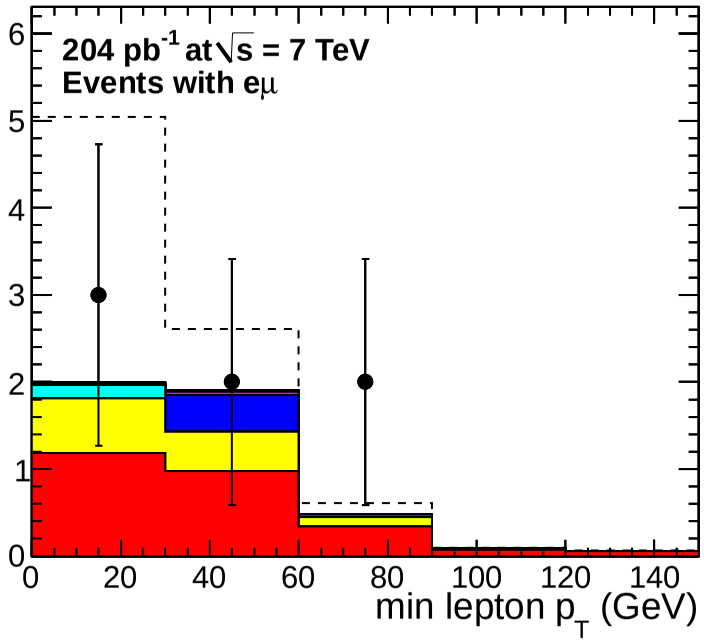
204 pb-1 at √s = 7 TeV
Events with eμ
min lepton pT (GeV)

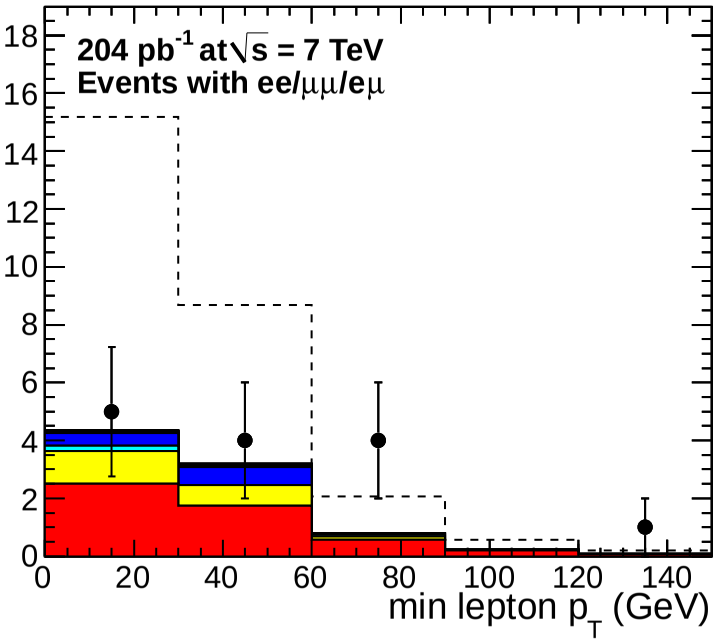
204 pb-1 at √s = 7 TeV
Events with ee/μμ/eμ
min lepton pT (GeV)

data
ttll
tttau
ttfake
DY
WW
WZ
ZZ
t
wjets
LM1

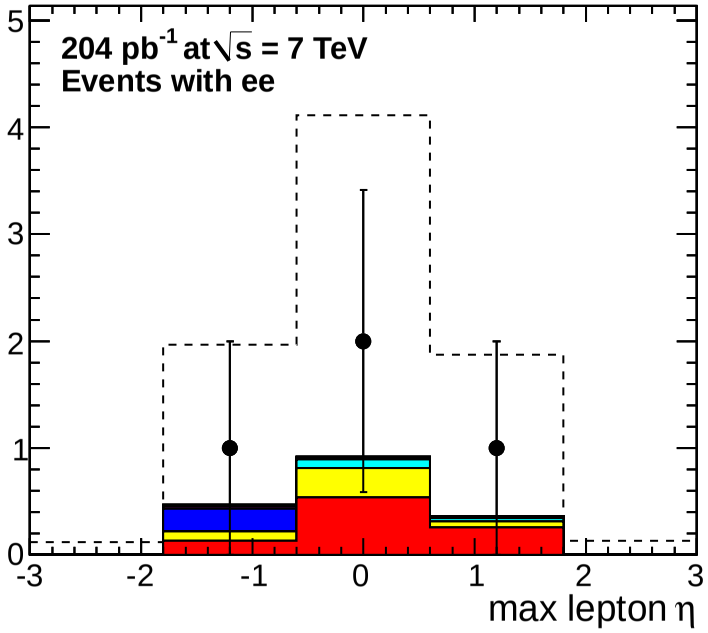
204 pb-1 at √s = 7 TeV
Events with ee
max lepton η

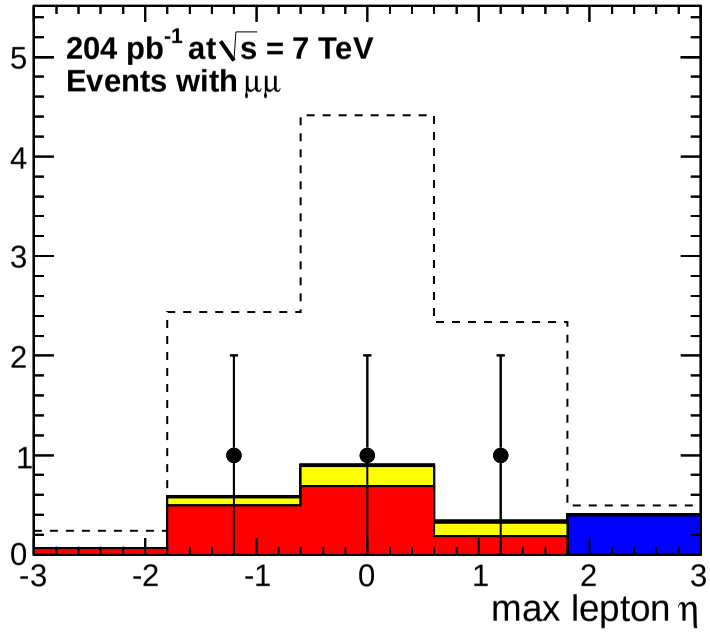
204 pb-1 at √s = 7 TeV
Events with μμ
max lepton η

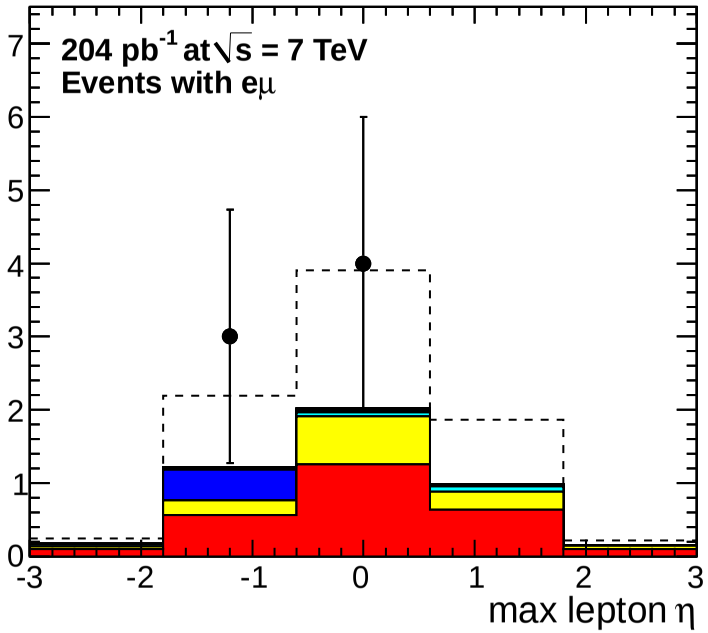
204 pb-1 at √s = 7 TeV
Events with eμ
max lepton η

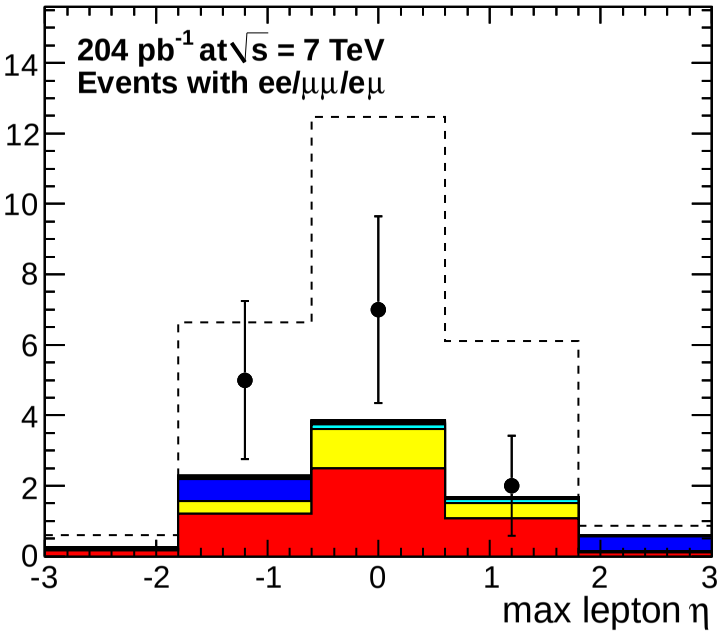
204 pb-1 at √s = 7 TeV
Events with ee/μμ/eμ
max lepton η

data
ttll
tttau
ttfake
DY
WW
WZ
ZZ
t
wjets
LM1

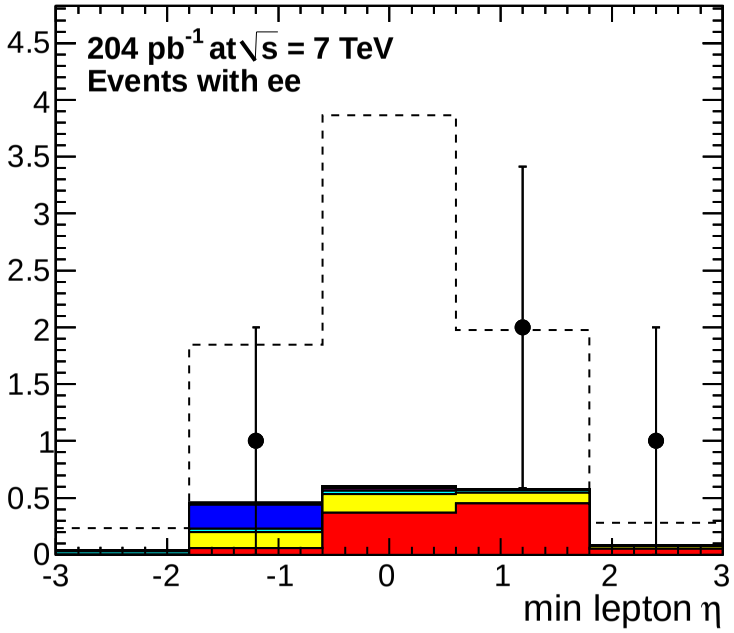
204 pb-1 at √s = 7 TeV
Events with ee
min lepton η

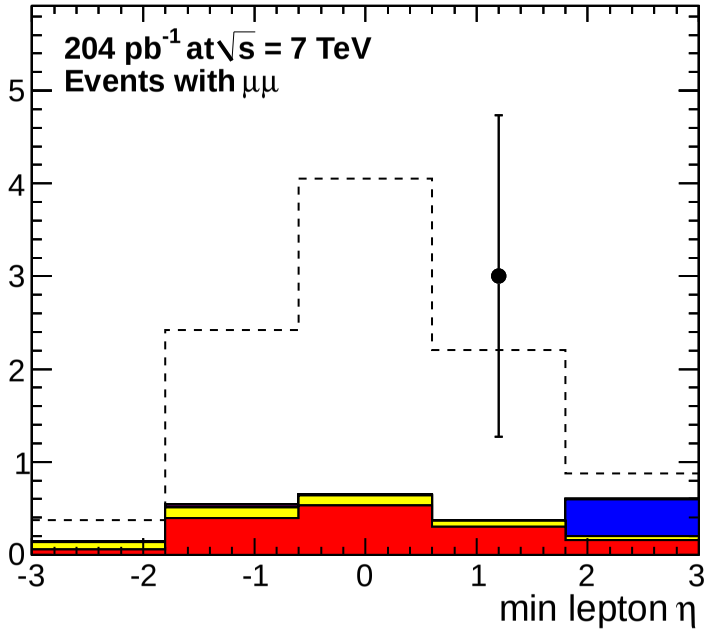
204 pb-1 at √s = 7 TeV
Events with μμ
min lepton η

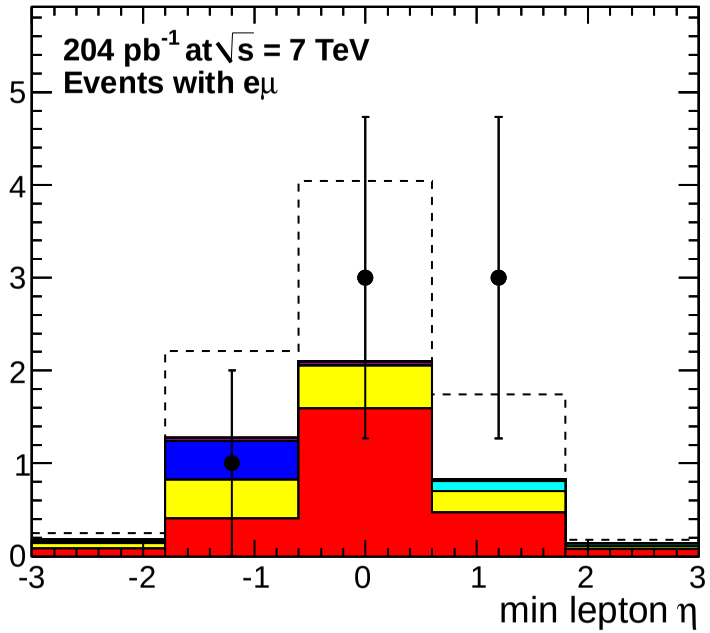
204 pb-1 at √s = 7 TeV
Events with eμ
min lepton η

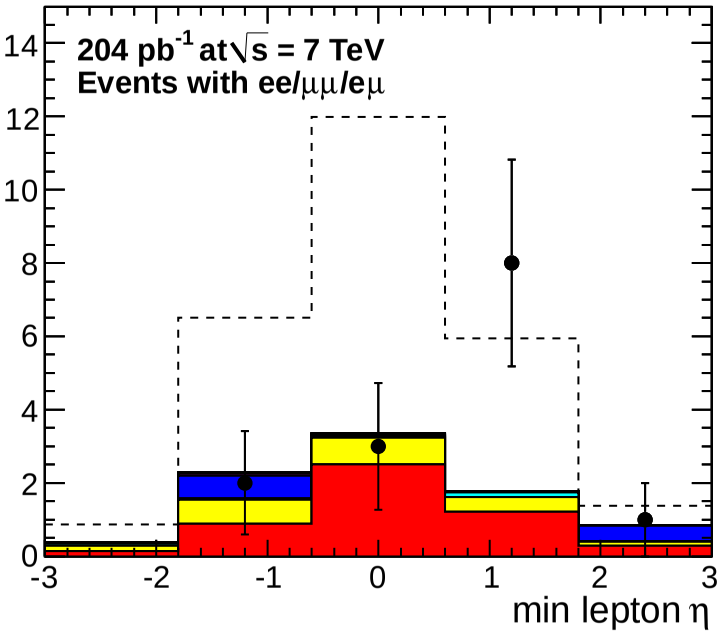
204 pb-1 at √s = 7 TeV
Events with ee/μμ/eμ
min lepton η

data
ttll
tttau
ttfake
DY
WW
WZ
ZZ
t
wjets
LM1

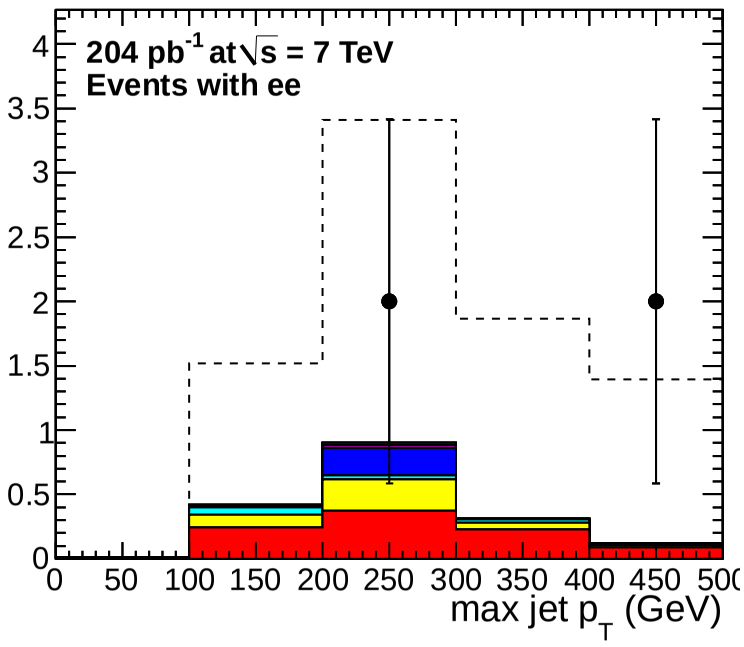

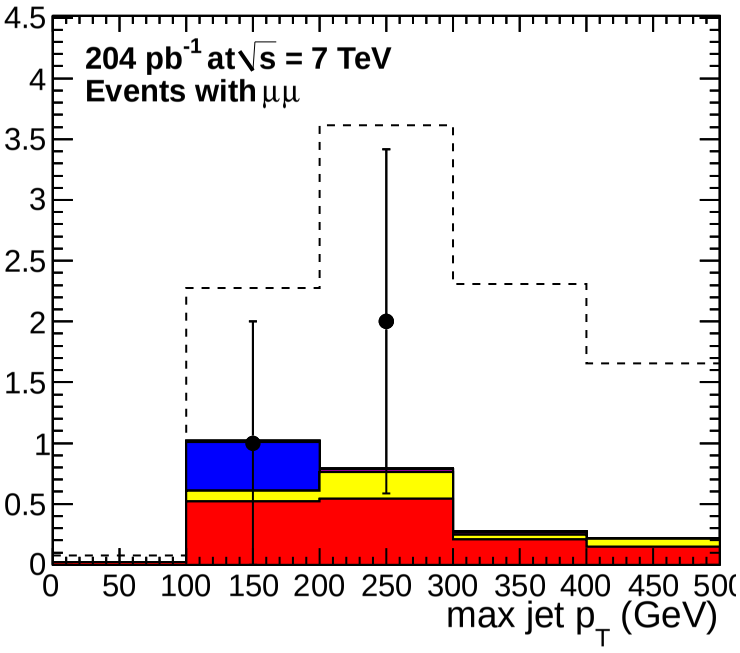

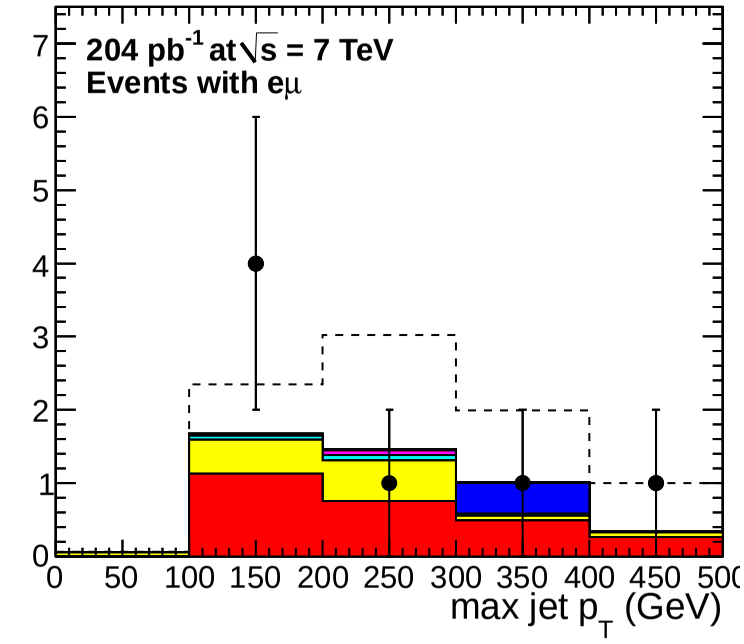

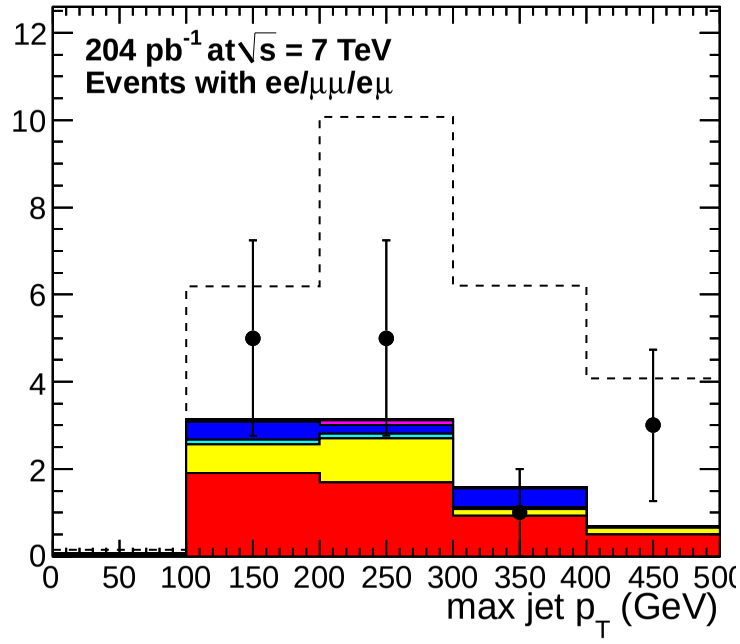

data
ttll
tttau
ttfake
DY
WW
WZ
ZZ
t
wjets
LM1

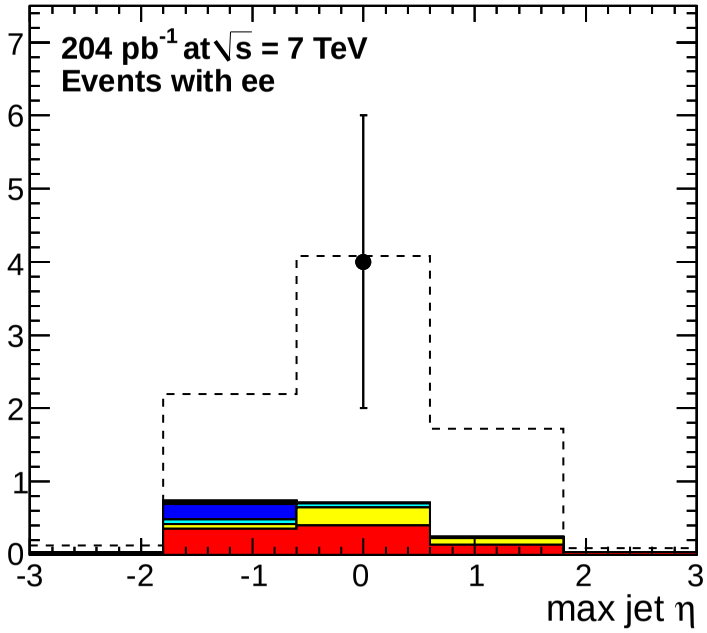
204 pb-1 at √s = 7 TeV
Events with ee
max jet η

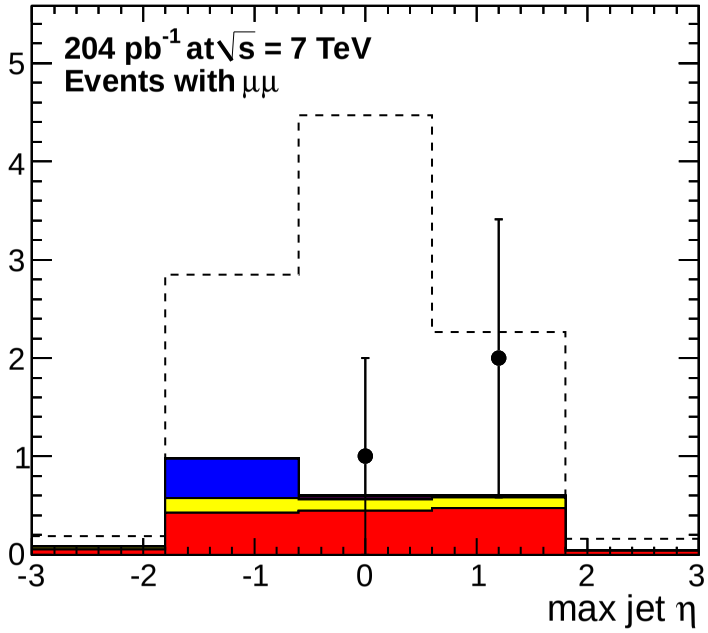
204 pb-1 at √s = 7 TeV
Events with μμ
max jet η

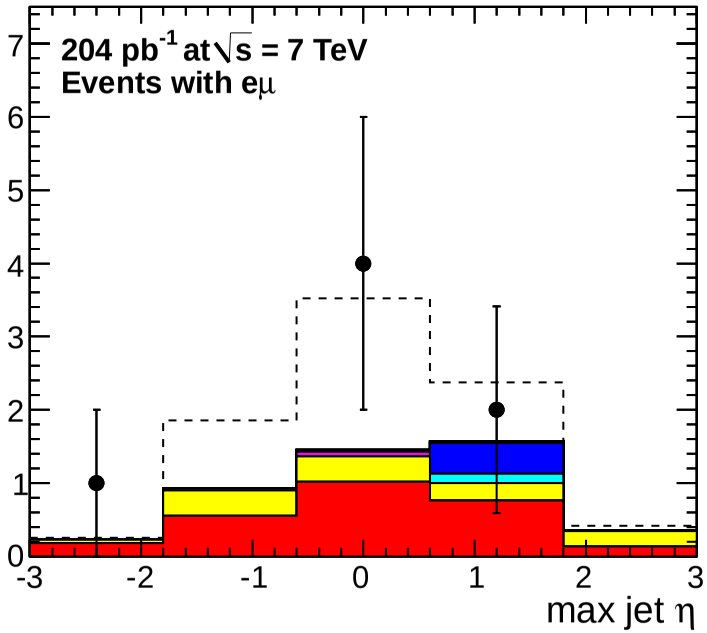
204 pb-1 at √s = 7 TeV
Events with eμ
max jet η

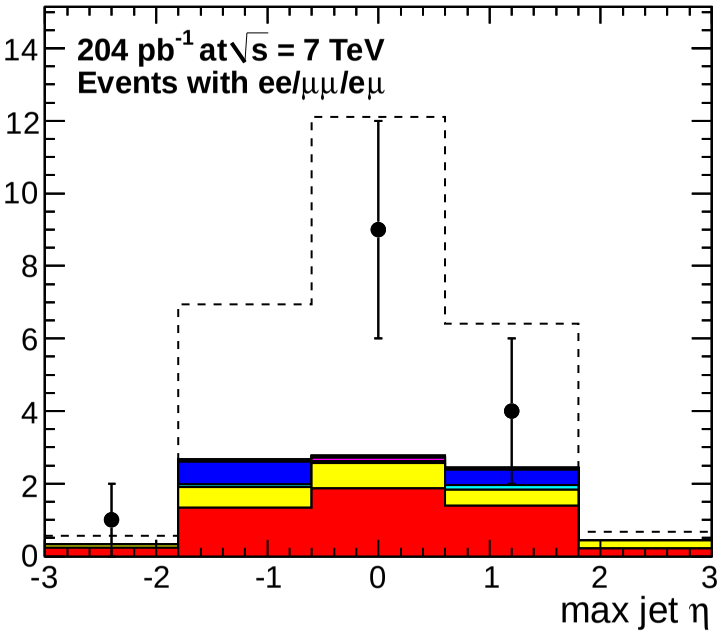
204 pb-1 at √s = 7 TeV
Events with ee/μμ/eμ
max jet η

data
ttll
tttau
ttfake
DY
WW
WZ
ZZ
t
wjets
LM1

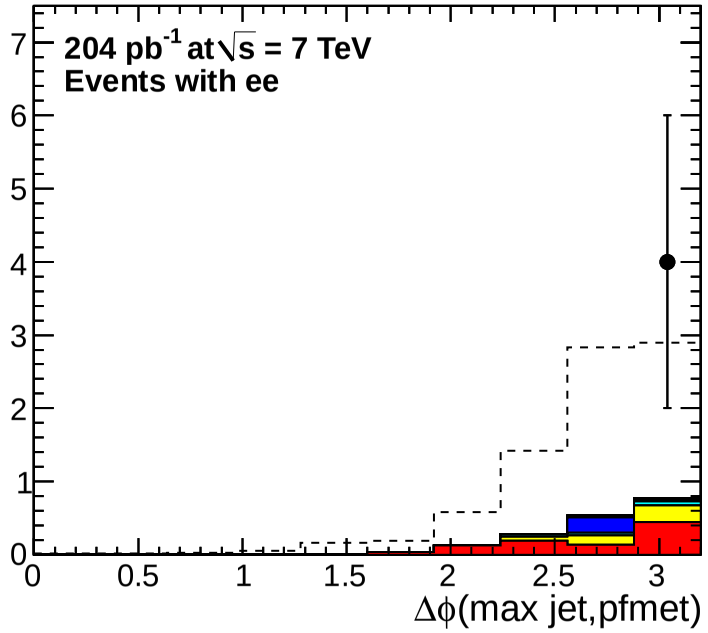
204 pb-1 at √s = 7 TeV
Events with ee
Δφ(max jet,pfmet)

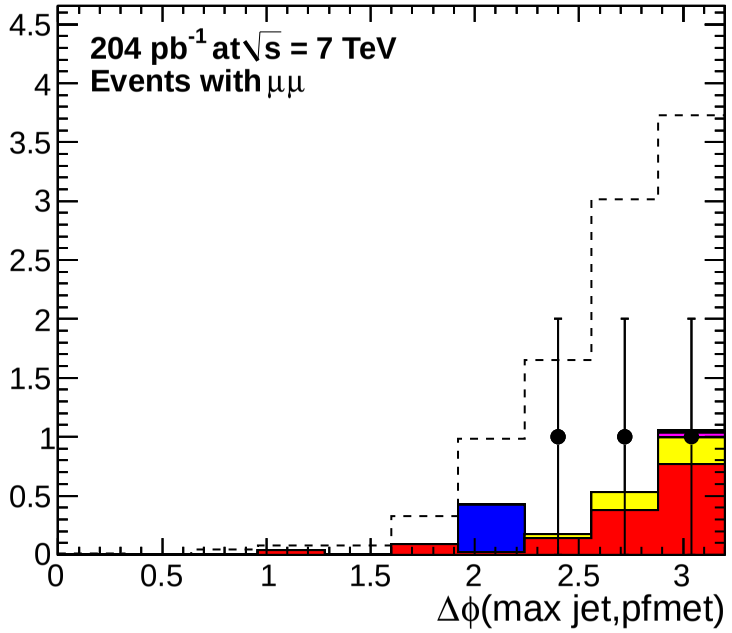
204 pb-1 at √s = 7 TeV
Events with μμ
Δφ(max jet,pfmet)

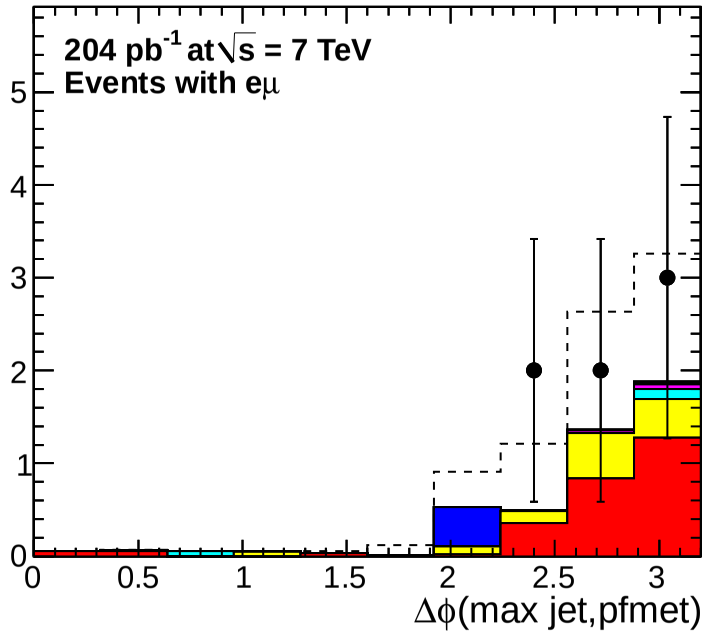
204 pb-1 at √s = 7 TeV
Events with eμ
Δφ(max jet,pfmet)

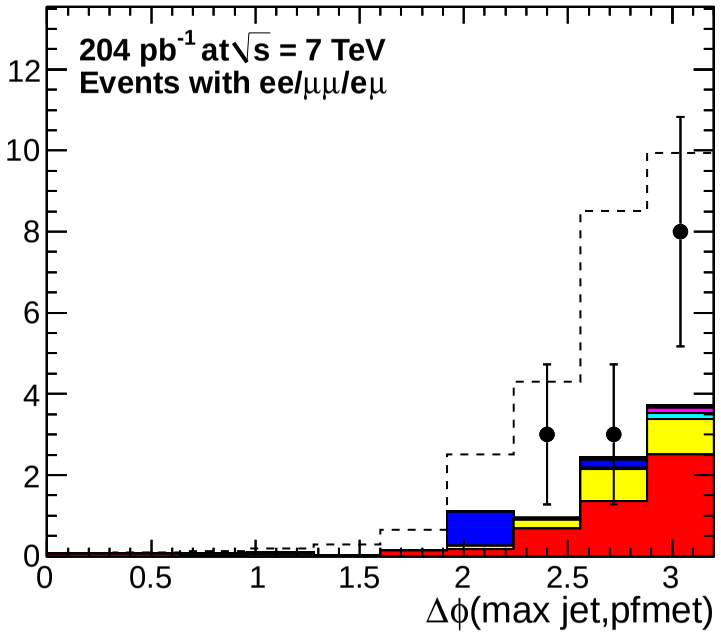
204 pb-1 at √s = 7 TeV
Events with ee/μμ/eμ
Δφ(max jet,pfmet)

data
ttll
tttau
ttfake
DY
WW
WZ
ZZ
t
wjets
LM1

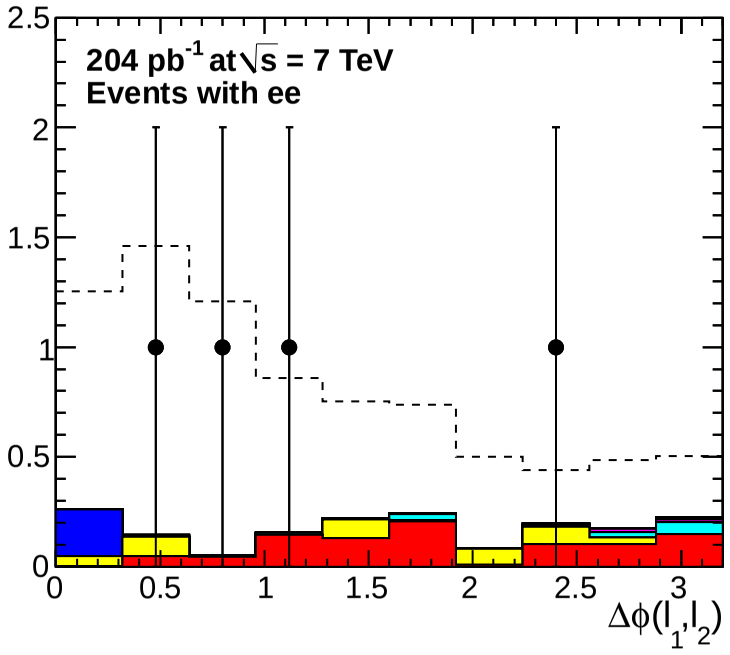
204 pb-1 at √s = 7 TeV
Events with ee
Δφ(l1,l2)

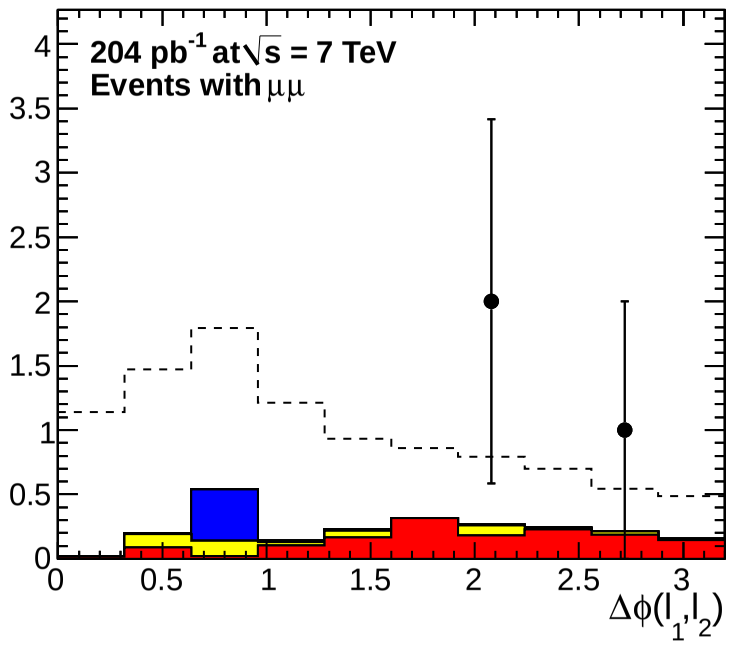
204 pb-1 at √s = 7 TeV
Events with μμ
Δφ(l1,l2)

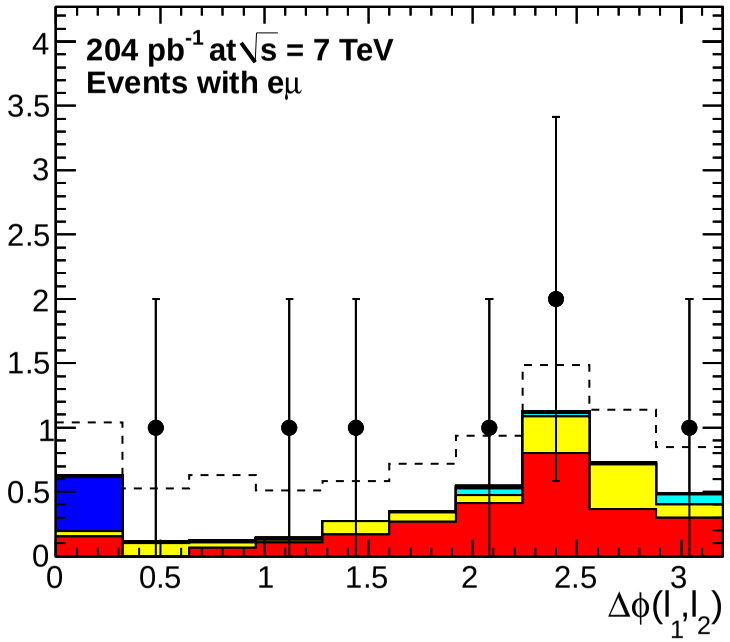
204 pb-1 at √s = 7 TeV
Events with eμ
Δφ(l1,l2)

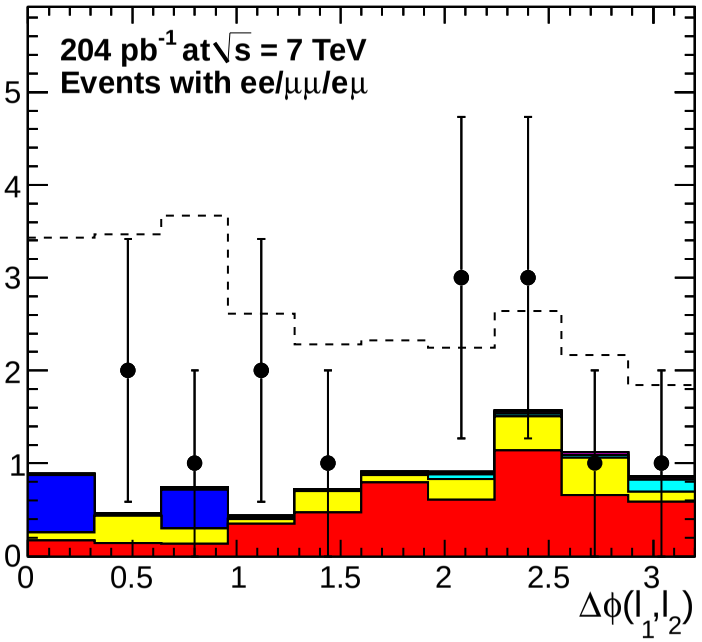
204 pb-1 at √s = 7 TeV
Events with ee/μμ/eμ
Δφ(l1,l2)

data
ttll
tttau
ttfake
DY
WW
WZ
ZZ
t
wjets
LM1

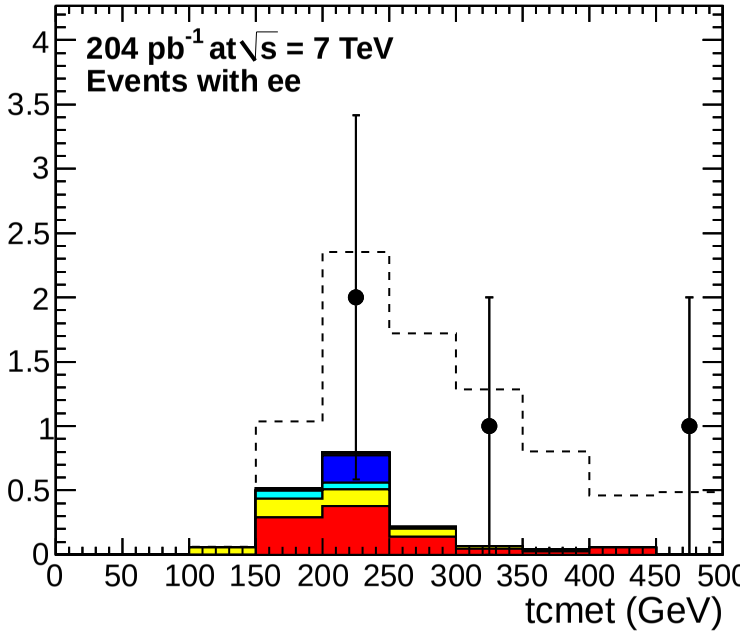

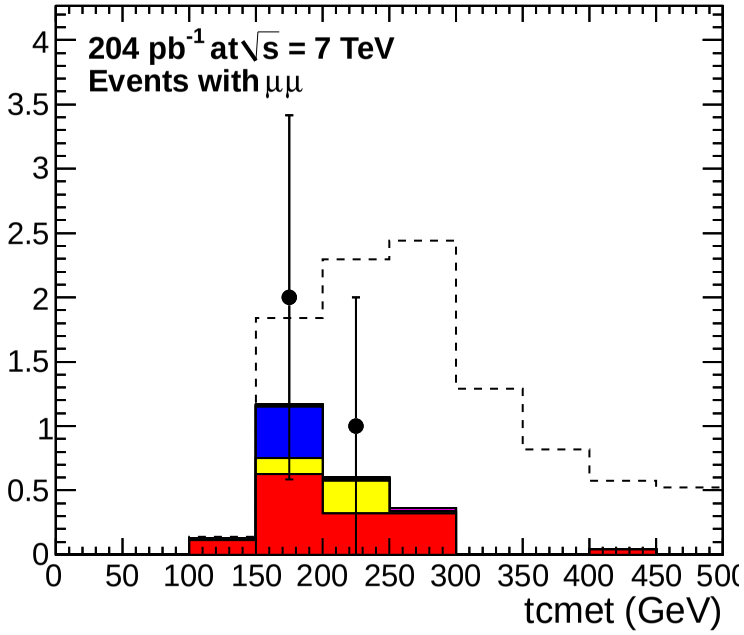

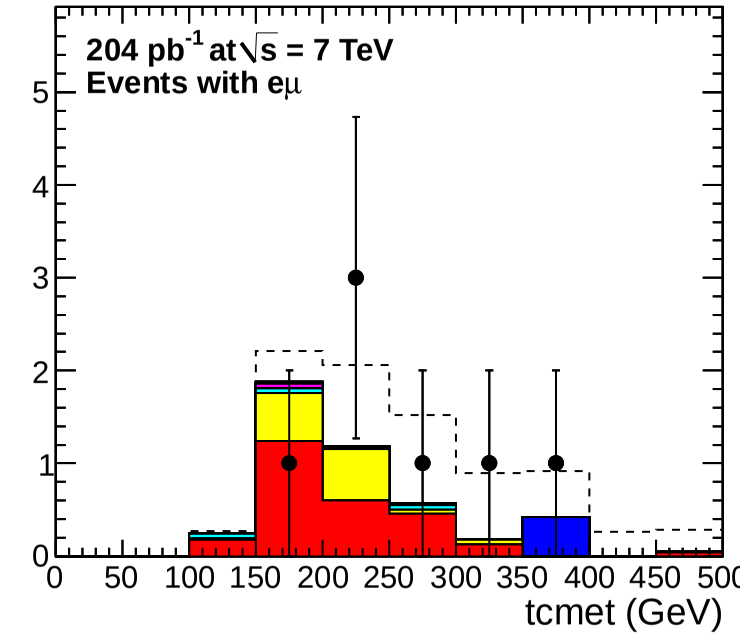

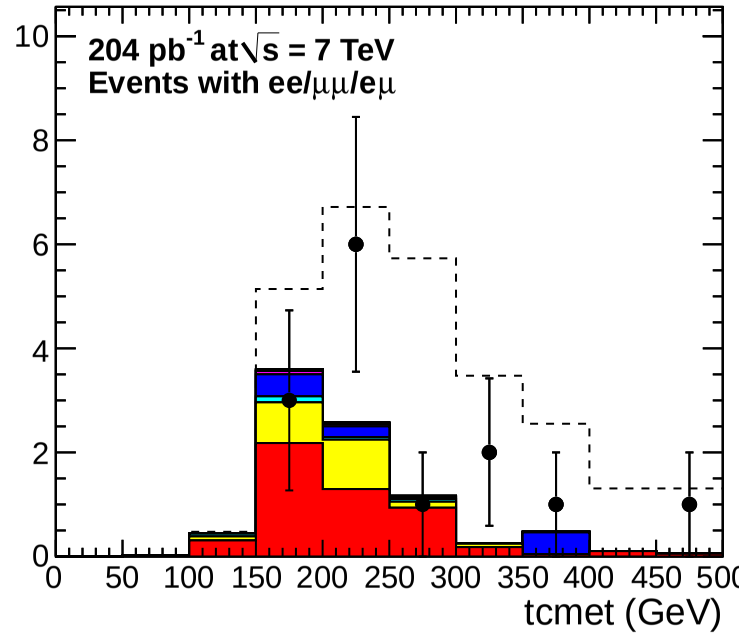

data
ttll
tttau
ttfake
DY
WW
WZ
ZZ
t
wjets
LM1

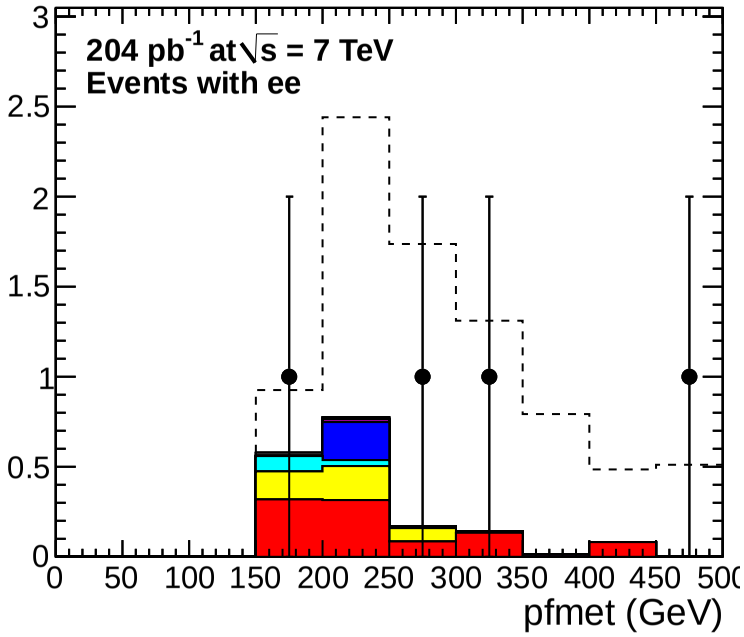

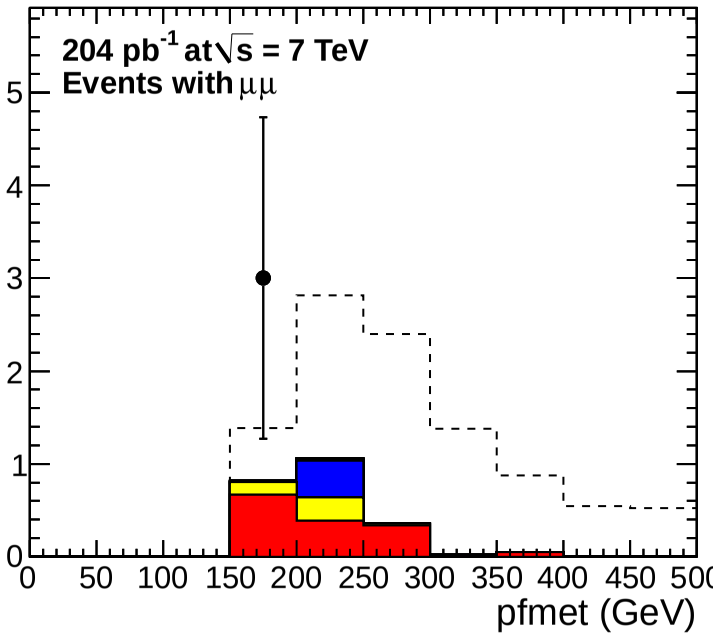

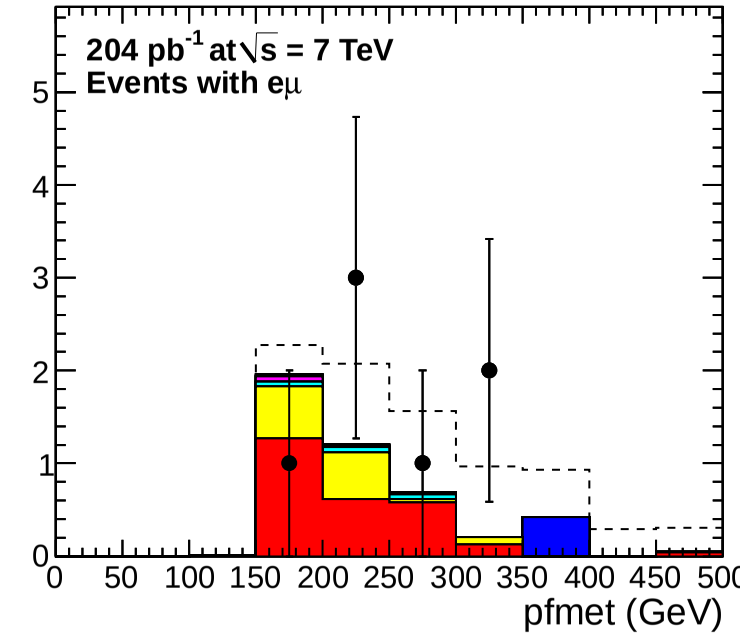

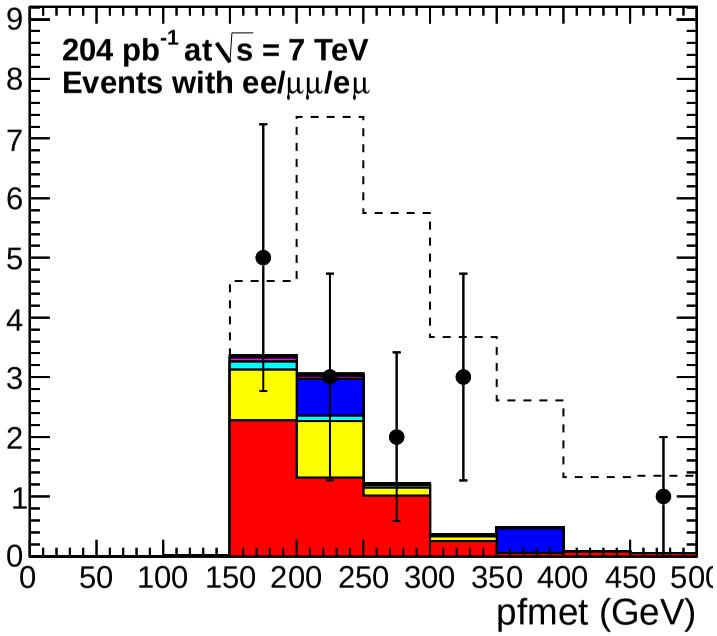

data
ttll
tttau
ttfake
DY
WW
WZ
ZZ
t
wjets
LM1

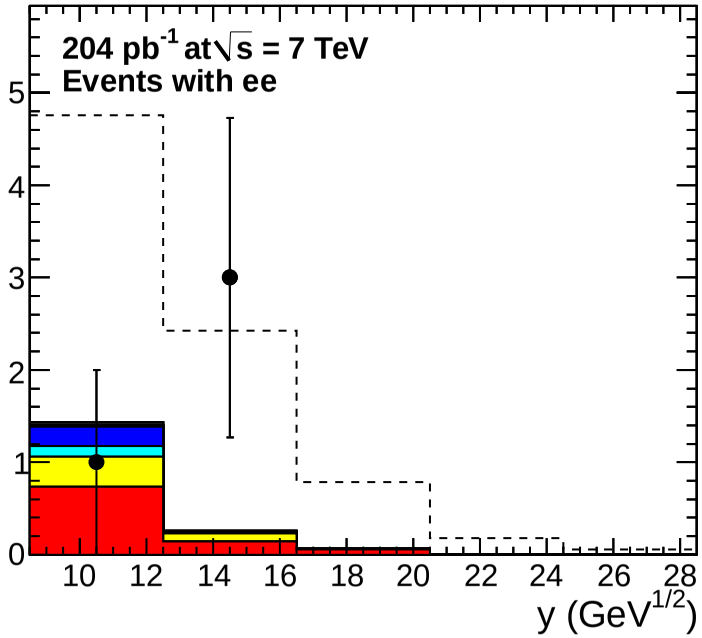
204 pb-1 at√s = 7 TeV
Events with ee
y (GeV1/2)

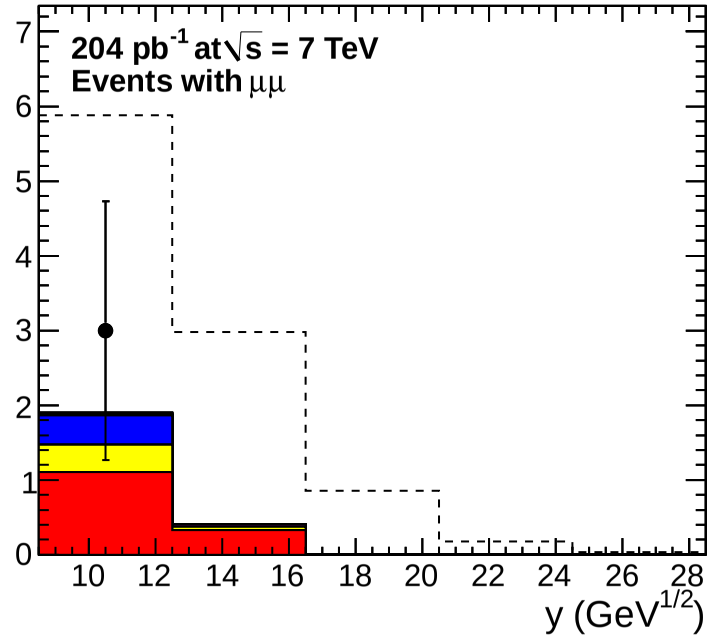
204 pb-1 at√s = 7 TeV
Events with μμ
y (GeV1/2)

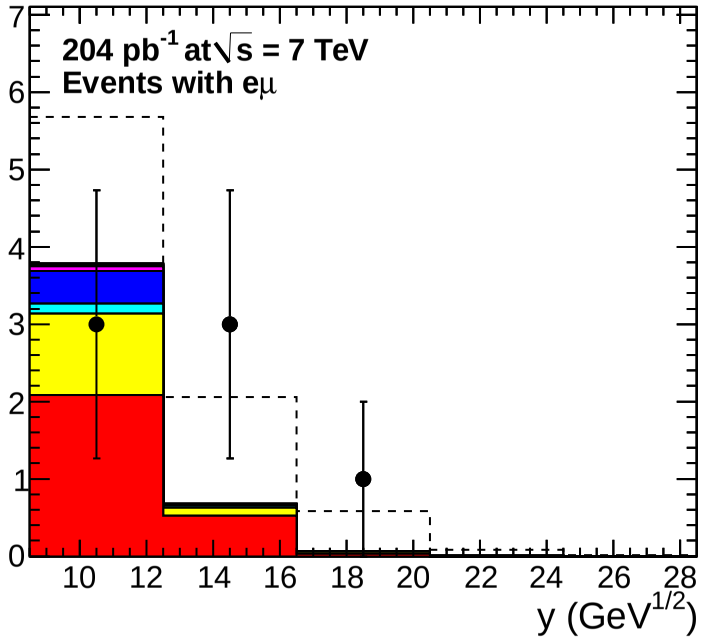
204 pb-1 at√s = 7 TeV
Events with eμ
y (GeV1/2)

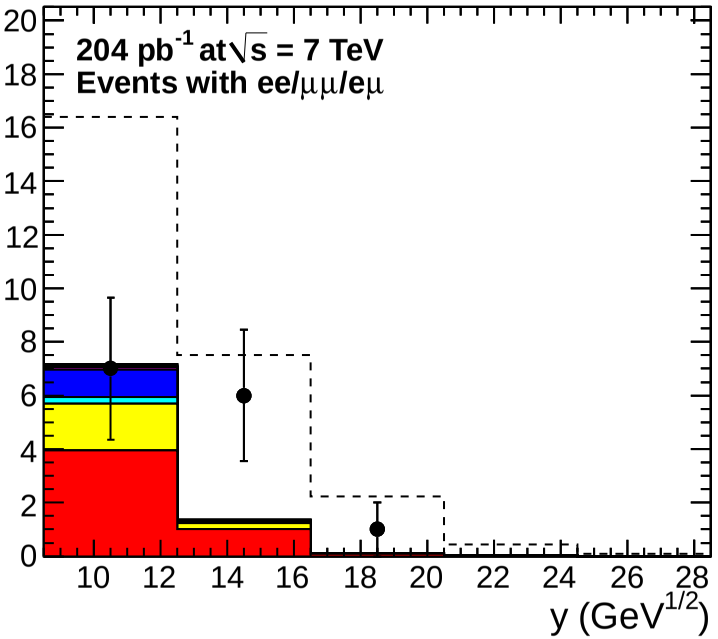
204 pb-1 at√s = 7 TeV
Events with ee/μμ/eμ
y (GeV1/2)

data
ttll
tttau
ttfake
DY
WW
WZ
ZZ
t
wjets
LM1

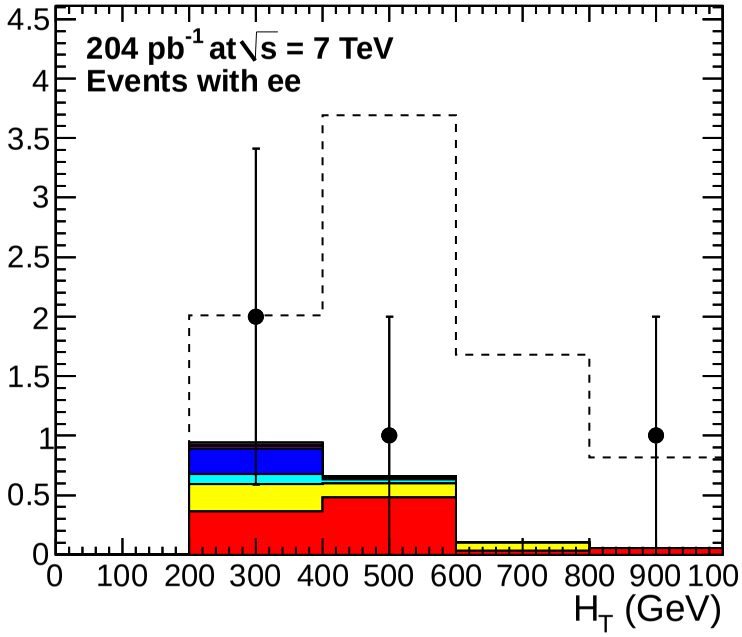
204 pb-1 at √s = 7 TeV
Events with ee
HT (GeV)

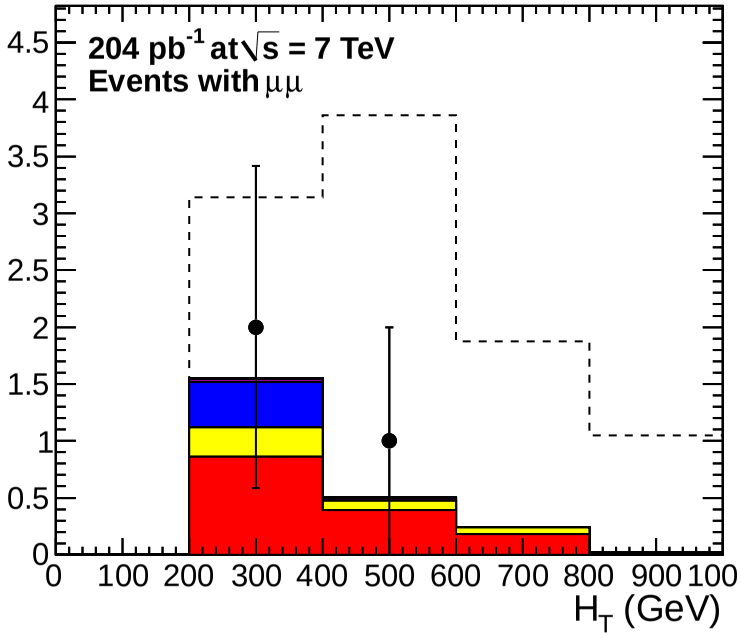
204 pb-1 at √s = 7 TeV
Events with μμ
HT (GeV)

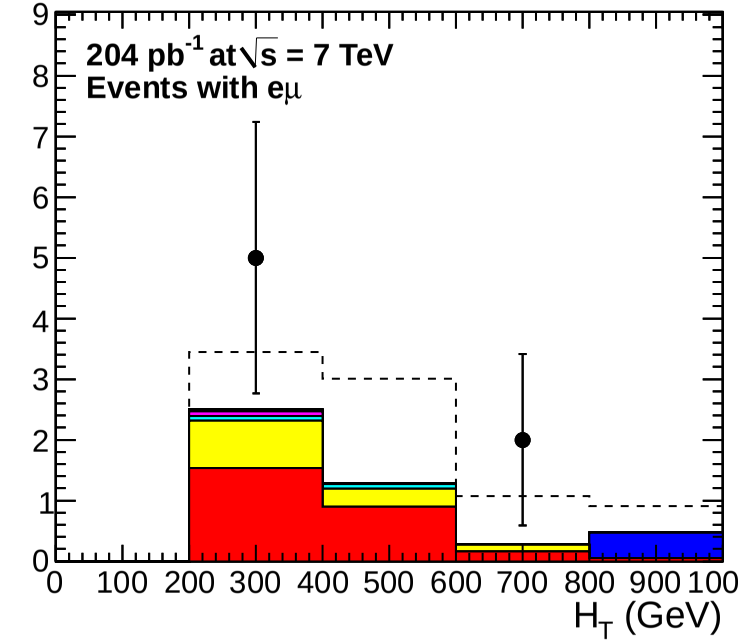
204 pb-1 at √s = 7 TeV
Events with eμ
HT (GeV)

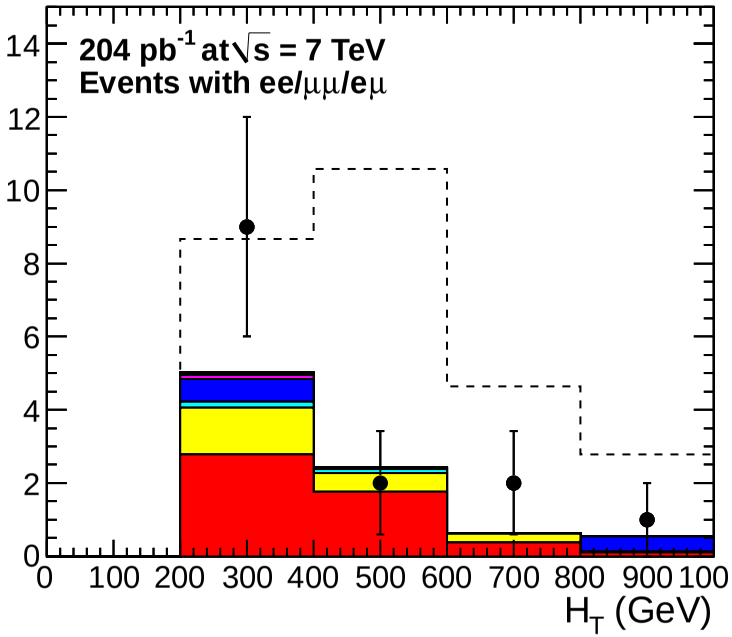
204 pb-1 at √s = 7 TeV
Events with ee/μμ/eμ
HT (GeV)

data
ttll
tttau
ttfake
DY
WW
WZ
ZZ
t
wjets
LM1

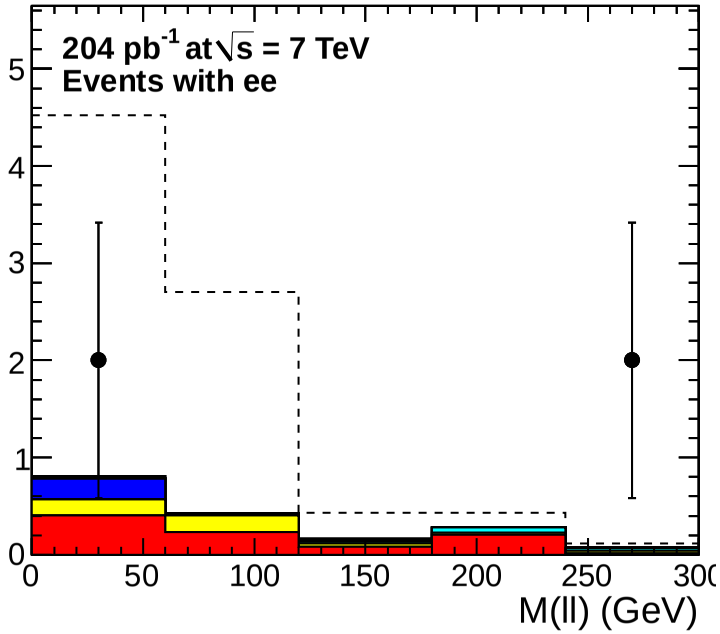
204 pb-1 at √s = 7 TeV
Events with ee
M(ll) (GeV)

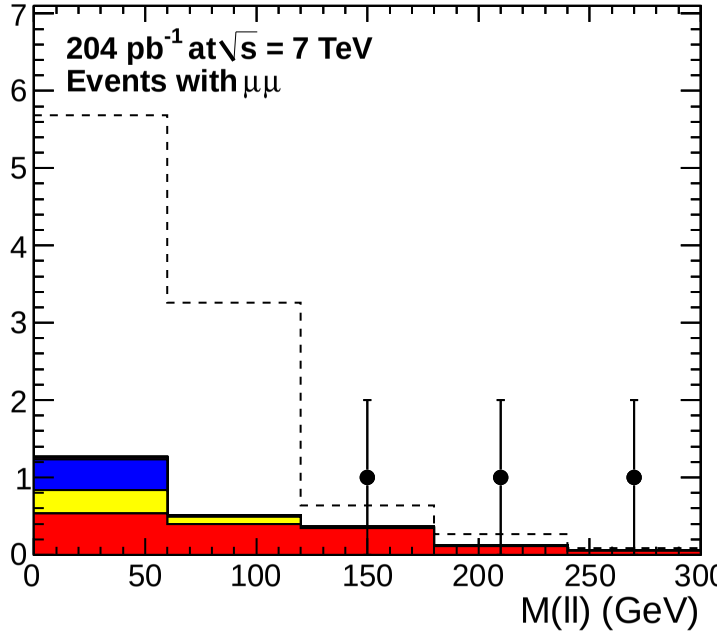
204 pb-1 at √s = 7 TeV
Events with μμ
M(ll) (GeV)

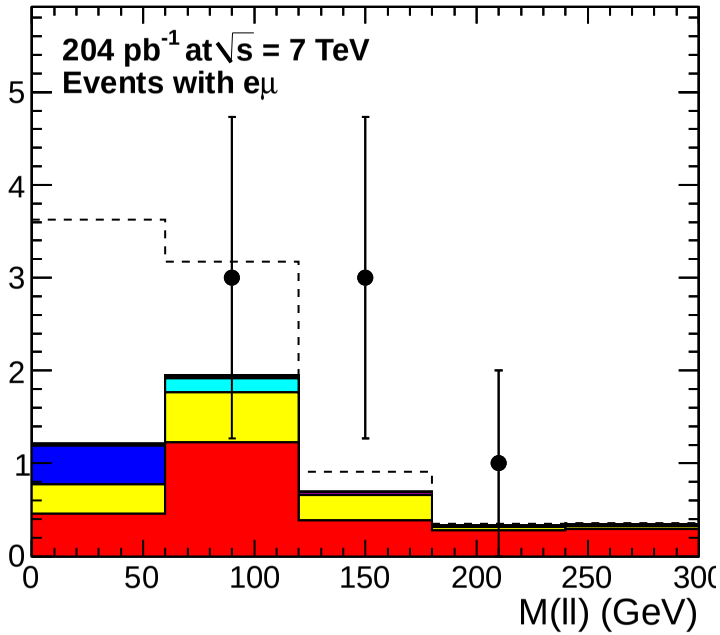
204 pb-1 at √s = 7 TeV
Events with eμ
M(ll) (GeV)

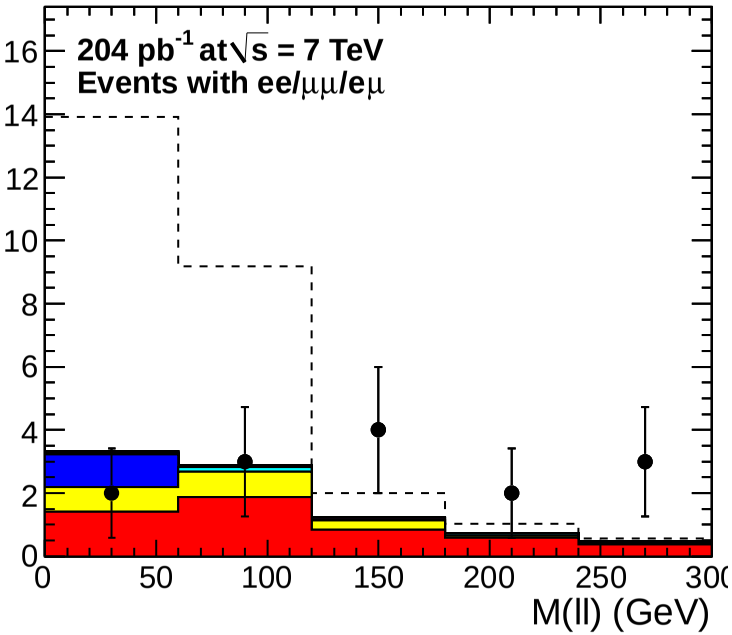
204 pb-1 at √s = 7 TeV
Events with ee/μμ/eμ
M(ll) (GeV)

data
ttll
tttau
ttfake
DY
WW
WZ
ZZ
t
wjets
LM1

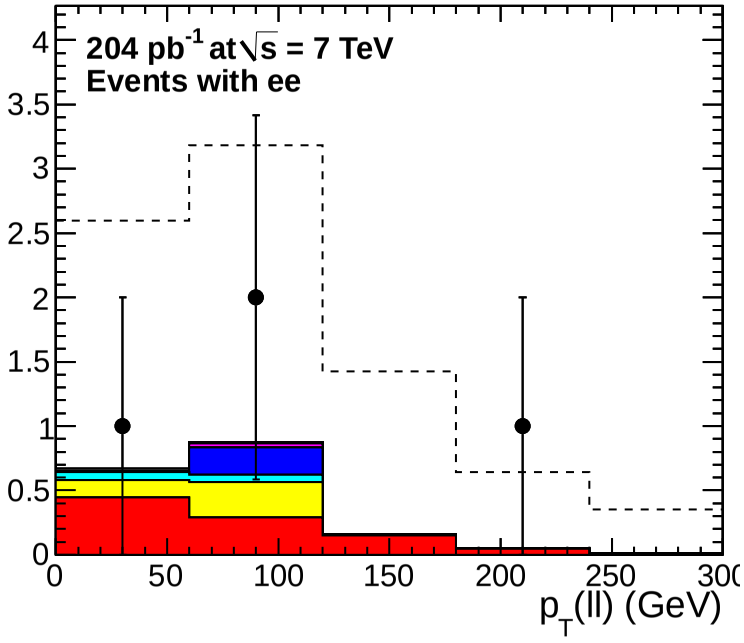
204 pb-1 at √s = 7 TeV
Events with ee
pT(ll) (GeV)

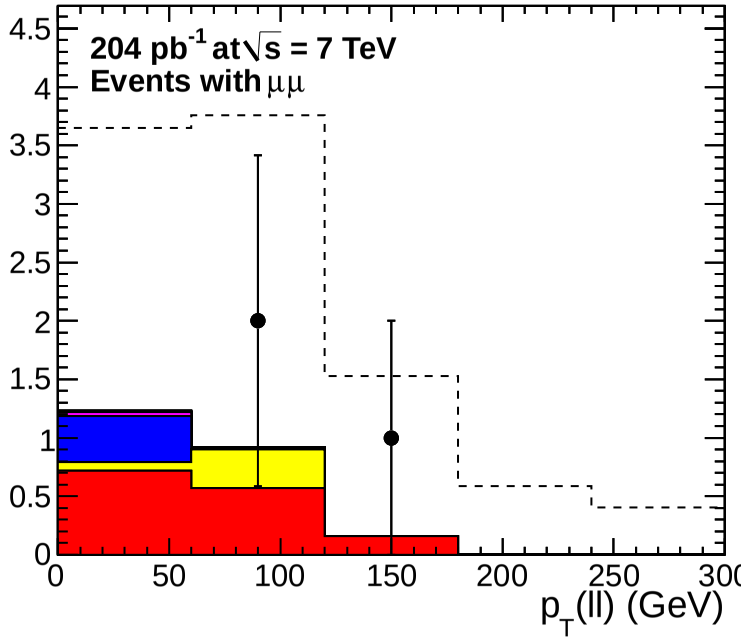
204 pb-1 at √s = 7 TeV
Events with μμ
pT(ll) (GeV)

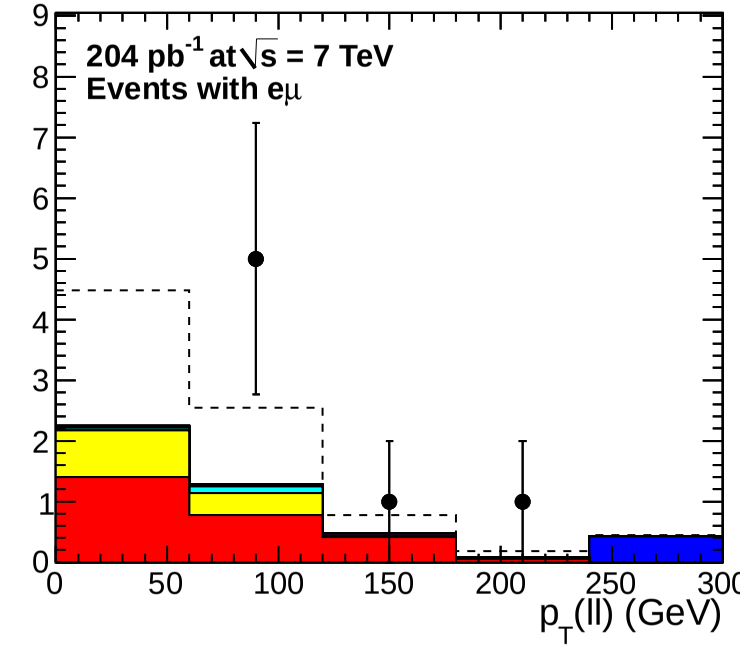
204 pb-1 at √s = 7 TeV
Events with eμ
pT(ll) (GeV)

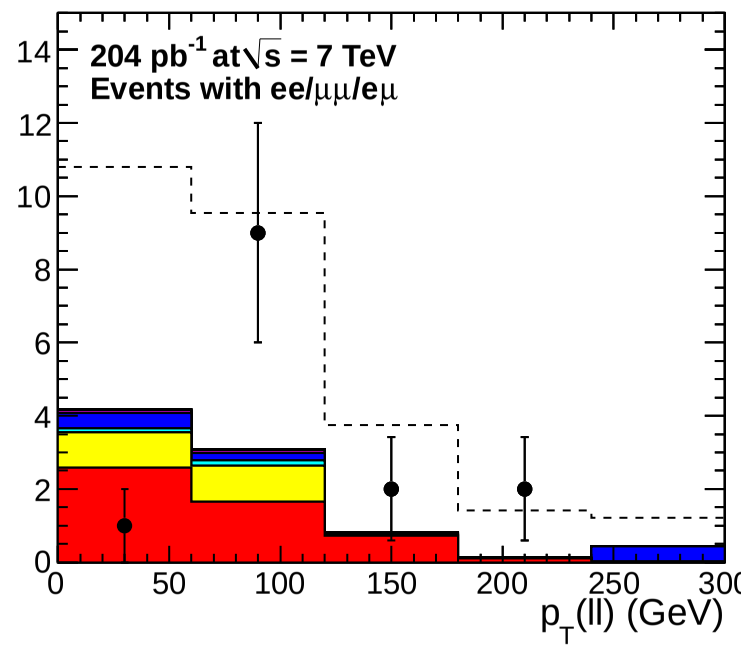
204 pb-1 at √s = 7 TeV
Events with ee/μμ/eμ
pT(ll) (GeV)

data
ttll
tttau
ttfake
DY
WW
WZ
ZZ
t
wjets
LM1

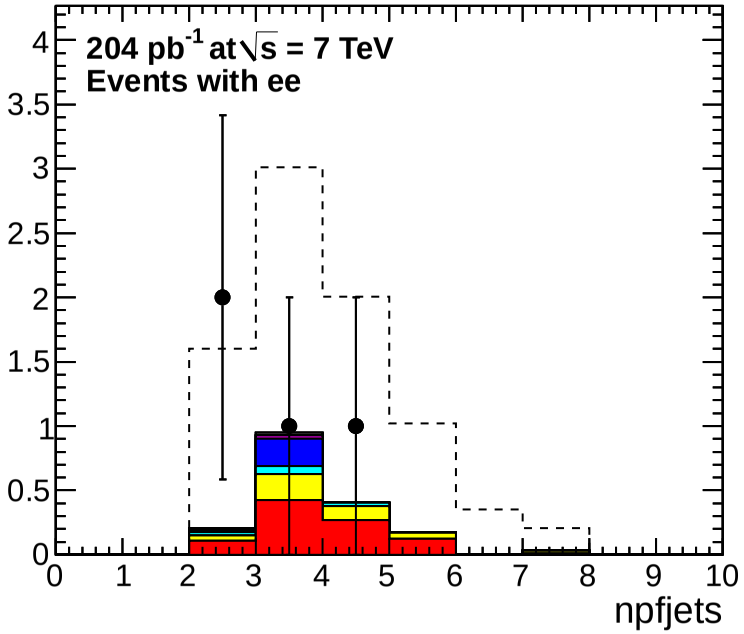
204 pb-1 at √s = 7 TeV
Events with ee
npfjets

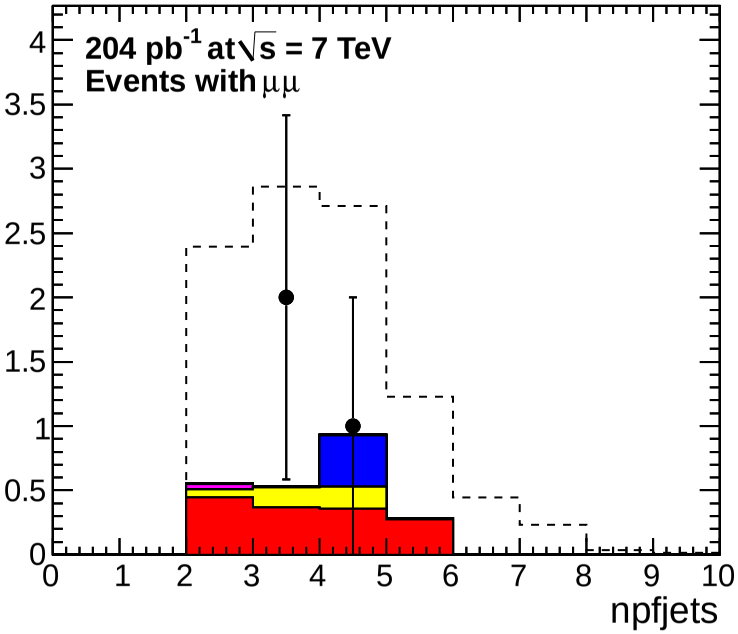
204 pb-1 at √s = 7 TeV
Events with μμ
npfjets

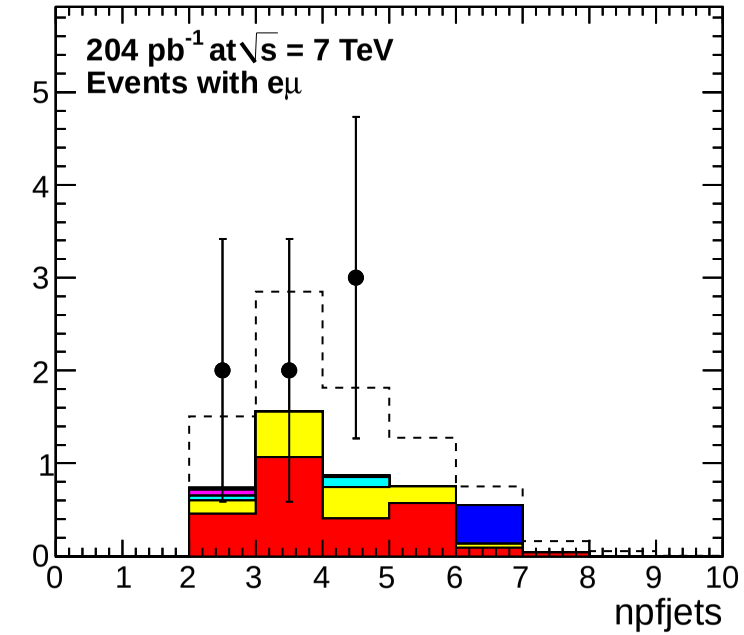
204 pb-1 at √s = 7 TeV
Events with eμ
npfjets

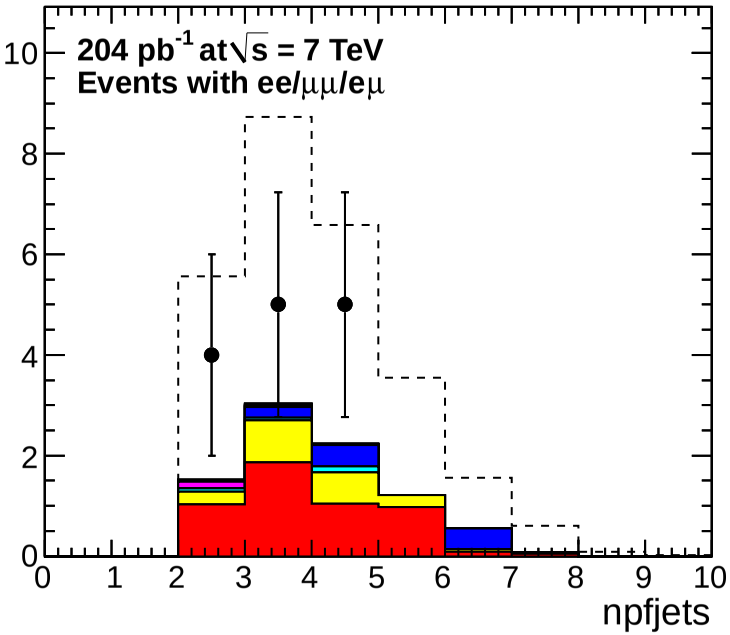
204 pb-1 at √s = 7 TeV
Events with ee/μμ/eμ
npfjets

data
ttll
tttau
ttfake
DY
WW
WZ
ZZ
t
wjets
LM1

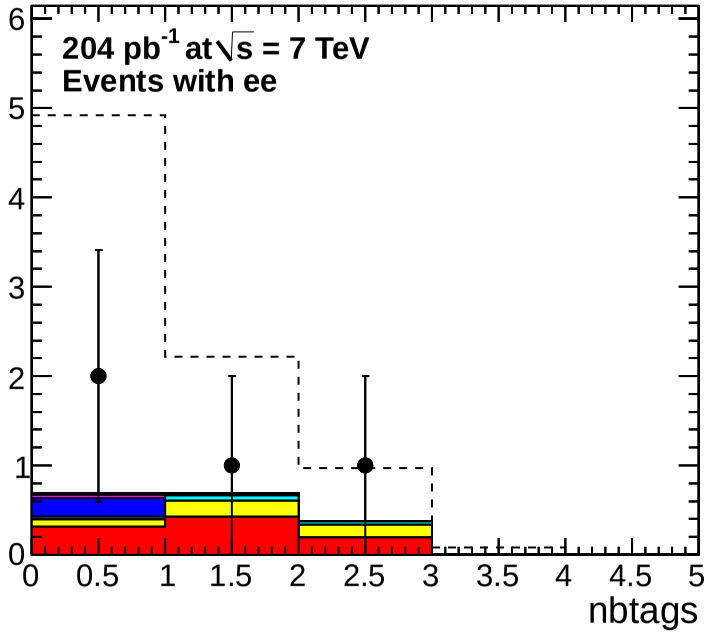
204 pb-1 at √s = 7 TeV
Events with ee
nbtags

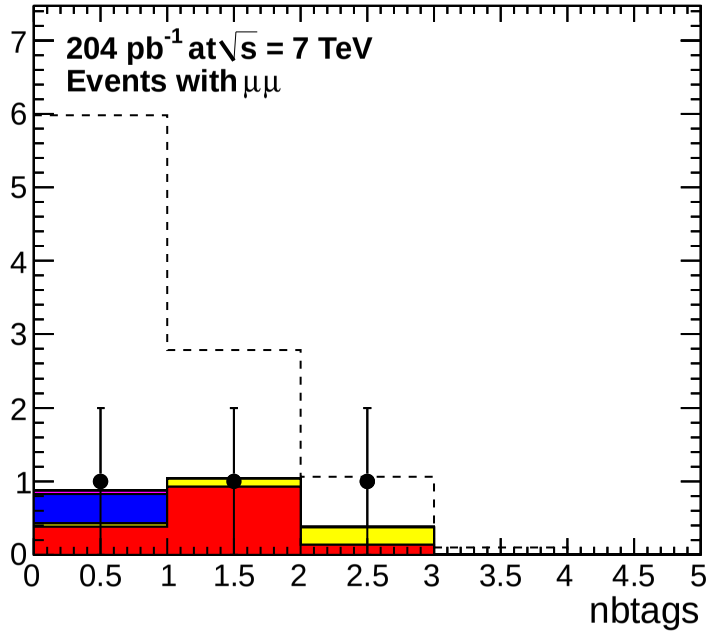
204 pb-1 at √s = 7 TeV
Events with μμ
nbtags

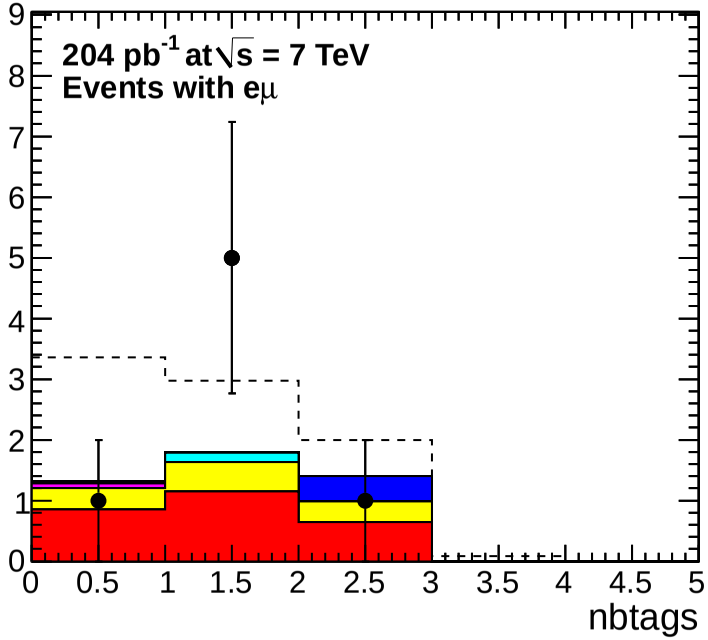
204 pb-1 at √s = 7 TeV
Events with eμ
nbtags

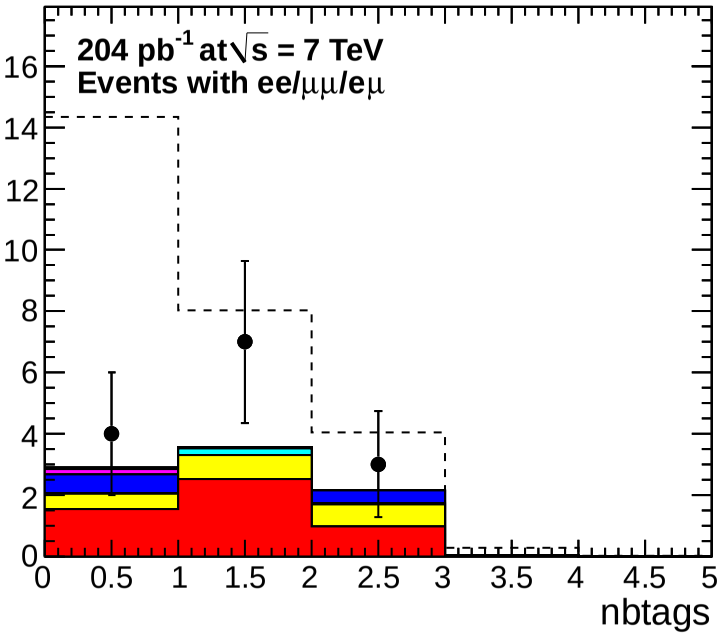
204 pb-1 at √s = 7 TeV
Events with ee/μμ/eμ
nbtags

data
ttll
tttau
ttfake
DY
WW
WZ
ZZ
t
wjets
LM1

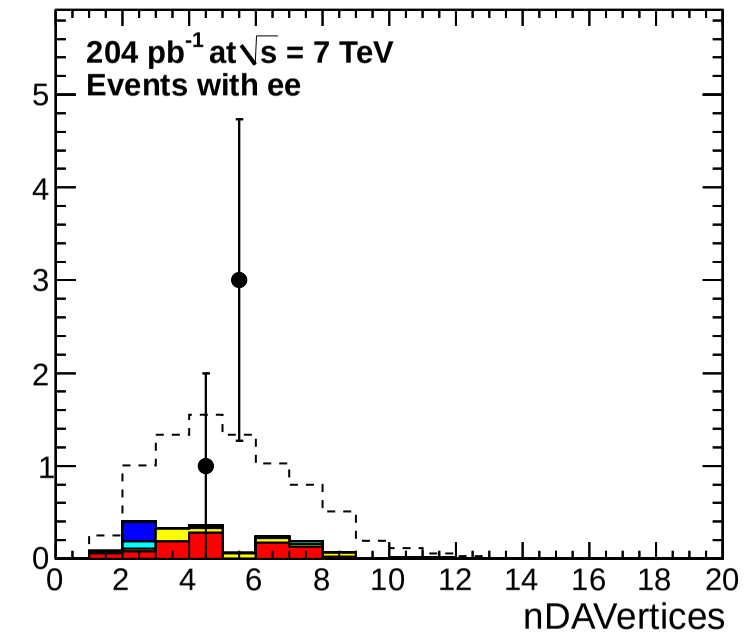
204 pb-1 at √s = 7 TeV
Events with ee
nDAVertices

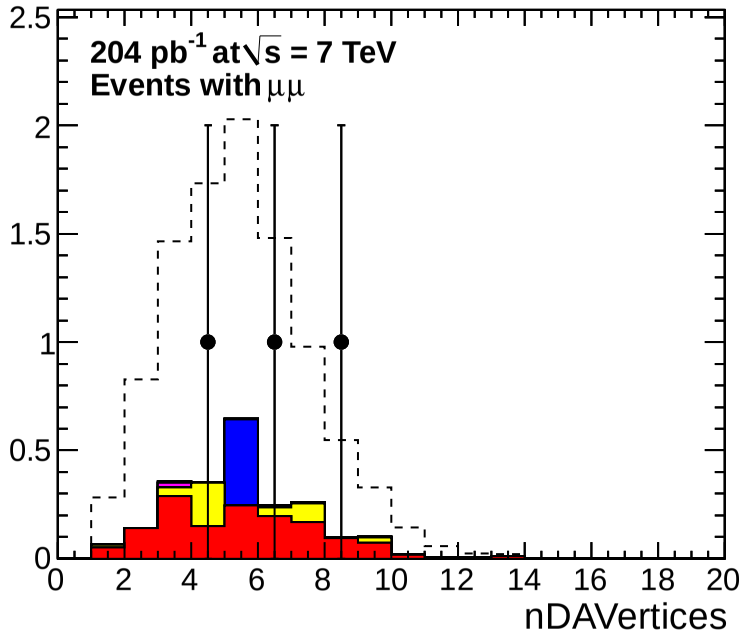
204 pb-1 at √s = 7 TeV
Events with μμ
nDAVertices

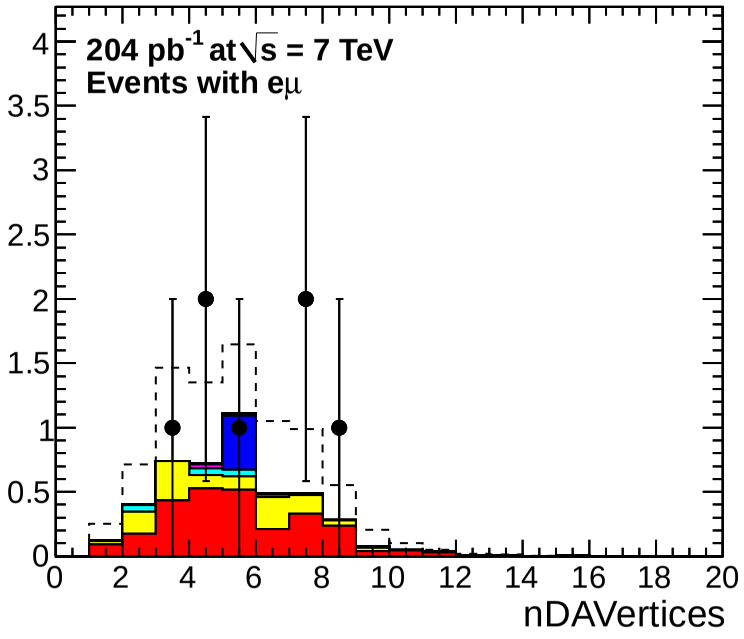
204 pb-1 at √s = 7 TeV
Events with eμ
nDAVertices

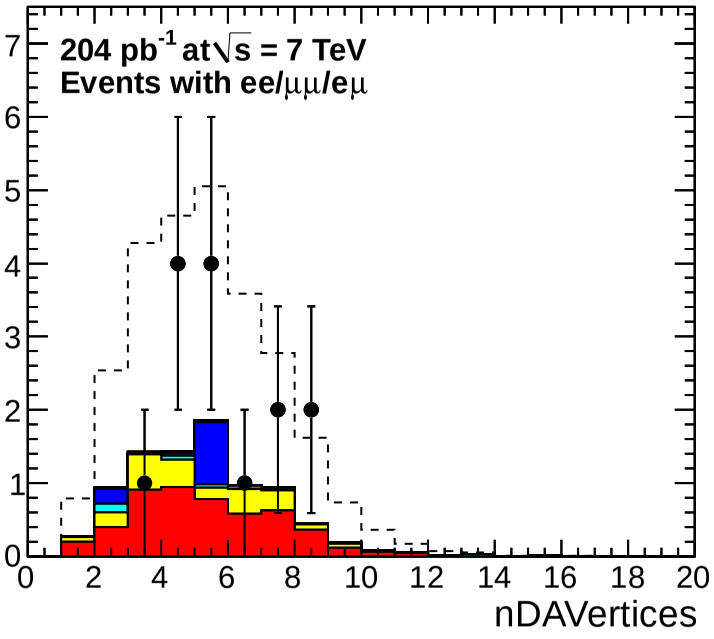
204 pb-1 at √s = 7 TeV
Events with ee/μμ/eμ
nDAVertices

data
ttll
tttau
ttfake
DY
WW
WZ
ZZ
t
wjets
LM1

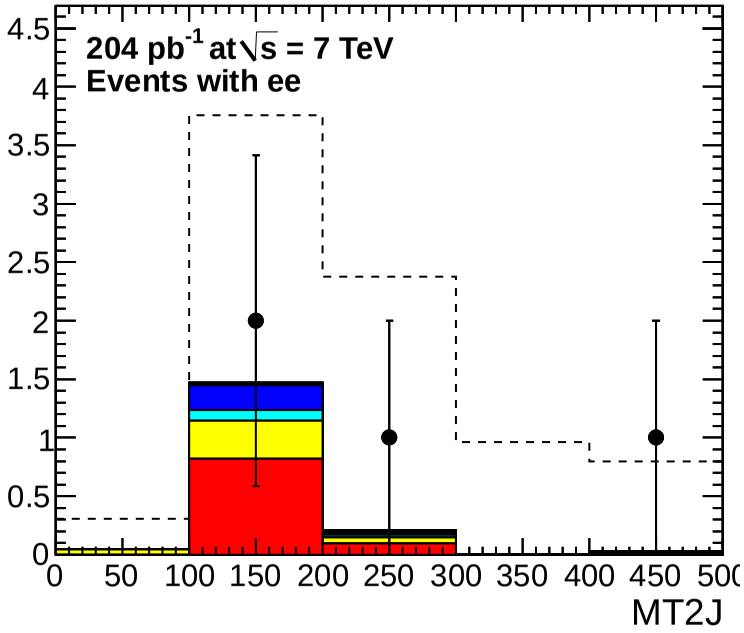
204 pb-1 at √s = 7 TeV
Events with ee
MT2J

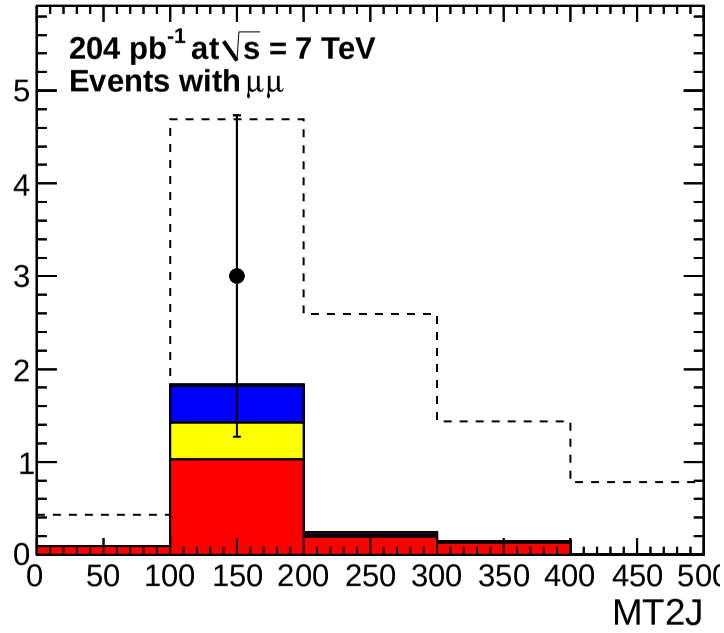
204 pb-1 at √s = 7 TeV
Events with μμ
MT2J

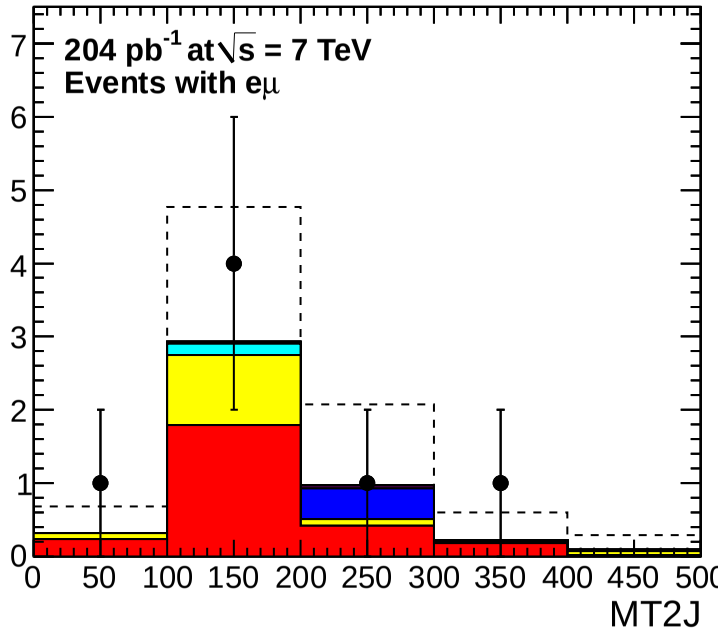
204 pb-1 at √s = 7 TeV
Events with eμ
MT2J

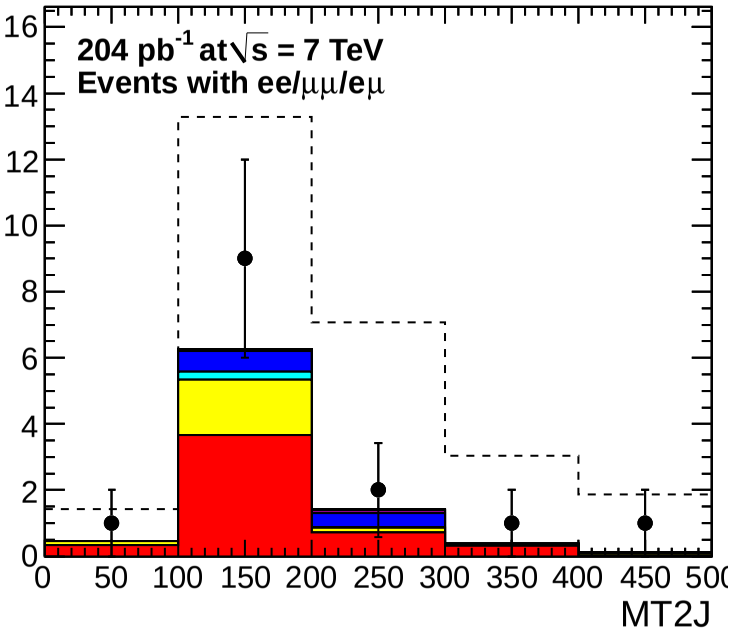
204 pb-1 at √s = 7 TeV
Events with ee/μμ/eμ
MT2J

data
ttll
tttau
ttfake
DY
WW
WZ
ZZ
t
wjets
LM1

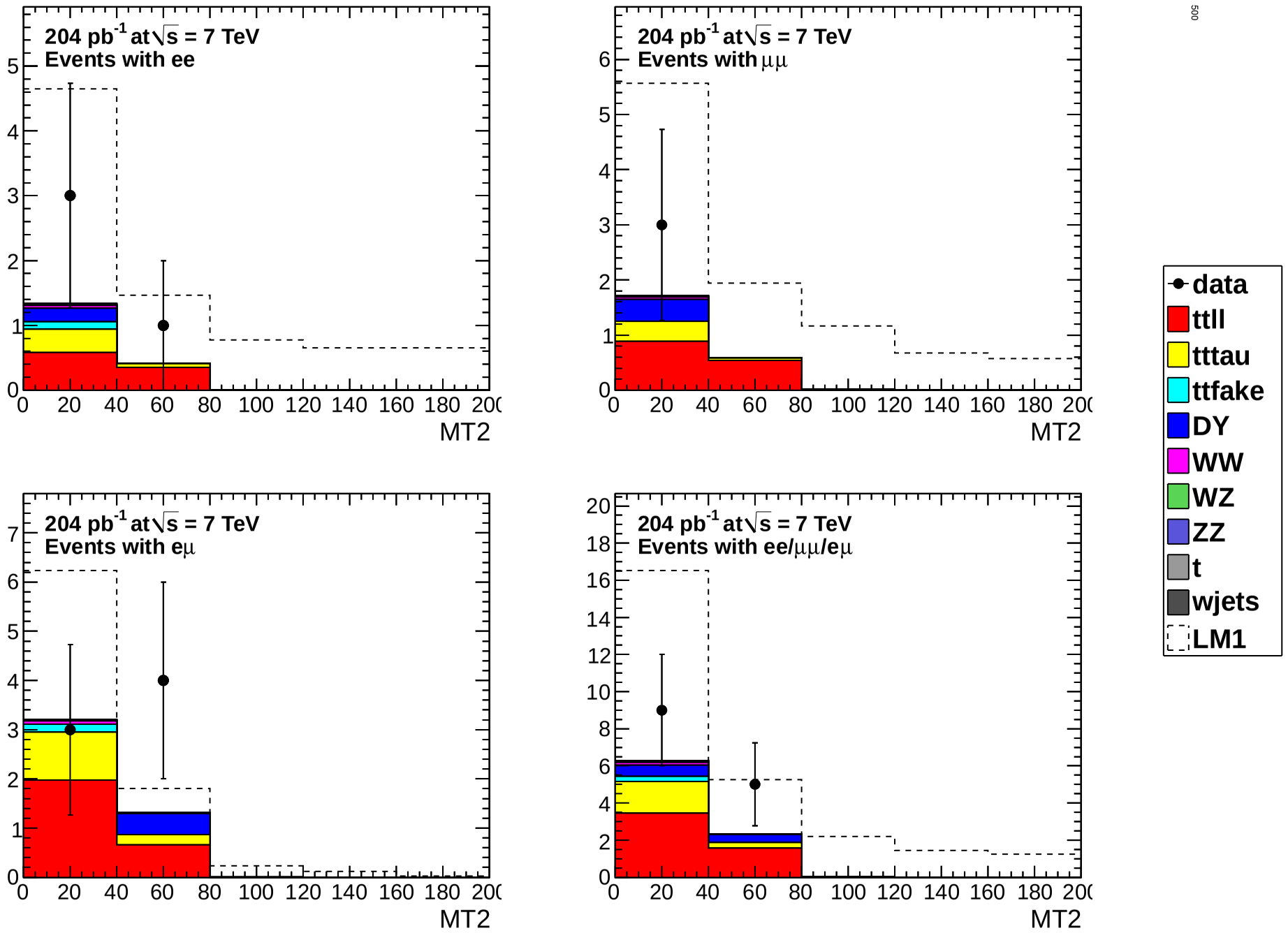
204 pb-1 at √s = 7 TeV
Events with ee
204 pb-1 at √s = 7 TeV
Events with μμ
204 pb-1 at √s = 7 TeV
Events with eμ
204 pb-1 at √s = 7 TeV
Events with ee/μμ/eμ
MT2
data
ttll
tttau
ttfake
DY
WW
WZ
ZZ
t
wjets
LM1

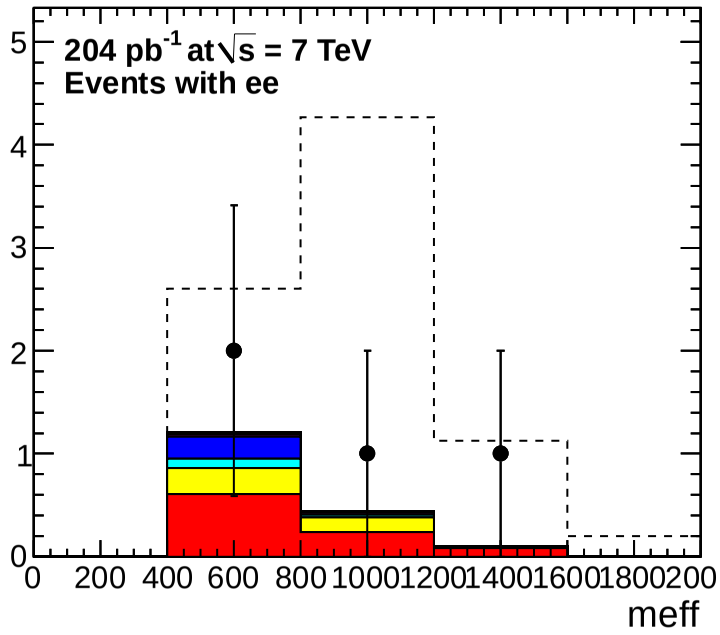
204 pb-1 at √s = 7 TeV
Events with ee
meff

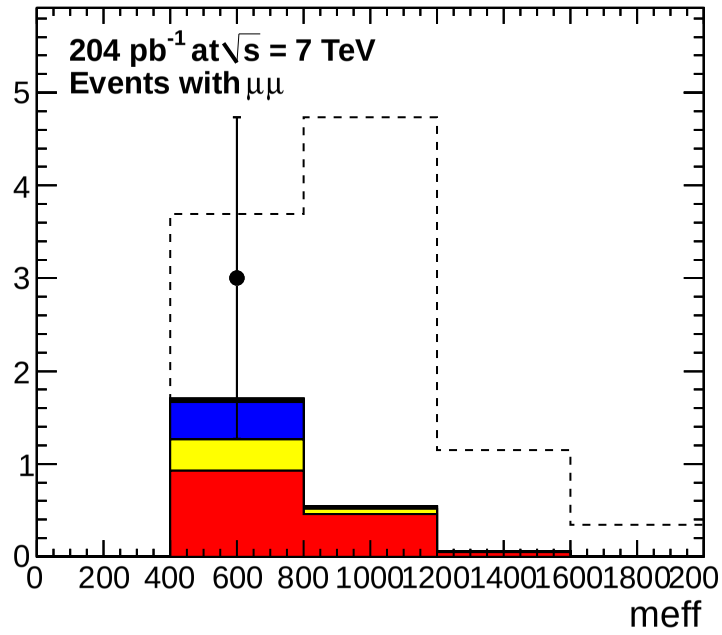
204 pb-1 at √s = 7 TeV
Events with μμ
meff

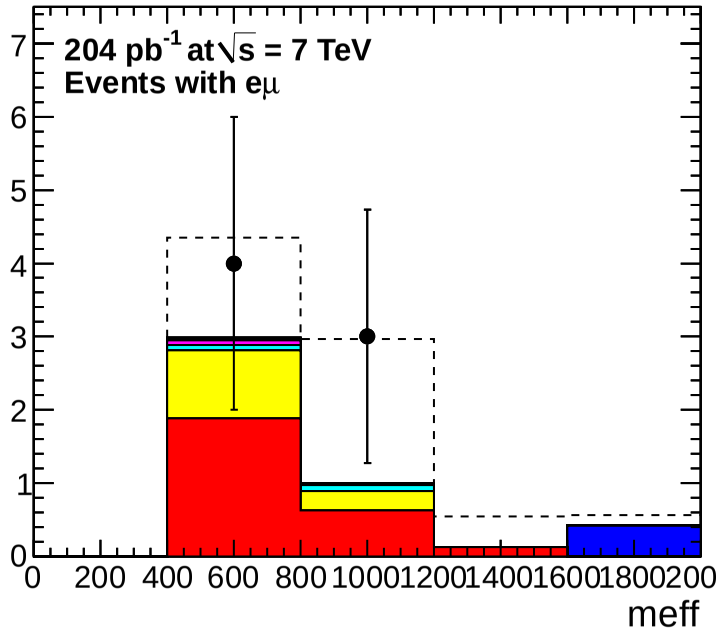
204 pb-1 at √s = 7 TeV
Events with eμ
meff

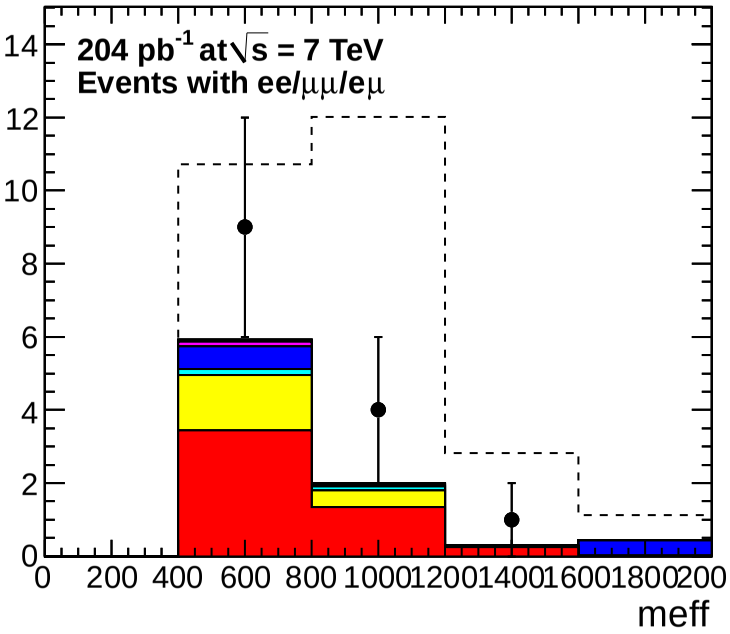
204 pb-1 at √s = 7 TeV
Events with ee/μμ/eμ
meff

data
ttll
tttau
ttfake
DY
WW
WZ
ZZ
t
wjets
LM1